MSc

2.º CICLO

FCUP
2021

U.PORTO

Interleukin-1 manipulation by *Mycobacterium tuberculosis*: impact to the infection establishment and progression

Rute Daniela Matos Gonçalves

FC

U.PORTO
FACULDADE DE CIÊNCIAS
UNIVERSIDADE DO PORTO

MSc

Interleukin-1 manipulation by *Mycobacterium tuberculosis*: impact to the infection establishment and progression

Rute Daniela Matos Gonçalves

Dissertação de Mestrado apresentada à
Faculdade de Ciências da Universidade do Porto em
Ciências da Vida

2020-2021

U.PORTO
FACULDADE DE CIÊNCIAS
UNIVERSIDADE DO PORTO

MSc

U.PORTO
FACULDADE DE CIÊNCIAS
UNIVERSIDADE DO PORTO
INSTITUTO DE INVESTIGAÇÃO
E INOVAÇÃO EM SAÚDE
UNIVERSIDADE DO PORTO

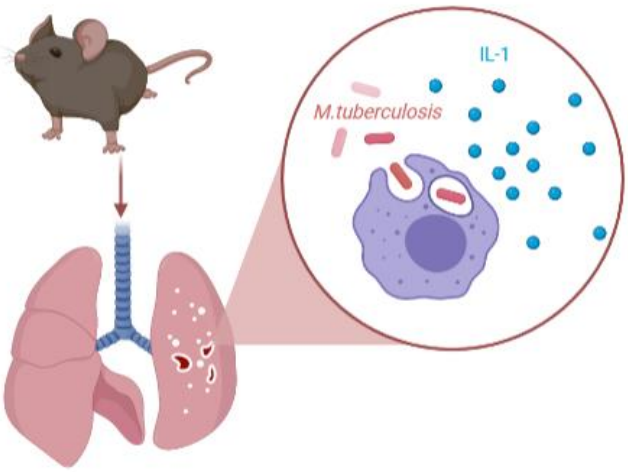

Interleukin-1 manipulation by *Mycobacterium tuberculosis*: impact to the infection establishment and progression

Rute Daniela Matos Gonçalves

Master's Degree in Cell and Molecular Biology

Department of Biology, Science College of University of Porto (FCUP)

2021

Supervisor

Margarida Saraiva, Principal Researcher and Group Leader,

Institute for Research and Innovation in Health (i3S), University of Porto

U.PORTO
FACULDADE DE CIÊNCIAS
UNIVERSIDADE DO PORTO

Todas as correções determinadas pelo júri, e só essas, foram efetuadas.

O Presidente do Júri,

Porto, _____/_____/_____

I, *Rute Daniela Matos Gonçalves* (student number 201606446), in the Cell and Molecular Biology master´s degree during the school year of 2020/2021, declare by my honour that I am the author of the totality of the presented document, and I acknowledge the consequences of plagiarism.

Agradecimentos

O desenvolvimento deste trabalho que culminou na presente tese não seria possível sem todas as pessoas que me ajudaram e apoiaram no meu percurso.

Primeiramente, quero agradecer à minha orientadora Dra. Margarida Saraiva, por me ter dado a oportunidade de integrar o seu grupo. Agradeço também todo o apoio, aprendizagens, motivação, disponibilidade e acompanhamento em todas as fases deste projeto. Por transmitir um gosto e empenho enorme em tudo o que faz e por ser um exemplo em todos os sentidos.

A todos os meus colegas do grupo Immune Regulation, em especial ao Diogo Silvério, por ser como um coorientador, me transmitir tudo o que aprendi, por me apoiar, pela confiança e pelo compartilhar de diversas horas no P3. Também à Raquel Maceiras, por todos os ensinamentos, conversas e conhecimento que me passou.

Ao Baltazar, um grande obrigado por tudo o que me ensinou, pela boa disposição e motivação.

À Deisy pelas aprendizagens que me passou, mas, principalmente por todas as conversas, risos, por ser uma pessoa querida, divertida e preocupada.

À Catarina por me fazer sentir logo bem-vinda ao grupo, por estar sempre disposta a ajudar, ser sempre muito amigável e espalhar cantorias pelo laboratório.

À Ana, por ser sempre muito prestável e mostrar dedicação e empenho em tudo o que faz.

À Marta, por termos sido as mais novas do grupo e por passarmos por etapas semelhantes, por todos os momentos divertidos, conversas e entreajuda. Obviamente a melhor companheira de azoto.

Aos colegas do III por me terem recebido bem no laboratório e por se demonstrarem disponíveis para qualquer ajuda. Em especial à Inês, um obrigado por me ouvires, por todas as conversas que tivemos e pelo apoio, principalmente nesta fase em que ambas estávamos a escrever a Tese.

Quero também agradecer à Kaori, que apesar de não estar no grupo, foi sempre muito prestável e simpática ao passar-me as suas aprendizagens em histologia.

Aos meus “Jamigos”, Ana, Andreia, Beatriz, Eduardo, Joel e Rita por todos os momentos de descontração, longas conversas, partilha e amizade. Tornaram este ano muito melhor!

Aos meus companheiros de BCM, Joana, Ricardo, Jéssica e Rita por compartilharem esta jornada comigo, tornando cada obstáculo um motivo para nos rirmos. O mestrado foi muito mais fácil e divertido com vocês.

Aos meus gémeos favoritos, Daniela e Ricardo, por serem os melhores amigos que podia ter. Obrigada por me ouvirem nas nossas caminhadas de sábado à tarde.

À Mónica e António, obrigada por estarem sempre dispostos a ouvir-me, acreditarem em mim e serem excelentes conselheiros.

Finalmente, à minha família pelo apoio incondicional e pela total confiança em mim e nos meus sonhos. O maior obrigado aos meus pais, que sempre abdicaram deles para eu ter o melhor. Aos meus irmãos, pelos momentos de lazer que me fazem esquecer das dificuldades.

Ao Bruno, pela compreensão, carinho e paciência inesgotáveis. Por me apoiar quaisquer que sejam as minhas decisões, sempre acreditando em mim. Obrigada por toda a ajuda e por me ouvires falar do projeto vezes e vezes sem conta.

Resumo

Mycobcaterium tuberculosis é um patogénio que causa mais de 1,4 milhões de mortes por ano. Intervenções inovadoras para o combate à tuberculose (TB) são, portanto, urgentes. A TB é uma doença heterogénea, apresentando-se como um espetro dinâmico, que varia de patologia ligeira a severa, formas disseminadas, e eventualmente, morte. Os primeiros eventos imunes no pulmão são críticos para definir a apresentação da doença e o papel da IL-1 neste processo tem sido realçado.

Um estudo recente do nosso grupo mostrou que *M. tuberculosis* isolado de pacientes com TB mais severa evadem mecanismos de resistência do hospedeiro, induzindo níveis baixos de IL-1. Baseando-me neste estudo e com recurso ao modelo animal, investiguei se e como diferentes isolados de *M. tuberculosis* recuperados de pacientes com TB ligeira ou severa manipulam a resposta imune *in vivo*. Investiguei ainda se esta manipulação afeta o estabelecimento e o curso da infeção. Para isso, ratinhos C57BL/6 foram infetados via aerossol com os isolados clínicos 4I2, 6C4 ou com HN878 (uma estirpe laboratorial hipervirulenta). Os resultados mostraram que foi possível recapitular, no modelo de ratinho, as diversas severidades de doença provocadas pelas diferentes estirpes de *M. tuberculosis* observadas em humanos. Especificamente, a infeção com o isolado 6C4 resultou em maiores cargas bacterianas no pulmão, lesões maiores e mais severas, maior recrutamento de células imunes para o local da infeção e maior expressão de genes que codificam citocinas pro-inflamatórias do que a infeção com o isolado 4I2. Como esperado, a estirpe HN878 foi ainda mais virulenta que as anteriores. Numa segunda fase do trabalho, usando ratinhos geneticamente modificados, com deficiência no recetor da IL-1 (IL-1R) nas células mieloides e infetando-os com os isolados de *M. tuberculosis,* pretendi investigar qual o impacto da sinalização por IL-1 no desenvolvimento da doença e estabelecimento da infeção. Os resultados mostraram que a infeção com a estirpe que induz mais IL-1 *in vitro, M. tuberculosis* 4I2, foi mais afetada pela falta de IL-1R, tornando-se mais virulenta e assemelhando-se à infeção pelo isolado 6C4. Já as infeções com os isolados 6C4 e HN878 não apresentaram diferenças significativas entre ratinhos *wild type* e deficientes para o IL-1R em células mieloides. Globalmente, a minha tese reafirma a importância da diversidade do *M. tuberculosis* na interação hospedeiro-patogénio e oferece uma perspetiva inovadora sobre os mecanismos da IL-1 na patogénese da TB.

Palavras-chave: Tuberculose, Interleucina-1, Diversidade do patogénio

Abstract

Mycobacterium tuberculosis is a pulmonary pathogen that causes over 1,4 million deaths per year. Novel interventions to tackle tuberculosis (TB) are therefore urgent. TB is an heterogeneous disease, presenting as a dynamic spectrum, which varies from mild to severe lung pathology, disseminated forms and eventually death. The early lung immune events critically define the outcome of TB and a role of IL-1 in this process has been highlighted.

A recent study from our group showed that *M. tuberculosis* isolated from patients with more severe TB presentations evade from mechanisms of host macrophage defence, ultimately inducing low levels of IL-1. Building upon this study and using the animal model, I investigated whether and how *M. tuberculosis* isolates recovered from patients with mild or severe TB can manipulate the immune response *in vivo,* and how that impacts the establishment and course of infection. For this, C57BL/6 mice were infected via aerosol with the clinical isolates 4I2, 6C4 and HN878 (a hypervirulent laboratory strain). The results showed that it was possible to recapitulate, in the mouse model, the diverse severities of disease caused by different strains of *M. tuberculosis,* observed in humans. Specifically, infection with *M. tuberculosis* isolate 6C4 resulted in higher bacterial loads in the lung, larger and more severe lesions, higher recruitment of immune cells to the site of infection and enhanced expression of genes encoding proinflammatory cytokines, than infection with *M. tuberculosis* 4I2. As expected, the HN878 strain presented more virulent traits than the other isolates. Furthermore, using genetically modified mice, deficient in the IL-1 receptor (IL-1R) on myeloid cells and infecting them with the different *M. tuberculosis* isolates*,* I intended to investigate the impact of IL-1 signaling on disease development and outcome of infection. The results showed that the infection with the high IL-1 inducer strain, *M. tuberculosis* 4I2, was more affected by the lack of IL-1R, resulting in a more severe infection that resembled the *M. tuberculosis* 6C4 infection. Infections with *M. tuberculosis* 6C4 and HN878 did not show significant differences between wild type (WT) and conditional knock out mice.

Collectively, my thesis reaffirms the importance of the pathogen diversity in host-pathogen interactions and offers new insights on the mechanism of IL-1 in the pathogenesis of TB.

Keywords: Tuberculosis, Interleukin 1, Pathogen diversity

Index

List of Figures

List of Tables

List of Abbreviations

CD	Cluster of differentiation
DNA	Deoxyribonucleic acid
ELISA	Enzyme-linked immunosorbent assay
ESAT-6	Early secretory antigen target-6
H&E	Haematoxylin and eosin
HIV	Human immunodeficiency virus
IFN	Interferon
IGRA	Interferon γ release assay
IL	Interleukin
LTBI	Latent tuberculosis infection
RNA	Ribonucleic acid
Mtb	Mycobacterium tuberculosis
MTBC	Mycobacterium tuberculosis complex
NI	Non-infected
PCR	Polymerase chain reaction
PFA	Paraformaldehyde
PGE2	Eicosanoid prostaglandin E2
TB	Tuberculosis
Th	T helper
TLR	Toll-like receptor
TNF	Tumor necrosis factor
TST	Tuberculin skin test
WHO	World Health Organization
ZN	Ziehl-Neelsen

Chapter I. Introduction

This work is a part of a review article publicised in mBIO:

Advances on the role and applications of IL-1 in tuberculosis
Diogo Fonseca Silvério, **Rute Gonçalves**, Rui Appelberg and Margarida Saraiva

Tuberculosis

Tuberculosis (TB) is the world oldest and more persistent pandemic. In fact, evidence shows the presence of ancient *Mycobacterium tuberculosis* (Mtb) DNA in Egypt mummies from 2400-3000 BC (1). Only in 1839 the word “tuberculosis” was suggested by J.L. Schönlein to designate the disease that until then had been called “White plague”, “Phthisis”, “Scrofula” or “King’s touch”. In 1882, the physician Robert Koch has firstly isolated the pathogen responsible for TB, setting aside the idea that TB is an inherited condition, but rather an infectious disease (2). TB is caused by microorganisms belonging to the *Mycobacterium tuberculosis* complex (MTBC) (3).

Despite being an ancient disease, TB remains a great health problem, currently considered one of the top 10 deadliest diseases worldwide and the leading cause of death by a single infectious agent, besides COVID-19 (4). Efforts are being made to contribute to the End TB Strategy, implemented by World Health Organization (WHO), which aims 95% reduction in TB deaths and 90% decrease in TB incidence until 2035. Achieving these goals relies on supportive systems and intensive research to the improvement of diagnosis, treatment, and prevention of disease (5, 6).

Epidemiology of Tuberculosis

According to the WHO, in 2019, TB caused over 1.4 million deaths, of which about 208 000 deaths were in HIV positive people, and an estimated 10 million people developed active TB disease. The death toll of TB is likely to further aggravate due to the COVID-19 pandemic situation, as it is estimated that a 50% decrease in TB case detection over 3 months may have resulted in 400 000 additional TB deaths last year (4).

Geographically, the incidence of TB cases is heterogeneous, wherein low-income, and middle-income countries are more affected. In 2019, South-East Asia (44%), Africa (25%) and Western Pacific (18%) were the regions with more incidence of TB cases (**Figure 1**). By contrast, high-income countries such as North America, New Zealand, Australia, and most countries of Western Europe registered the lowest rates of TB. Although affecting people from all demographic groups, TB cases are more prevalent in adult men (56%) followed by adult women (32%) and children (12%) (4).

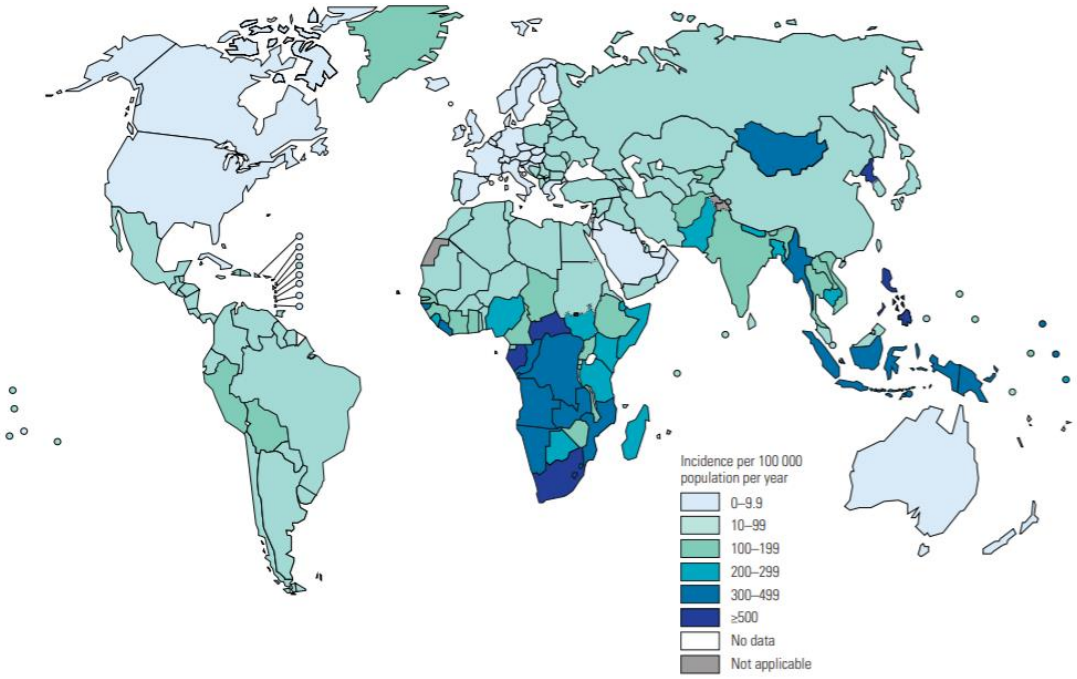

Figure 1. Global incidence rates of active TB (cases per 100 000 population per year) in 2019. Figure from (4).

Historically, the advances in TB research were very slow, but some important events resulted in great changes in the TB burden. The improvement of hygiene and socioeconomic conditions in the beginning of the 20th century decreased TB-related deaths in Western Europe and United States (7). Later, this decline was highly amplified by the discovery of effective antibiotic treatments and vaccination. However, these advances did not reach the low-income countries so rapidly. In fact, TB incidence in Africa increased due to the HIV epidemic, which remains a major risk factor in disease development (7). Currently, the TB incidence rate is slowly decreasing worldwide but the prevalence of the HIV coinfection, the emergence of new drug resistant strains and the impact of COVID-19 are massive challenges in the fight against TB (6).

The Spectrum of Tuberculosis

From a simpler clinical point of view, Mtb–infected individuals can be categorized in one of two defined states: latent TB infection (LTBI) or active TB. Nevertheless, TB is a heterogeneous disease, presenting as a dynamic spectrum, which varies from mild to severe lung pathology, disseminated forms and eventually death (**Figure 2**) (7-12).

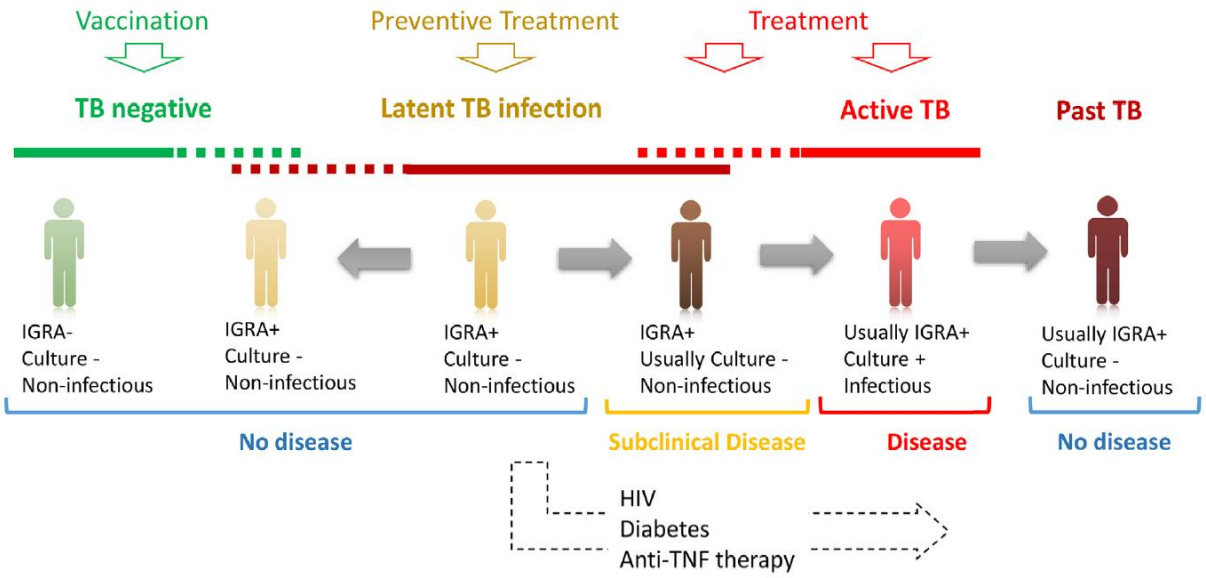

Figure 2. The different outcomes of *M. tuberculosis* infection (spectrum of disease). From (9).

After *M. tuberculosis* exposure, our immune system can successfully eliminate the pathogen, or the bacteria can escape our defence mechanisms. The pathogen can be eliminated via innate or adaptative immune response, in which individuals do not present symptoms nor need treatment. LTBI is a non-symptomatic and non-contagious state (7-9, 11). Notably, mathematical studies estimate that a quarter of the world's population are latently infected with *M. tuberculosis,* even without realizing it (13). This constitutes a massive reservoir of unceasingly TB infection. Even without showing signs of illness, some of these individuals may eventually progress to active TB throughout their lifetime. This reactivation process normally happens when the host immune system is compromised, such as in HIV coinfection, immunotherapies, and diabetes (7, 8, 14-16). Within the definition of LTBI, there is a range of infection presentation, from a well-contained and quiescent state to a subclinical infection, whereas patients are already progressing to active disease. This outcome stratification could be extremely helpful to differentiate patients who are in increased risk of TB and need preventive treatments (7-9).

When the host immune system is not able to clear or control the infection, individuals infected with *M. tuberculosis* develop active TB, showing clinical symptoms such as fever, cough, weight loss and lack of appetite, night sweats, fatigue, chest pain and even haemoptysis (presence of blood when coughing) in more severe pulmonary states (7). Even within active TB, there is a wide spectrum of TB severity with several clinical presentations, varying from mild to severe outcome and life-threatening disease. Active

TB is symptomatic and contagious, in which the bacteria is transmissible by aerosol droplets expelled by an infected person through coughing. It is very important that these individuals are treated, since 50% of non-treated active TB patients succumb to disease (17). Although *M. tuberculosis* is not highly infectious, one person infects approximately 3-10 people per year, and thus households contacts of TB patients must be followed and examined regularly (9, 12).

Diagnose, treatment and prevention

There are several diagnostic tests and techniques to determine if a person has been exposed to *M. tuberculosis* and developed disease.

Tuberculin skin test (TST) is a diagnostic method based on the Mantoux technique, which involves an intradermal injection of purified protein derivative (PPD) – a mixture of proteins from *M. tuberculosis*. Then, if the person has been in contact with *M. tuberculosis* and developed cell-mediated immunity against the PPD, a delayed-type hypersensitivity reaction (redness skin) will occur in the next 2-3 days (7, 18).

Interferon-γ release assay (IGRA) is a blood test which measures the IFN-γ released *in vitro* by T cells, after stimulation with antigens encoded by genes in the region of difference 1 (RD-1). In contrast to TST, which uses antigens also present in the Bacillus Calmette-Guérin (BCG) vaccine and other non-tuberculous mycobacteria, the IGRA test is performed with *M. tuberculosis* specific antigens. For that reason, this test is useful to detect LTBI in populations vaccinated with BCG (19).

Both TST and IGRA show a low predictive value, since neither allow to distinguish between LTBI and active TB (19, 20). For the diagnose of active TB disease, other methods are used, namely chest X-rays and Positron-Emission Tomography/Computed Tomography (PET-CT) scan (imaging techniques), sputum smear microscopy, microbiology culture methods and molecular tests. A definitive diagnose requires culture validation and an imaging screening of potential lung lesions (7, 9). Xpert MTB/RIF is a recent and easy molecular test, based on the polymerase chain reaction (PCR) technique that detects *M. tuberculosis* DNA and the presence of rifampicin resistance gene at the same time. It is recommended by the WHO as first-line diagnosis, and it has been used in low-income countries (6, 21).

The common treatment for active TB includes a six-month regimen of antibiotics: two intensive months with four drugs (rifampicin, isoniazid, pyrazinamide, and ethambutol), followed by two months with two drugs (rifampicin and isoniazid).

Despite the high success rate, this standard treatment is very aggressive and toxic for the patients (8). Furthermore, the emergence of drug resistant (DR), multidrug resistant (MDR) and extensively drugs resistant (XDR) strains constitutes a major problem (22-25). The resistance to one (DR) or at least to isoniazid and rifampicin drugs (MDR), require a long-term treatment with second line anti-TB drugs, such as linezolid, moxifloxacn, delamanid, which have low efficiency and high toxicity. Nevertheless, resistance to all first line antibiotics, fluoroquinolones and some second line antibiotics (XDR) can occur. Thus, it is important to search for new anti-TB drugs, optimizing the existing ones and understanding the mechanisms of resistance (23, 26).

Currently, BCG is the only licensed vaccine for the prevention of TB disease (7). It was developed over 100 years ago, and it still takes part of the plan of vaccination in several countries, being administered to newborns. Indeed, BCG is known to confer protection to young children against *M. tuberculosis* infection, severe and disseminated forms of TB, with 50-80% of efficacy (27). However, the efficiency in adolescents and adults, who are the groups presenting higher TB prevalence and transmission rates, is lower and variable (0-80%) (28, 29). Therefore, the majority of TB vaccines in development are intended for these age group. Vaccine candidates and the current research aim to prevent the progression of LTBI to active TB, affording protection against the pulmonary form of disease and ultimately preventing the infection (27, 30).

The *Mycobacterium tuberculosis* complex

The MTBC includes several closely related species, which show a similarity of 99,9% of DNA sequence between them. However, the different members of the MTBC are known to differ in their primary host and in some virulence traits (7, 31). Members of the MTBC are characterized as acid fast bacilli, with a thick and impermeable cell wall which only stains with Ziehl Neelsen coloration. Most cases of TB are caused by the human-adapted MTBC species *M. tuberculosis (sensu stricto)* and *Mycobacterium africanum*. A few TB cases are related to zoonotic species as *Mycobacterium bovis* and *Mycobacterium caprae* (32).

The human adapted species of the MTBC are obligate human pathogens and do not have any environmental reservoir. Hence, these species are professional pathogens, in other words, they need to cause disease in humans to allow transmission from host to host (7, 31, 32). Moreover, these pathogens cause chronic infections and grow more slowly than most bacteria (33).

Until very recently, the human adapted MTBC members comprised seven phylogenetic lineages (L1-L7) (7), but in the last year, two new lineages were discovered (L8 and L9) (34, 35). L1-L4, L7 and L8 are *M .tuberculosis* lineages (35), while L5, L6 and L9 are *M .africanum (34).* All lineages have derived from the same ancestor (*Mycobacterium canettii*) but they are geographically distinct (36). For instance, *M.tuberculosis* lineages are commonly widespread, in contrast to the *M. africanum* ones which are highly limited to West Africa. Also, L7 is restricted to Ethiopia (37) and L8, firstly reported in 2020, seems to be restricted to the African Great Lakes region (31, 35)

The greatest diversity of the MTBC human adapted species is found in Africa. This is one of the reasons why several studies suggest an African origin for these bacteria. Furthermore, it is described that *M .tuberculosis* emerged and accompanied the “Out-of-Africa” migration by modern humans, 70 000 years ago (**Figure 3**) (38). Thenceforth, a co-evolution between MTBC species and humans is likely to have occurred, with pathogen diversification and mutual adaptation (39-41).

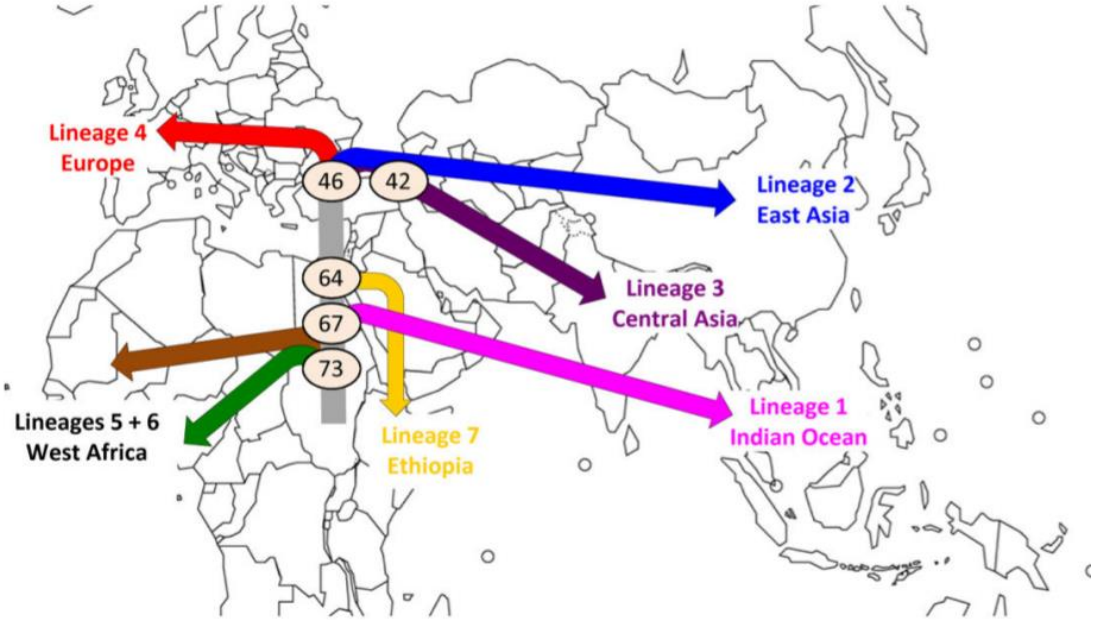

Figure 3. MTBC phylogenetic expansion and the "Out-of-Africa" representation. Different colours represent different lineages. In circles the major splits between lineages are dated (in thousands of years). Figure reproduced from (38).

Genetic diversity of the pathogen

Although *M. tuberculosis* and *M. africanum* are genetically similar and both infect humans, differences in growth rate, virulence and disease presentation were found (40). Indeed, several studies, in both mice and humans, show lower virulence and slower progress of disease upon infection with *M. africanum*. (42, 43). Moreover, variability in the pathogenicity of different lineages is also documented. For instance, L1 was associated with higher rates of extrapulmonary TB as compared to L2 and L4. Also, studies with human macrophages and animal models have shown that L2 and L4 present higher replicative abilities (32). It is worth mentioning that some variable results from these studies may possibly be due to the complex host-pathogen interactions, depending not only on pathogen diversity, but also on host genetic factors (8).

Importantly, even within each lineage, heterogeneity of the infecting bacteria, once considered irrelevant, impacts the transmission, host immune response, clinical presentation, and, even, disease outcomes (44). Understanding how different strains of *M. tuberculosis* associate with variable TB manifestations would be important to develop better clinical control decisions and adequate adaptation of patient care. Ultimately,

unveiling the impact of *M. tuberculosis* diversity is a crucial part to understand host-pathogen interactions and TB itself (8, 9).

The immune response to tuberculosis

A brief overview

TB is an airborne infection, whereas after inhalation, *M. tuberculosis* is transported to the lower respiratory tract, and internalized by the resident alveolar macrophages and dendritic cells (**Figure 4**) (7). In the alveolar space, these cells recognise the bacteria and phagocyte it through specific receptors in their surface. Once internalized, *M. tuberculosis* has several mechanisms for escaping the host immune protection, such as the ability to block the fusion between phagosome and lysosome (45). Hence, the bacillus can evade the acidic environment of phagolysosome and abide. In addition, the ESAT-6 secretion system-1 (ESX-1) disrupts the phagossomal membrane, allowing the release of bacterial material into the cytosol. Then, *M. tuberculosis* products activate cytosolic surveillance systems, promoting a type I Interferon (IFN) response, beneficial to the intracellular growth of the bacteria (46-49). Indeed, patients with active TB or progressing to active disease present a transcriptional blood signature dominated by genes inducible by type I IFN (10). However, the activation of the cytosolic surveillance systems also induces interleucin-1β (IL-1β), a proinflammatory cytokine important for the host defence against TB (44) .

This early stage of infection has proven essential to determine bacterial clearance or persistence. If the bacteria survives the first line of host defence, it accesses the lung interstitium, either by cross through the epithelial cells or by transmigration of infected macrophages across the epithelium (50, 51). Alveolar macrophages are the first cells to interact with the bacteria, mediating its dissemination to the lung interstitium and initiating the recruitment of other immune cells (50, 52). In the interstitium, *M. tuberculosis* multiplies, infects other cells, and triggers the recruitment of immune cells to the local of infection, such as macrophages, monocytes, neutrophils and dendritic cells (45, 50, 52). Interestingly, the two populations of macrophages (alveolar versus recruited) present different transcriptional profiles and distinct metabolic states upon *M. tuberculosis* infection (53). Studies have shown that alveolar macrophages are associated with a fatty acid uptake and metabolic shift towards β-oxidation, being more permissive to *M.*

tuberculosis replication. In contrast, recruited macrophages are associated with up-regulation of glycolysis, make them more restrictive to the survival of the bacteria (53).

Neutrophils are one of the first cell types recruited to the lung after infection. There, neutrophils can play a protective role either by phagocyte the bacteria or release antimicrobial mediators, cytokines and chemokines, which prevent bacterial growth or promotes recruitment of immune cells (45, 54, 55). Despite of being important to the host defence during the early stages of infection, neutrophils may be detrimental in later stage (56). Indeed, in both humans and mouse models, when the disease is established, higher levels of neutrophils correlate with negative outcomes of TB (57). Due to their highly cytotoxic content and short lifetime, neutrophils are linked to advanced inflammation and tissue damage (56).

Establishing the connection between innate and adaptative immunity, antigen presenting cells (APCs), such as dendritic cells, migrate to the lymph node to prime T cells into differentiation. Specifically, naïve cluster of differentiation 4 (CD4+) T lymphocytes differentiate into T helper 1 (Th1) or Th17 cells, which produce IFN-γ or IL-17, respectively (7, 10, 58). IFN-γ plays a strong protective role in TB, mainly due to the activation of the macrophage microbicidal functions, such as the production of antimicrobial peptides and reactive species of oxygen (11, 58). IL-17 is involved in the recruitment of neutrophils (59, 60). CD4+ T cells play a central role in the immune response to TB, since the lacking of a competent CD4+ T cell response, for instance in HIV infected individuals (61), is associated with increased susceptibility to infection and uncontrolled bacterial growth. Although not so prominent, CD8+ T cells also perform a protective role, mainly due to their cytotoxic granule-mediated function or by their production of proinflammatory cytokines (62).

Immune cells are recruited to the infection site, becoming organized in structures called granulomas (discussed in the next section). At this point, *M. tuberculosis* can be contained in the lung (latent) or disseminate to other organs inflicting disease (active TB) (7). Therefore, the balance in host immune responses is critical to determine the outcome of TB (8, 11).

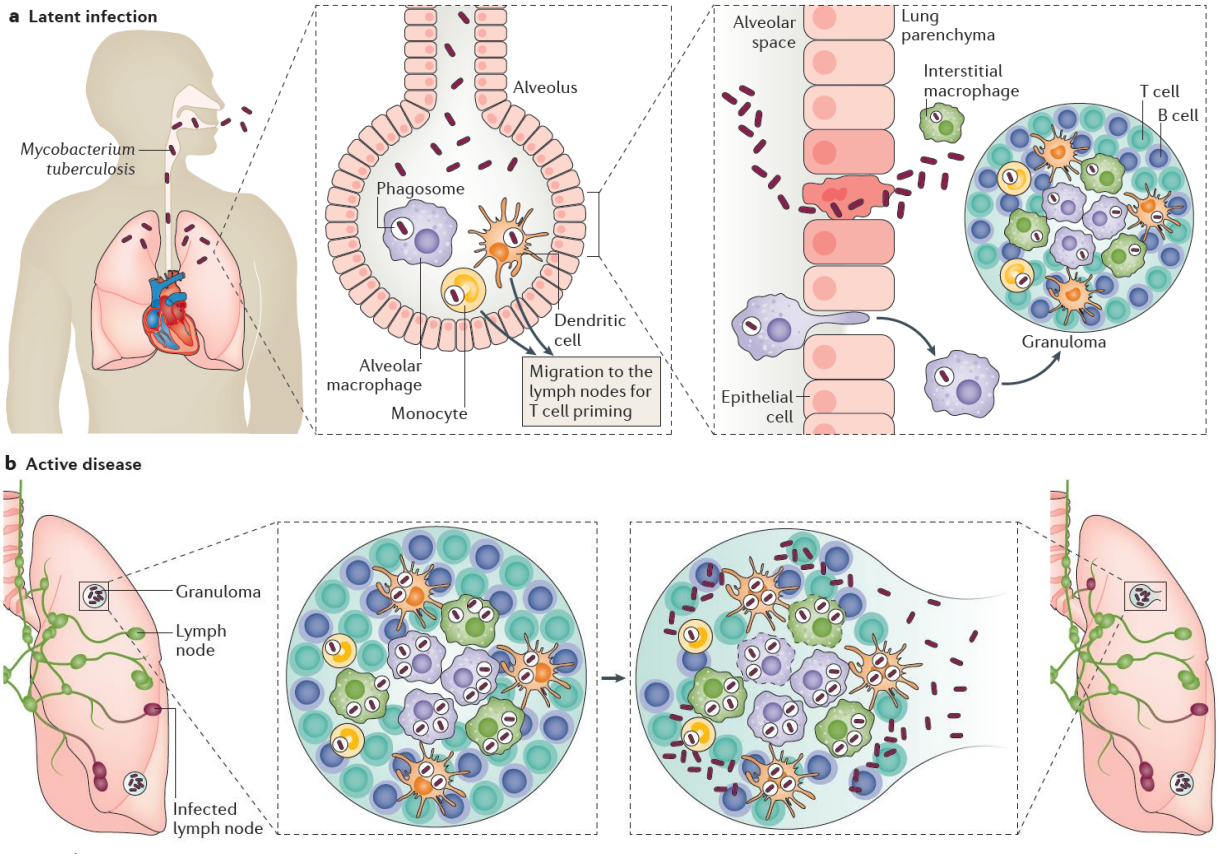

Figure 4. Immune events after infection with *M. tuberculosis* in latent and active disease. Figure from (7).

The Tuberculosis granuloma

The TB granuloma is a multicell structure with high spatial organization, formed at the sites of *M. tuberculosis* infection (**Figure 5**). This pathological hallmark of human TB is constituted by immune cells, such as macrophages, neutrophils, lymphocytes, dendritic cells, natural-killer cells (NK) recruited in response to persistent stimuli (11, 58, 63). Although granulomas can be morphologically diverse, most share a typical organization: a caseum and hypoxic centre, limiting the bacteria in an acellular mass of necrotic debris, surrounded by infected macrophages and innate cells, delimitated by adaptative B and T cells. The granuloma can be surrounded by an outer fibrotic capsule. Macrophages play an important role in the establishment of the granuloma and can present themselves in multiple differentiation forms, such as the epithelioid cells, foamy macrophages, and multinucleated giant cells (11).

Although granulomas are lesions of inflammatory cells that can be detrimental to the lung (58), when balanced, this pathological architecture can be vital to control and restrain the bacteria, preventing progression to active disease. However, granulomas may benefit the pathogen too, given that bacteria persist and continue to replicate inside the granuloma. When the host system is dysregulated, the expansion and disruption of the granuloma can lead to lung cavitation (11). Then, bacteria can escape the granuloma, disseminate through pulmonary tract and potentially be transmitted to other hosts via coughing droplets. Interestingly, the antigens related to T cell activation in *M. tuberculosis* are hyperconserved (32, 64). This constitute an immune strategy for the benefit of the bacteria, since it is necessary a robust immune response to form cavitary lesions, which potentiate the spread and transmission of *M. tuberculosis* (7).

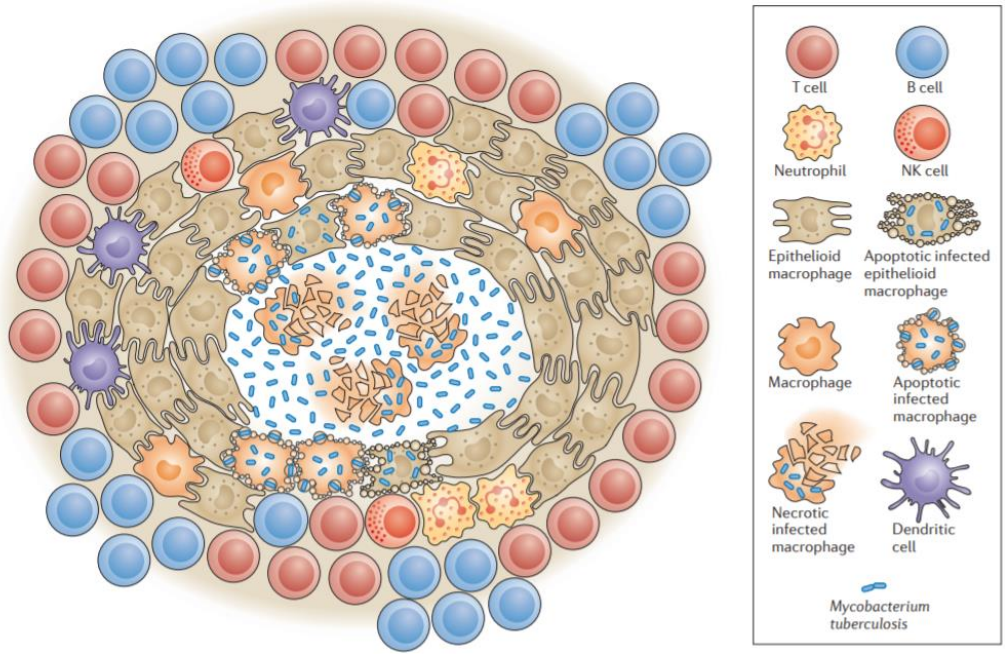

Figure 5. Representation of the composition and organization within a human granuloma. Figure reproduced from (11).

Cytokines in Tuberculosis: focus on Interleucin-1

The immune response to TB relies on the production of several cytokines. Proinflammatory cytokines, such as TNF-α, IL-1β, IFN-γ, IFN-β and IL-17, and the anti-inflammatory cytokine IL-10 are particularly important. Due to the focus of my thesis in

the role of IL-1β during *M. tuberculosis* infection, I will provide a more detailed description of its participation in the protection or pathogenesis of TB.

IL-1 is a pleiotropic and pro inflammatory cytokine belonging to the IL-1 superfamily, which is constituted by several cytokines and membrane receptors. (**Figure 6**). IL-1 comprised two forms: IL-1α that is constitutively expressed in epithelial and mesenchymal tissues and IL-1β which is induced under disease and damage conditions. Macrophages are the predominant IL-1 producers, but this cytokine is also produced by a variety of other cell types, such as neutrophils, lymphocytes, fibroblasts, keratinocytes, epithelial and endothelial cells (65, 66). Furthermore, IL-1 is also expressed in different organs and tissues, including lymphoid organs, lung, liver, kidney and others. Both IL-1β and their agonist, IL-1α, bind to the Interleucin-1 Receptor (IL-1R1), triggering important functions in immunity and inflammation, such mediating the immune response to infection, regulating vascular permeability and angiogenesis. The antagonist IL-1RA, also binds to IL-1R1, then blocking the biological functions of IL-1. This mechanism is used in the treatment of rheumatoid arthritis through the administration of Anakinra (recombinant IL-1RA) (66, 67).

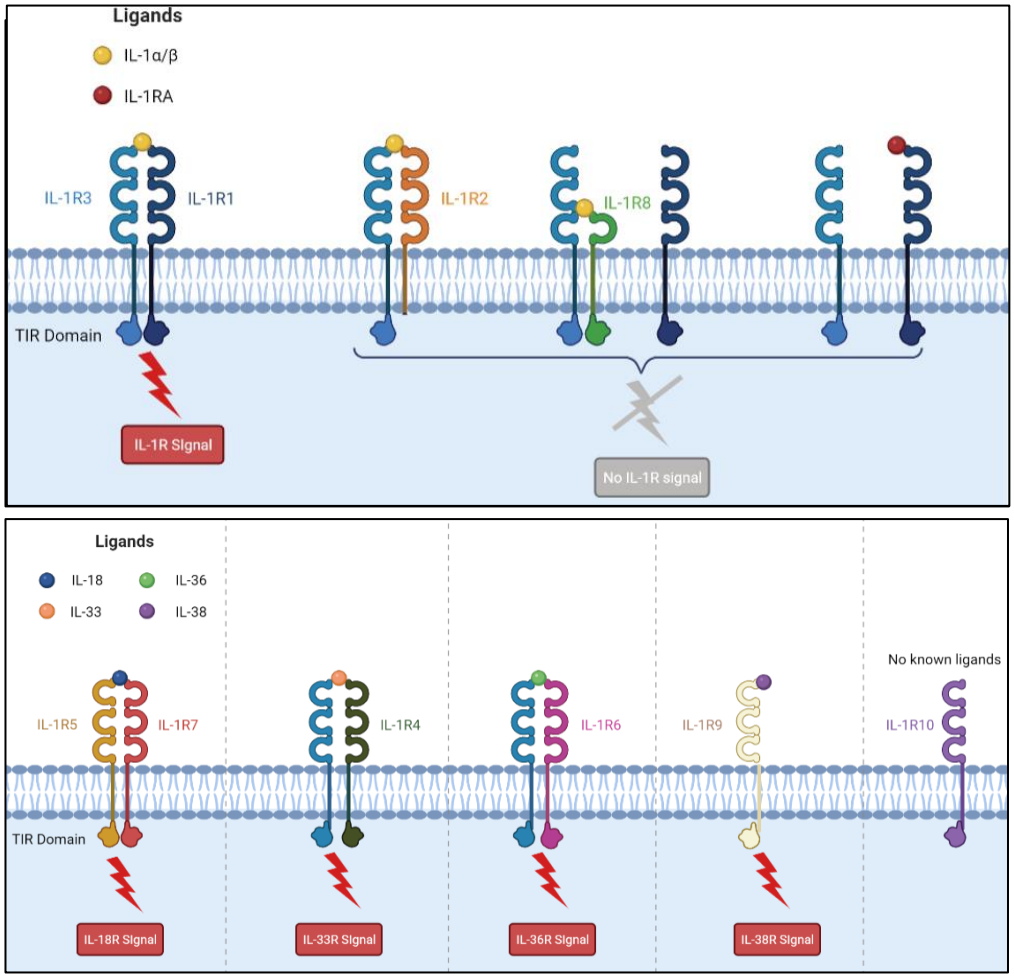

Figure 6. IL-1 superfamily of cytokines and respective membrane receptors. Both IL-1α and IL-1β bind to IL-1R1 and his co-receptor IL-1R3, which triggers a structural change. This interaction promotes a signal transduction cascade through the Toll-Interleucin-1 Receptor (37) homology domain leading to a strong pro inflammatory signal. IL-1 signalling does not occur when: the antagonist IL-1RA binds to IL-1R1 and IL-1R3 is not recruited; IL-1 interact with IL-1R2, which does not possess a functional TIR domain; or when co-receptor IL-1R8 is recruited and blocks the interaction between IL-1R1 and IL-1R3 (panel above). Other members of IL-1 superfamily are shown in the panel below: IL-18R signal requires binding of IL-18 to IL-1R5 and the recruitment of IL-1R7; IL-33R signal requires binding of IL-33 to IL-1R4 and the recruitment of IL-1R3; IL-36R signal requires binding of IL-36 to IL-1R6 and the recruitment of IL-1R3; IL-38 binds to IL-1R9 but the mechanism for IL-38R signaling is still unknown; IL-1R10 has no know ligands. Figure created in Biorender.

The role of IL-1β in Tuberculosis

IL-1β is a cytokine of great importance to the early protection against TB, since several experimental studies in mice show that deficiency in the IL-1 signaling results in rapid establishment of infection, increased bacterial burdens, extensive lung pathology and death (68-74). Upon *M. tuberculosis in vivo* infection, innate myeloid cells are the main source and target of IL-1β action (50, 75). The protection afforded by the IL-1 signaling relies on multiple mechanisms, from the induction of several antimicrobial cytokines, recruitment of immune cells to the local of infection, as well as the production of prostaglandins (particularly PGE2) and reactive oxygen species (ROS) (76).

Although the protective role of IL-1β is indisputable, an excessive production of this cytokine can also be detrimental for the infection control. Whereas it is true that an initial IL-1 response is essential to fight the pathogen, it is also important that this is correctly regulated, especially in later stages, so that it does not leads to inflammatory damage (77). For instance, both in non-human primates and in a susceptible mouse, the administration of Anakinra two weeks post- *M. tuberculosis* infection, as an adjunct to Linezolid treatment, proved beneficial in controlling of inflammation and lung damage (77). This dynamic role of IL-1 has been also demonstrated in other infectious diseases (78), where excessive production leads to inflammatory damage, but too little of this cytokine is insufficient to trigger an immune response to fight off the pathogen (79) .

Regulation of IL-1β during *M. tuberculosis* infection

The production of IL-1β in myeloid cells is regulated at the transcriptional and post transcriptional levels, in which an intermediate inactive form of IL-1β (pro-IL-1β) is formed (65, 80). Regarding *M. tuberculosis* infection, the bacteria is recognized by specific pattern recognition receptors (PRR), particularly by the Toll-like receptor (TLR) 2/6 or Nucleotide Binding Oligomerization Domain Containing 2 (NOD2) (**Figure 7**). This interaction activates an intracellular signaling cascade which culminates in the transcription of the *Il1b* gene through mechanisms involving the signaling molecules ERK, p38 and Rip2 (81). Then, the *Il1b* mRNA exits the nucleus and is translated to pro-IL-1β protein, which needs to be cleaved for the bioactive form IL-1β to be produced.

Biological activation of IL-1β may be achieved through a canonical or a non-canonical mechanism. Canonical activation consists of the assembly of inflammasome components and on the enzymatic action of caspases (69). Non-canonical activation is not well described in the context of *M. tuberculosis* infection, but the processing of pro-IL-1β may be mediated by other molecules, such as other CASP, matrix metalloproteases (MMPs), chymases, elastases, and cathepsins (82).

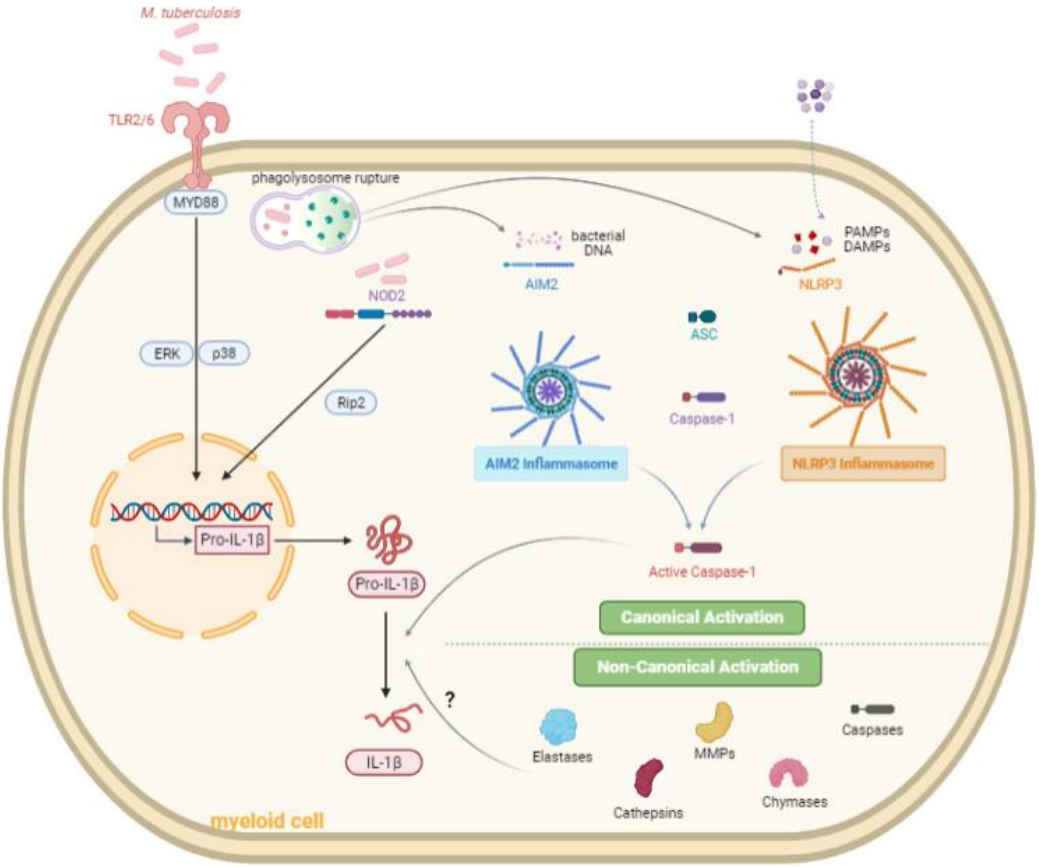

Figure 7. Molecular mechanism leading to IL-1β production in *M. tuberculosis*-infected cells. The recognition of *M. tuberculosis* molecular patterns by TLR2/6 or by NOD2 induces a series of signaling cascades that culminate in the transcription of the IL-1β mRNA. Biological activation of IL-1β requires cleaving of the pro-IL-1β through canonical or non-canonical mechanisms. Canonical activation consists on the assembly of NLRP3 and AIM2 inflammasomes, which are triggered by recognition of PAMPs/DAMPs or bacterial DNA, respectively, resulting from the export of bacterial products from the phagolysosome. The assembly of the inflammasomes leads to the recruitment of CASP1 by ASC. CASP1 becomes activated and cleaves pro-IL-1β into active IL-1β. Non-canonical activation is much less studied in the context of *M. tuberculosis*, but may be mediated by elastases, MMPs, other caspases and chymases. Figure created in Biorender.

Manipulation of IL-1 responses by *M. tuberculosis*

A competent bacterial ESX-1 secretion system is an important virulence factor, determinant for the induction of IL-1 in *M. tuberculosis*-infected cells. As described above, the ESX-1 secretion system also mediates the export of bacterial DNA and RNA from the phagosome into the cell cytosol, thus triggering the production of type I IFNs through cGAS and RIG-I recognition, respectively (83, 84). Thus, the bacterial mechanisms leading to IL-1 production potentiate, at the same time, the synthesis of type I IFN. The pathogen may be able to take advantage of this cross-regulation by manipulating IL-1 levels, assuring its survival and progression of disease (83, 85, 86). Other mechanisms interfer with the inflammasome activation, thus ultimately modulating the secretion of IL-1β, for instance the *M. tuberculosis* protein encoded by the *zmp1* gene was found to prevent inflammasome activation and IL-1β production (**Figure 8**) (87). Mice infected with bacteria lacking *zmp1* displayed higher production of IL-1β, lower bacterial burden in the lungs and enhanced bacterial clearance, resulting in a positive outcome of the disease (**Figure 8**) (87). More recently, differential induction of IL-1β by genetically distinct *M. tuberculosis* clinical isolates was found to associate with disease severity (88). Clinical isolates recovered from patients with mild TB disease consistently induced high secretion of IL-1β in human PBMCs, THP-1 cells and mouse bone marrow-derived macrophages, which related to a stronger activation of the inflammasome (**Figure 8**) (88).

As discussed above, *M. tuberculosis* infection drives a metabolic shift in the macrophage towards glycolysis, which is linked to IL-1β production (89). By upregulating the host production of miR-21, *M. tuberculosis* interferes with *PFK-M*, preventing the glycolytic shift and lowering the production of IL-1β, a process that culminates with enhanced bacterial replication within macrophages (**Figure 8**) (90).

Another example of cross-modulation between metabolism and IL-1 is seen in macrophages infected with *M. tuberculosis* strains carrying a rifampicin drug resistance mutation. The presence of the mutation altered the expression of *M. tuberculosis* lipid wall components, impacting the macrophage metabolic reprograming, bypassing the IL-1 signaling, driving the induction of IFN-β and inhibiting glycolysis (**Figure 8**) (91).

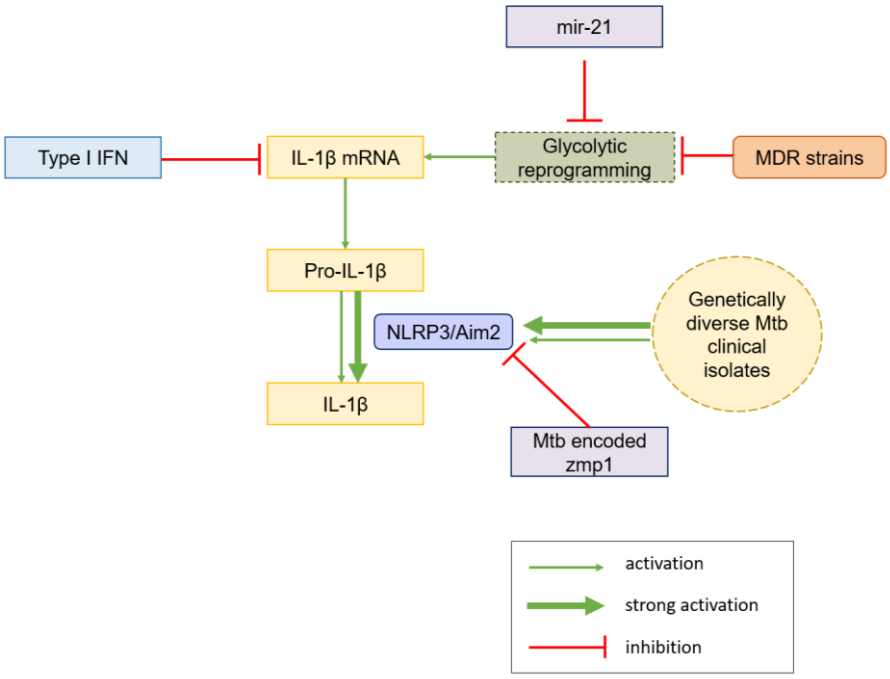

Figure 8. Mechanisms of pathogen manipulation of IL-1 during *M. tuberculosis* infection. Since both IL-1 and type I IFN are activated through similar mechanism, bacteria can beneficiate from this cross regulation between to ensure their survival. Another mechanism relies on the production of the protein encoded by zmp1 gene that interferes with the NRLP3/AIM2 inflammasome, ultimately regulating IL-1 levels. Genetically diverse *M. tuberculosis* strains can also modulate the levels of IL-1 through differential activation of the inflammasome. Regarding, glycolytic reprogramming, both production of mir-21 or even *M. tuberculosis* strains carrying a rifampicin drug resistance mutation, inhibit the glycolysis shift, lowering the IL-1 production.

Aims

Recently, our group has described that *M. tuberculosis* clinical isolates associated with mild (4I2) or severe (6C4) TB in humans induce high or low levels of IL-1β, respectively, in human PBMCs, THP-1 cells and mouse bone marrow-derived macrophages. Clinical isolates recovered from patients with mild TB exhibited a stronger activation of the inflammasome, while those recovered from severe TB escaped macrophage cytosolic surveillance systems, such as cGAS and the inflammasome (44). Therefore, the characteristics of the infecting bacteria may potentially explain why some patients develop a more severe disease (8). To tackle this interesting question, I proposed to unveil the *in vivo* impact of the aforementioned immune evasion mechanism on the establishment and progression of the infection, using the mouse model of experimental TB (**Figure 9**). To attain this aim, my thesis is divided in the analysis of two specific goals:

1. To compare the progression of *in vivo* infection in mice infected with different *M. tuberculosis* clinical isolates under study in the host lab (isolates 4I2 and 6C4) or with a hypervirulent control strain (HN878).

2. To decipher the impact of cell-specific IL-1 receptor signalling on the pathogenesis of TB, using a IL-1R1 knockout mice for myeloid cells (IL-1R^{flox} LyzM.Cre).

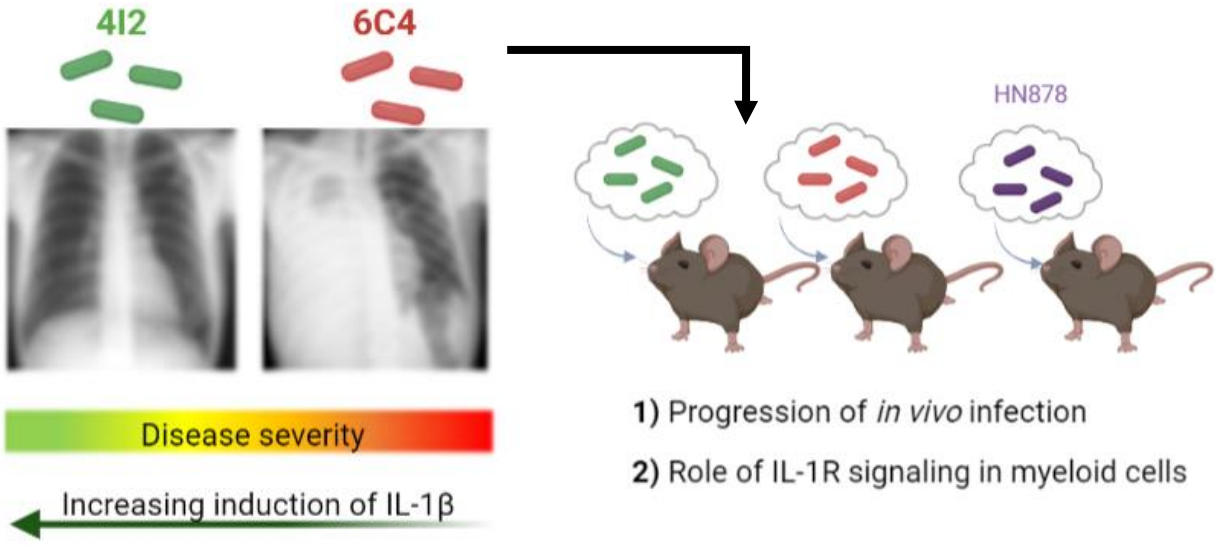

Figure 9. Representation of *M. tuberculosis* clinical isolates recovered from patients with different severities of TB and differential IL-1β levels. X-rays show distinct pulmonary manifestations in human patients infected with 4I2 and 6C4 strain. Clinical isolates were used to infect mice via aerosol. Figure created in Biorender.

Chapter II. Methodologies

Ethics Statement

This project uses the mouse model of aerosol infection with *M. tuberculosis.* Mice were bred and maintained at i3S (AAALAC accredited animal house). Genetically modified strains were used. We adhere to the 3Rs Principle. Mice exhibiting signs of distress were euthanized by CO_2 inhalation (refinement). Animal experiments were performed in the absence of alternatives (replacement). Groups were tested in G*power to minimize the number of animals (reduction). Animal experiments complied with the EU Directive 2010/63/EU, National legislation, and local ethics committees. The PI is FELASA C certified.

Animal model

Eight to twelve-weeks-old male or female C57BL/6 WT or IL-1R1^{flox} LyzM.Cre were housed under contention conditions in the Animal Biosafety Level 3 (ABSL3) facility at i3S. Mice were kept under controlled temperature and humidity, with food and water *ad libitum* and humanely euthanized by CO_2 asphyxiation or by intraperitoneal injection of sodium pentobarbital.

To study the impact of the IL-1R1 sinaling in the myeloid compartment, conditional knock out mice were obtained through the Cre/lox recombination technology (92). The engineered modified mice have the *Il1r1* gene flanked by loxP sites (flox/flox), which can be deleted by Cre recombinase expression in specific cells or tissues. In this study, mice with deficiency in the IL-1R1 in myeloid Lysozyme M cells (LyzM) (93, 94) were generated. This process and the maintenance of IL-1R1^{flox} LyzM Cre mice were performed by the animal facility at i3S.

Aerosol infection

Mice were infected with *M. tuberculosis* via aerosol, to mimic the natural route of entry, using an inhalation exposure system (Glas-Col apparatus) to nebulize a bacterial suspension into the lungs. Mice were infected with clinically relevant and well-characterized *M. tuberculosis* isolates selected from TB patients presenting mild (4I2) or severe TB (6C4), as well as a hypervirulent control strain (HN878). High dose delivered more than 500 CFU of viable bacteria to the lung. This is a well-established technique in

our laboratory, that has already been used in other studies from the group (42, 55). Infection dose was determined by colony forming units (CFU) count in the lungs of 3–5 mice, 3 days after infection.

Animal welfare

The progression of infection in mice were investigated over time. The general welfare of the infected animals was monitored through a score sheet by evaluating their weight loss (until the maximum 20% of weight loss), respiratory capacity, anemia and reaction to stimuli over time (**Table 1**).

Table 1: Parameters established in an infection score sheet to evaluate the animal welfare.

Parameter	Score (0-16)
Appearance	Normal to above and eyes half closed (0-4)
Behaviour	Normal to restless or very still, not alert (0-3)
Hydration	Normal or abnormal skin pinch test (0 or 5)
Respiratory movement	Normal rate to marked abdominal breathing and cyanosis (0-4)

Organ harvesting and processing

At specific time points (days 15, 30, 45 and 60 or 90 post infection), infected and non-infected mice were euthanized by CO_2 inhalation or, in experiments where we collected bronchoalveolar lavage (BAL), by intraperitoneal injection of a lethal dose of sodium pentobarbital. BAL is isolated by inserting a catheter in the trachea of mice, injecting a saline solution (FACS buffer), and then, retrieving the maximum fluid. The blood in the lung was pre-cleaned by perfusing PBS through the heart. For each animal, lungs, liver, and spleen were harvested and processed on the same day, to study the site of infection (lungs) and the bacterial dissemination to other organs (spleen and liver). The organs were homogenized into a cellular suspension in complete DMEM medium (10% Fetal bovine serum, 1% sodium pyruvate, 1% HEPES and 1% L-glutamine; cDMEM) (GIBCO). For the lungs of each animal, digestion with 2 ml of Collagenase D 0,1% (prepared in HBSS 1X) was performed to prepare single cell suspensions with integrity of cell-surface proteins. Cell suspensions were filtered to remove possible aggregates and 1ml was used for CFU determination. For the lysis of red blood cells, lung suspensions were incubated with ACK solution for 5 minutes. Cells were counted using a Neubauer chamber and diluting cells in Trypan blue stain 0,04%. Blue dyed cells are non-viable

cells, so were excluded. Cell suspensions were used for bacterial burden determination, RNA analysis and flow cytometry.

CFU enumeration

Bacterial burdens in the lung, liver, spleen and BAL were performed by CFU enumeration. After organ processing, *M. tuberculosis* are released from the cells using a saponin 10% solution; then, serial 1:10 dilutions were prepared in PBS, plated in 7H11 enriched with OADC plates and cultured at 37ºC. *M. tuberculosis* is a slow growing bacteria, so, colonies were counted after 3 weeks of incubation.

Histology and morphometric analysis

From each animal, the right upper lung lobe was excised and fixed in 4% phosphate-buffered formalin (PFA) for 1 week, whilst the other four lobes were processed as described above. Lung tissues were embedded in paraffin, cut into 3 µm-thickness sections, and stained with Haematoxylin-Eosin (H&E) or Ziehl-Neelsen (ZN) in "Histology and Electron Microscopy" facility at i3S. Images were acquired with a NanoZoomer 2.0-HT Whole Slide Imager, Digital Pathology Slide Scanner.

To study the dynamics of pulmonary lesions formation during infection, tissue histology was morphometrically analyzed. Qualitative and quantitative analysis of lung pathology were performed. For qualitative analysis, through H&E sections, pathological features were scored using the scale parameters present in **Table 2**.

Table 2. Lesion score established for the evaluation of histopathological features in the lung.

Score	Description
0	No lesions
1	Few minor lesions
2	Intermediate or multiple minor lesions
3	Multiple intermediate lesions
4	Extensive and severe lesion

Quantitative morphometric analysis of lung pathology was performed using two softwares: Interactive Learning and Segmentation Toolkit (Ilastik) and CellProfiler Analyst software (version 3.1.5). Firstly, probability maps for whole lung tissue and lesion areas were obtained in ilastik, after training manually the software with several lung

images (**Figure 10**). Probability maps were then analyzed in CellProfiler, which creates final overlapping images, where it is possible to distinguish and calculate the area of the whole tissue (green line), lesion and cell infiltrates (red lines) and lung holes (blue lines) (**Figure 10**). To the whole lung area was subtracted the area occupied by the holes. Percentage of lesion per lung was calculated by the quotient between the area of cell infiltrates and the whole lung area.

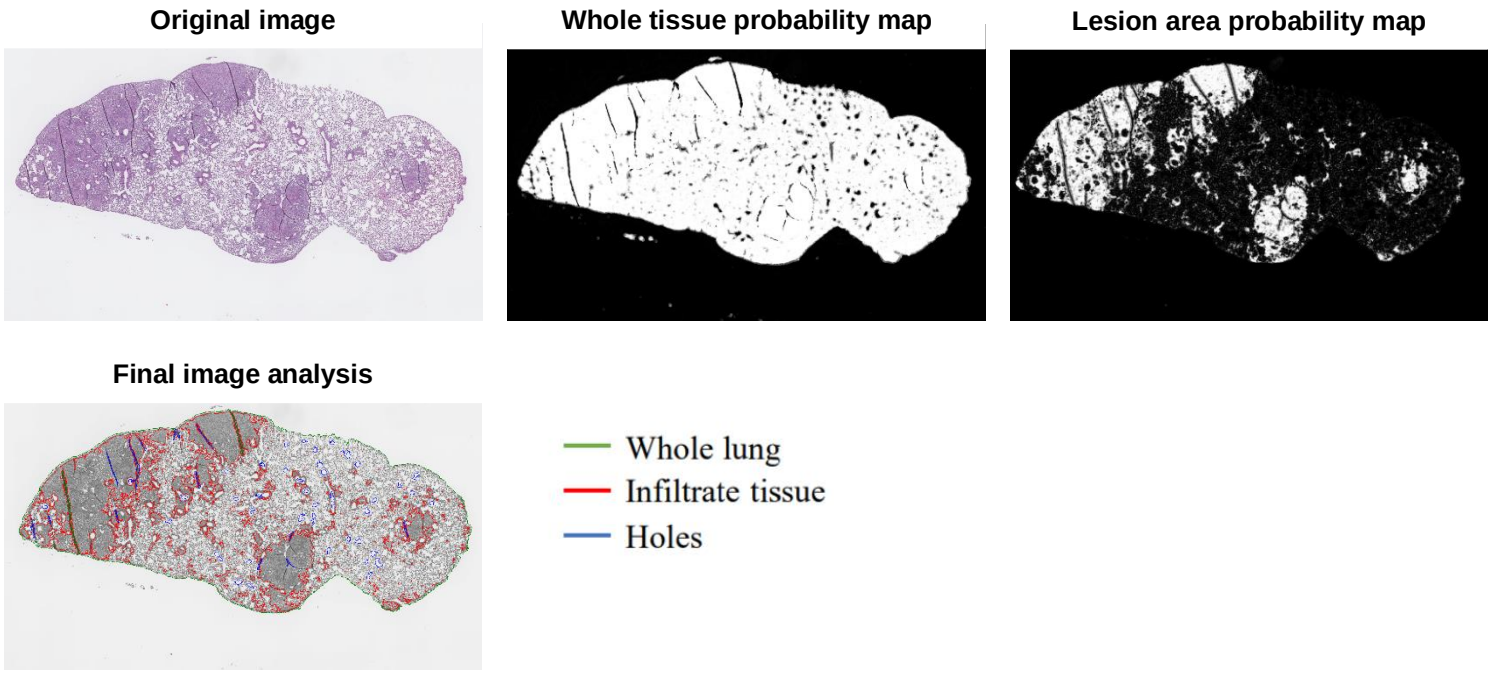

Figure 10. Representative images obtained by morphometric analysis of lung histopathology. Whole tissue and lesion probability maps show background in black, and the lung tissue and cell infiltrates in white, respectively. Whole lung tissue (green line), lung infiltrates (red line) and lung holes (blue line) are delimited in the final image analysis.

mRNA analysis by real-time quantitative PCR

RNA was extracted from $1x10^6$ cells of mouse lungs using with TRIzol Reagent (Invitrogen), according to the manufacturer's instructions. mRNA was converted in cDNA using the ProtoScript First Strand cDNA Synthesis kit (Biolabs). Gene expression was quantified by real-time quantitative PCR (qPCR), using SYBR Green dye and gene specific oligonucleotides, and normalized to ubiquitin mRNA levels. The analyses were performed using the comparative CT method ($2^{-\Delta\Delta Ct}$).

Characterization of the immune cell populations by Flow Cytometry

To evaluate the dynamics of the immune response, such as immune cell recruitment and infiltration to the site of infection, cell populations (myeloid and lymphoid) were analyzed by multiparametric flow cytometry. Mouse BAL and lung cells were stained for surface antigens for 30 min (4 °C) and fixed for 20 min in 4% of PFA. Dead cells were excluded using Zombie Green (Biolegend) viability dye. Cells were stained with the appropriate antibody mixes, showed in **Table 3**. Samples were acquired on a BD FACS Canto II and data were analyzed using FlowJo software version 10.1.r7.

Table 3. Antibody used in flow cytometry analyses, respective dilution and clone.

Antibody	Conjugate	Dilution	Clone
CD11b	APC	1:200	M1/70
Ly6C	Pacific Blue	1:400	RB6-8C5
Ly6G	PercpCy5.5	1:400	1A8
CD11c	PECy7	1:200	HL3
CD45	PE	1:400	2D1
CD3	PercpCy5.5	1:100	UCHT1
CD4	APC	1:200	OKT4
CD8	PECy7	1:200	SK1
CD19	APCCy7	1:100	TS2/16

Statistical analysis

Data were analyzed using GraphPad Prism software, version 7.04. Student's t test was used to determine differences between two different groups and one-way ANOVA when more than two groups were included. Data was checked for normality and log normality. Differences were considered significant for $p \leq 0.05$ and represented as follows: *$p \leq 0.05$; **$p \leq 0.01$; ***$p \leq 0.001$ and ****$p \leq 0.0001$.

Briefly, **Figure 11** shows a summary of the methodologies used in this project and the setup of the experiments developed.

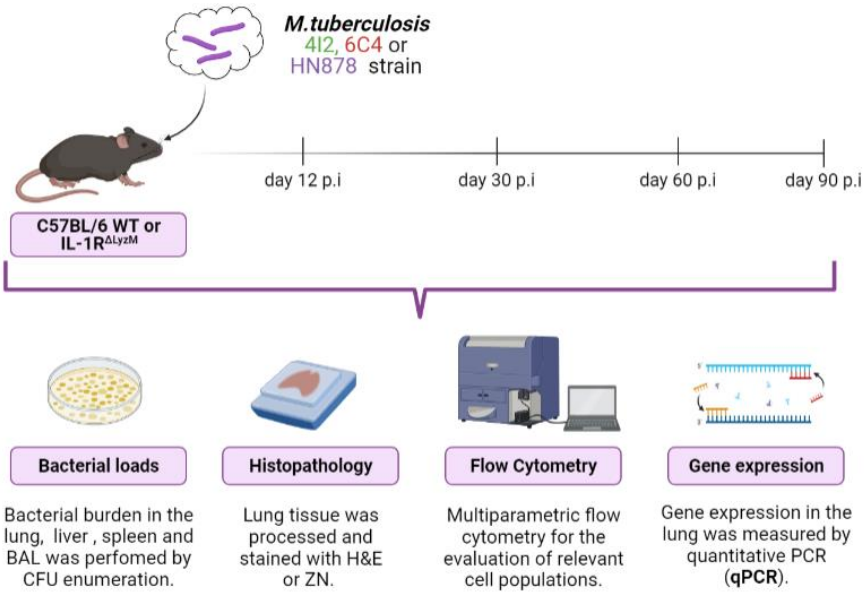

Figure 11. Summary image of methods used to perform the *in vivo* experiments in this project. Figure created in Biorender.

Chapter III. Results and discussion

Part of this work was presented as:

1. Poster on the 14ª Edition of “Encontro de Investigação Jovem da Universidade do Porto” (5 to 7 May 2021) - Interleukin-1 manipulation by *Mycobacterium tuberculosis*: impact to the infection establishment and progression (**Rute Gonçalves** et al.).
   1.1 Work distinguished by the Scientific Committee of IJUP’21

2. Poster on the VI Edition of “Jornadas da Bioquímica da Universidade do Porto” (7-10 May 2021) - Interleukin-1 manipulation by *Mycobacterium tuberculosis*: impact to the infection establishment and progression (**Rute Gonçalves** et al.).

Impact of *M. tuberculosis* diversity for the progression of infection and disease establishment in the mouse model

Genetic diversity of *M. tuberculosis* is now accepted to play an essential part on host-pathogen interactions, possibly translating into different disease manifestations. Recent work from our group highlighted a relation between *M. tuberculosis* genetic diversity, TB severity in humans and the modulation of the macrophage IL-1β response by the infecting pathogen (44). From this previous work, two *M. tuberculosis* isolates were selected: isolate 4I2, associated with mild TB and high IL-1β response; and isolate 6C4 associated with severe TB and low IL-1β response. In the first part of my thesis, I used these two isolates to study the impact of *M. tuberculosis* diversity during an *in vivo* infection and decipher if the outcome differences in humans were recapitulated in the mouse model. Additionally, a well-studied hypervirulent *M. tuberculosis* strain (HN878) (95, 96) was included in the study. 4I2 and 6C4 are clinical isolates from lineage 4, collected from patients with similar age. HN878 is a lineage 2 strain associated with reduced survival of infected mice when compared to other clinical isolates. These three isolates of *M. tuberculosis* were used to infect C57BL/6 mice via aerosol, using a high dose of bacteria (**Figure 12**). The infection conditions were based on a previous report showing that C57BL/6 mice infected with high dose of *M. tuberculosis* displayed a blood immune signature that recapitulated the one seen in human patients (97).

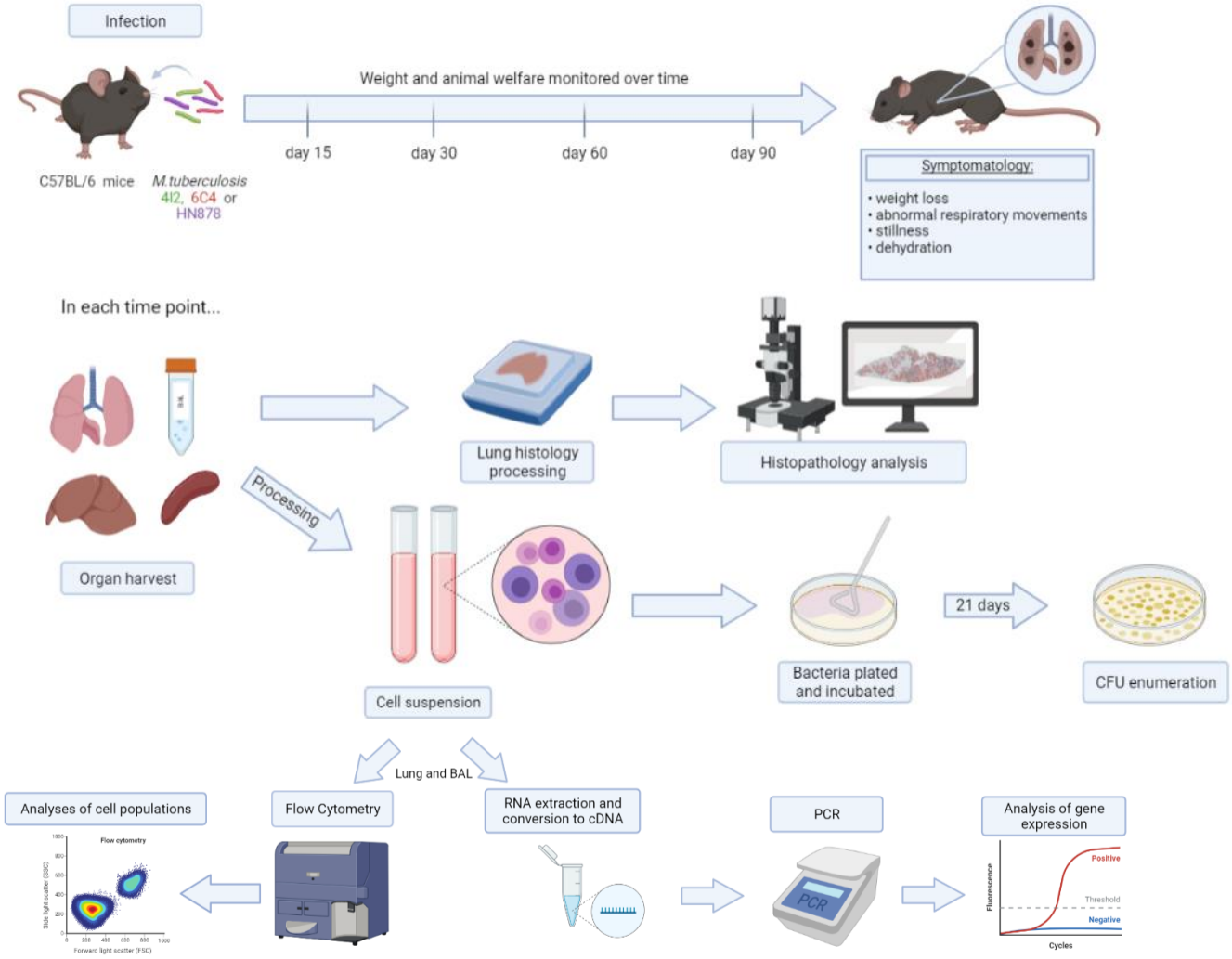

Figure 12. Experimental setup for the evaluation of disease and immune response in mice infected via aerosol with the Mtb clinical isolates 4I2, 6C4 or HN878. During the experiment, animals were monitored through the evaluation of weight loss and symptomatology. In certain time points, lung, BAL, liver and spleen of each animal were harvested. Histological images of the lung were obtained, and histopathology were evaluated through a relative disease score and morphometric analysis. Organs were processed into a cell suspension and bacteria were cultured to obtain CFU enumerations. Lung and BAL cell suspensions were analysed by flow cytometry. Relative gene expression in the lung was evaluated by real time qPCR, after RNA extraction and conversion to cDNA. Figure created in Biorender.

Evaluation of the infection progression and disease severity

C57BL/6 mice were infected with high doses of *M. tuberculosis* 4I2, 6C4 or HN878 and followed over time to define the dynamics of disease progression, the peak of disease and the TB severity. Infections with isolates 4I2 and 6C4 were monitored over 90 days, whereas those with HN878 were monitored for 47 days. Two independent experiments with *M. tuberculosis* HN878 were carried out with similar goals, in which one evaluated the survival of infected mice and the other was designed for the study of infection in two time points (day 15 and 30 post infection). During the entire experimental period, we monitored the survival and general welfare of infected mice as compared to control non-infected mice. At specific time-points, we investigated more specific parameters, namely the bacterial burden and histopathology in the lung, and the dissemination.

Mice infected with the clinical isolates 4I2 and 6C4 either maintained or gained weight over time **(Figure 13A)**, surviving throughout the 90 days of experiment (**Figure 13B)**. These animals did not present any symptomatic manifestation, such as marked respiratory movements and abnormal behaviour or appearance, showing a total disease score of zero in the animal welfare score sheet (**Figure 13C**). In general, the results for mice infected with *M. tuberculosis* 4I2 or 6C4 are very similar to non-infected mice.

In contrast, *M. tuberculosis* HN878 infected mice showed a sharp decrease on their weight starting on day 21 post-infection, which led us to monitor weight variations more often in this case **(Figure 13A)**. Furthermore, 50% of mice infected with *M. tuberculosis* HN878 succumbed to disease before day 30 **(Figure 13B)**. These mice had to be humanely euthanized when their percentage of weight loss was above 20% or when they began to display severe symptoms, in which dehydration, slower movements and no reaction to human touch were predominant. *M. tuberculosis* HN878-infected mice that did not survive to infection were those showing a very high disease score as soon as day 25 post infection, while those with less disease score and reduced weight loss coped with the infection until the end of the experiment (**Figure 13C**).The results for *M. tuberculosis* HN878 infection are in line with other studies (55, 96) that showed that a relevant percentage of HN878-infected mice die, whilst others recover their weight and survive.

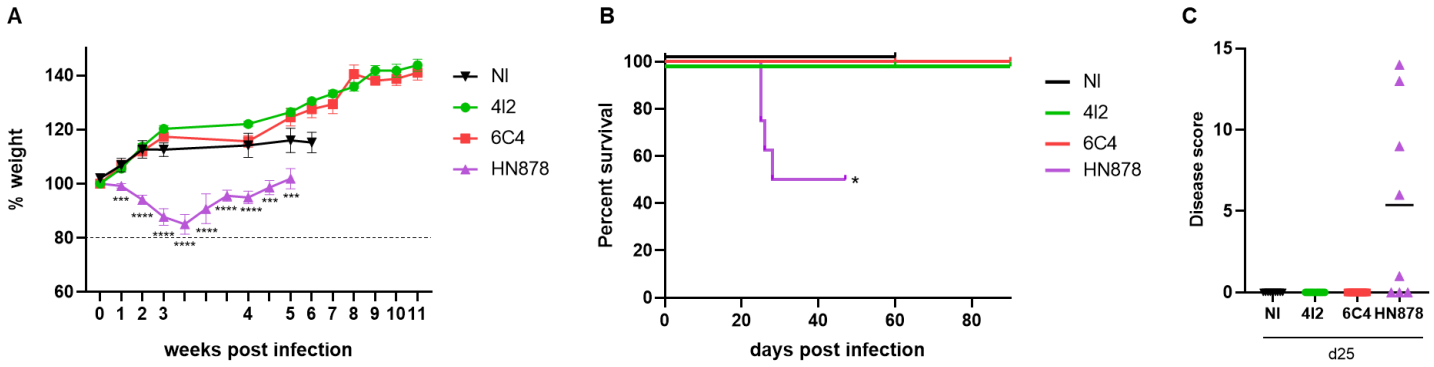

Figure 13. Survival and general welfare of mice infected with high doses of *M. tuberculosis* 4I2, 6C4 or HN878, compared to control non-infected mice (NI). The weight of the animals was monitored over time **(A)** to determine survival curves **(B)**. In **A** the dotted line at 80% indicates the minimum weight a mouse can achieve before being euthanized. **(C)** Disease score presented for day 25 post infection (d25). In **A** each dot represents the Mean ± SEM and in **C** each dot represents an individual mouse. Statistical analysis was performed using multiple t-test **(A)** and with a log-rank (Mantel-Cox) test for the Kaplan Meyer curve **(B)**. *p < 0.05; ***p < 0.001; ****p < 0.0001.

Collectively, our findings position *M. tuberculosis* strain HN878 as more virulent than the clinical isolates 4I2 and 6C4, which at the overall level did not appear to modulate disease severity. Importantly, in the human patients infected with *M. tuberculosis* 4I2 and 6C4 the differences in TB severity were mainly dictated at the pulmonary level (9, 44). Thus, we next investigated the progression of the infection with either isolate in terms of lung bacterial burden and pathology.

To further evaluate the progression and impact of the infection, bacterial burden in lungs, was determined by CFU enumeration at different time points. For days 15 and 30 post infection, mice infected with *M. tuberculosis* isolate 6C4 presented higher bacterial loads in the lung than those infected with isolate 4I2 (**Figure 14A**). After day 30, while the lung bacterial burden for 4I2 infections continues to increase, reaching a maximum burden at 90 days post infection, bacterial loads for 6C4 infections stabilize (**Figure 14A**).

For a more extended analyses of bacterial burden, including in other organs and with isolate HN878 as a control, we focused on day 30. Both in the lung tissue and BAL, HN878 infection resulted in the highest bacterial burdens (**Figure 14B-C**), which is in line with a more hypervirulent profile for this strain. Although not statistically significative, for this time point, we detected higher values of CFU in the liver of mice infected with 6C4 than with 4I2 (**Figure 14D**). In contrast, 4I2 infection led to increased bacterial loads in the spleen compared to 6C4 infection (**Figure 14E**). Of note, these are preliminary data

that need to be repeated with a higher sample size, in order to explore the dynamics of bacteria dissemination in these infections. In fact, the tendency observed in the liver was expected since it was in line to what happen in the lung, but the results for the spleen were surprising and require more investigation, if validated. Furthermore, we may include in future experiments other time points and a parallel with HN878.

.

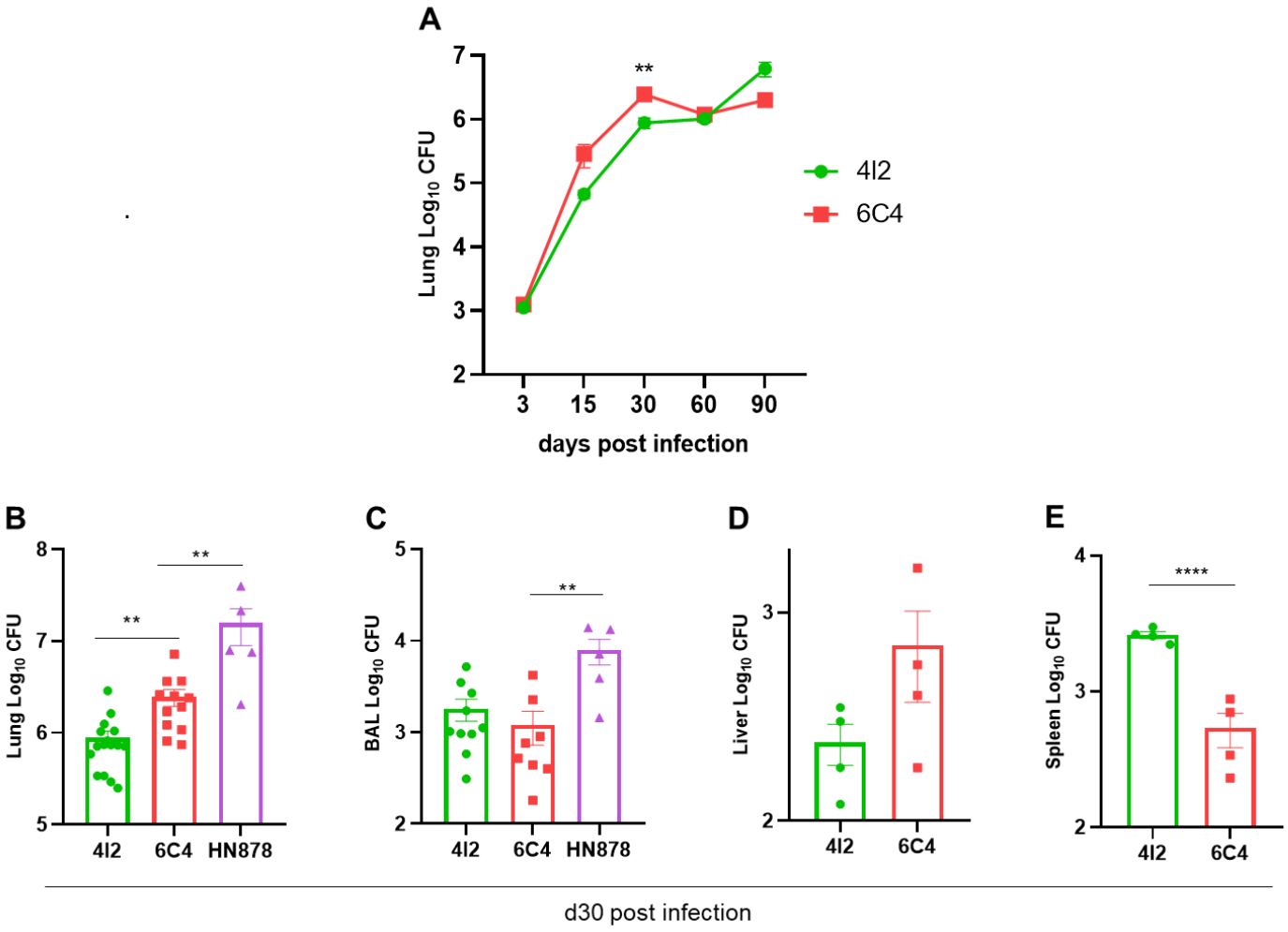

Figure 14. Bacterial loads in the lung, BAL, spleen and liver of C57BL/6 mice infected with 4I2, 6C4 or HN878. **(A)** Evolution of bacterial burden in the lung of mice infected with 4I2 and 6C4 isolates throughout different time points. For day 30 post infection, differences in the CFU count for the lung are highlighted **(B)**, together with bacterial loads in BAL **(C)**, liver **(D)** and spleen **(E)** for the 4I2 and 6C4 infections. In **A** each dot represents the Mean ± SEM and in **B-E** each dot represents an individual mouse and Mean ± SEM are represented for each group. Statistical analysis was performed using multiple t-test **(A)** and unpaired t-test **(B-E)**. **p < 0.01; ****p < 0.0001.

Another important way to assess pulmonary disease severity is the evaluation of the histopathology of infected lungs. Temporal development of lesions is shown in **Figure 15** for the 4I2 and 6C4 infections. At day 15 post infection, where predominantly the innate immunity is triggered, mice infected with either *M. tuberculosis* isolate 4I2 or 6C4 displayed lung histology features that were very similar to non-infected mice. Contrarily, at day 30 post infection, where adaptative immunity is already actively responding, lesions in both infections were prominent. At this stage, lesions were formed by infiltrates of mononuclear cells and lymphocytes, with no level of organization (**Figure 15A**). At day 60 post infection, both infections resulted in a progress in lung pathology, with extensive areas of cell infiltrates and areas of necrotic debris. At day 90 post infection, whereas the majority of mice infected with 6C4 show similar or more mild lesions compared to day 60 (**Figure 15A**), with less lesions scores (**Figure 15B**) and %Lesion (**Figure 15C**), 4I2 infected lungs present larger areas of infiltrates than the previous time point. Although the experimental sample size is reduced in certain time points (n=4 for each infection at day 90), it is possible to observe a tendency, in which 4I2 infection seems to have a slower progression of infection, with development of severe lesions at later time points than 6C4.

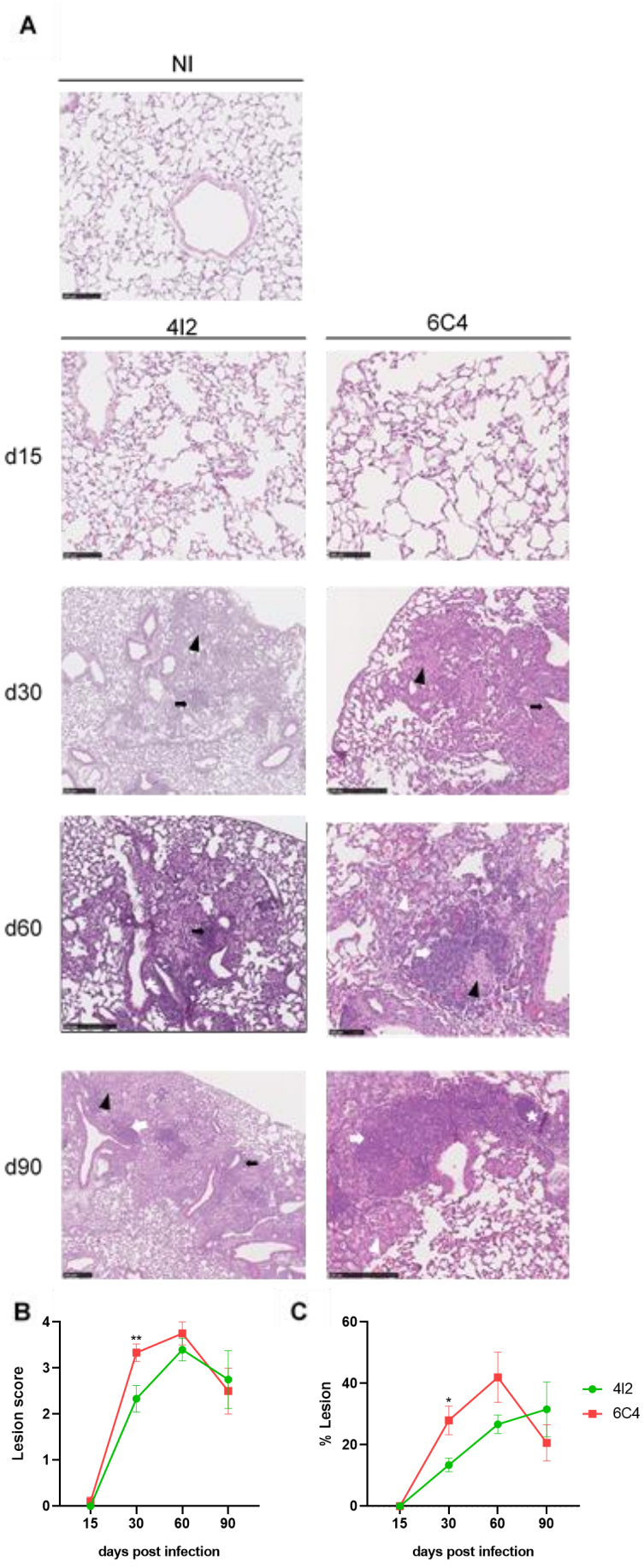
A
NI
4I2
6C4
d15
d30
d60
d90
B
Lesion score
days post infection
C
% Lesion
days post infection
4I2
6C4

Figure 15. Evolution of lung pathology over time for the *M. tuberculosis* 4I2 and 6C4 infections. **(A)** Representative images of lung stained with H&E are showed for each time point and each infection. Lung pathology was evaluated qualitatively **(B)** and quantitatively **(C)**. Pathologic features were analysed and evaluated through a relative lesion score attributed **(B)**. Histopathology was defined as the percentage of cell infiltrates/lesion per lobe (%Lesion), upon H&E staining and morphometric analysis **(C)**. Black Arrowheads point to macrophage infiltrates, white arrowheads point to foamy macrophages, white stars point to bronchiolar debris, black arrows point to perivascular lymphocytes and white arrows point to peribronchiolar lymphocytes. Scale bars for NI and day 15 correspond to 100 µm and for the other time points correspond to 250 µm. In **B-C** each dot represents the Mean ± SEM. Statistical analysis was performed using multiple t-test **(B-C)**. *p < 0.05; **p < 0.001.

We next focused on day 30 post infection, which is the time point showing most differences between strains. Two lesion types could be distinguished depending on the *M. tuberculosis* isolate: 4I2 and 6C4 infected mice exhibited cellular lesions with mixed mononuclear cell composition, such as lymphocytes and macrophages (**Figure 16A**); however, HN878 infection led to an uncontrolled lesion with substantial necrotic areas (**Figure 16A**). Perivascular and peribronchiolar lymphocytes were observed across the three infections, normally surrounded by macrophages and by some neutrophil infiltrates (**Figure 16A**). In general, lungs from mice infected with isolate 4I2 presented more localized and contained lesions, as compared to mice infected with isolate 6C4 (**Figure 16A**). Furthermore, less infiltrates and cellular debris were encountered in 4I2 infected lungs (**Figure 16A**). Although present in most lungs, neutrophilic infiltrates were more common in the case of 6C4 infection, which is compatible with the observed increased lung damage seen in this infection and the over inflammation associated with neutrophils in TB (46, 55). These results illustrate a higher histopathology severity associated with 6C4 infections as compared to 4I2 ones, which is compatible to what was observed in the x-rays of the corresponding TB patients (44). As expected, HN878 induced the most pronounced pathology, where visible large necrotic areas with accumulation of cells with nuclear fragmentation (karyorrhexis), dense inflammation and, occasionally, presence of edema, were all observed. Extracellular bacteria seems to concentrate within necrotic lung lesions (**Figure 16A**). Moreover, in the largest magnification it was possible to observe that lymphocytic infiltration is more delimited in the case of HN878 infection (**Figure 16A**). In more quantitative terms, infection with the isolate 6C4 resulted in more severe (**Figure 16B**) and larger lesions (**Figure 16C**) than the observed in 4I2 infection,

but with minor severity and area than lesions resulting from HN878 infection (**Figure 16B-C**).

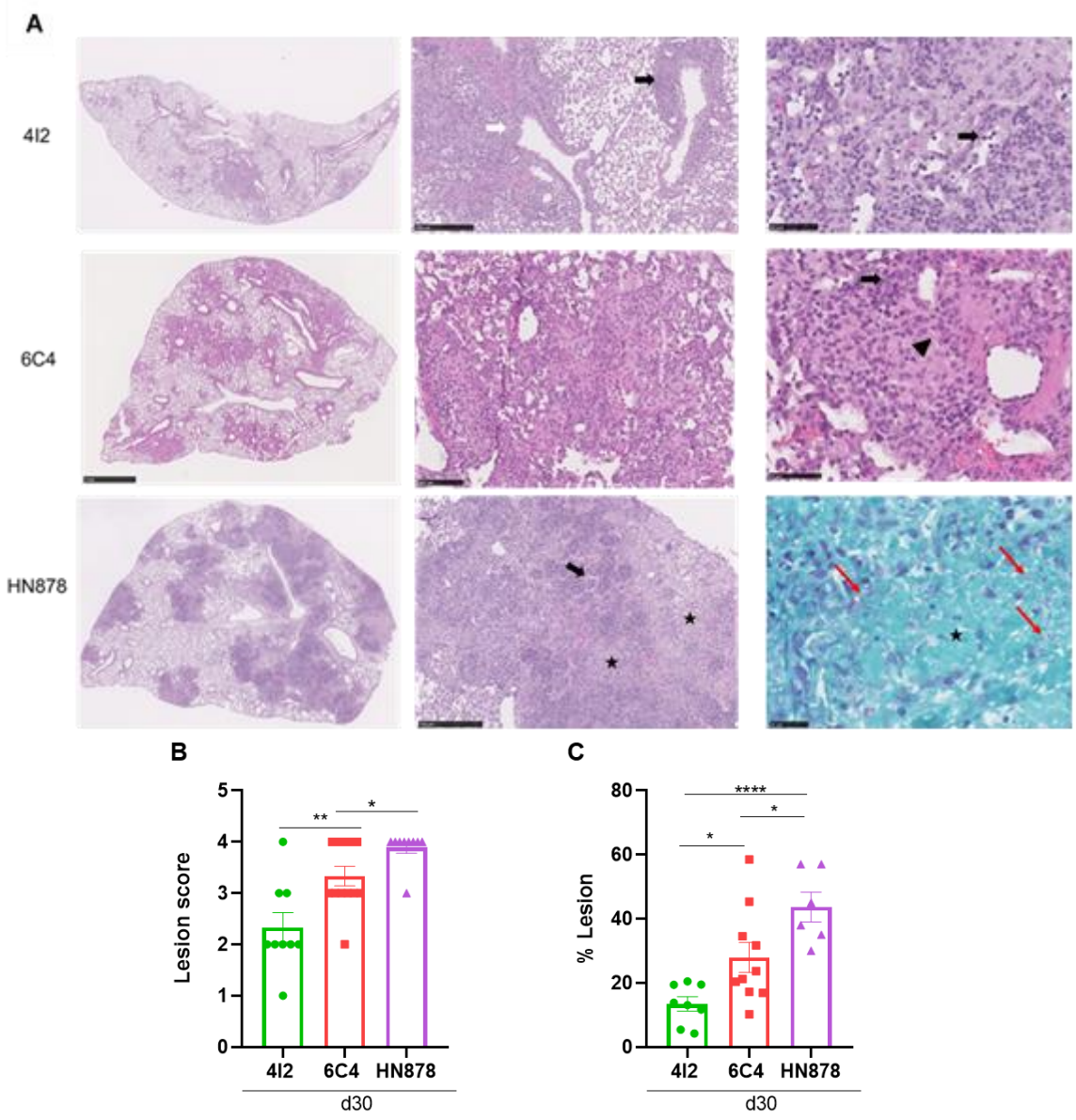

Figure 16. Histopathology of the lung at day 30 post infection for the *M. tuberculosis* isolates 4I2, 6C4 and HN878. **(A)** Representative images of lung stained with H&E and one picture of lung stained with ZN are shown. Lung pathology was evaluated qualitatively **(B)** and quantitatively **(C)**. Pathologic features were analysed and evaluated through a relative lesion score attributed **(B)**. Histopathology was defined as the percentage of cell infiltrates/lesion per lobe (%Lesion), upon H&E staining and morphometric analysis **(C)**. Black stars point to intra-alveolar necrosis, black arrows point to perivascular lymphocytes, white arrows point to peribronchiolar lymphocytes, black arrowhead point to neutrophils, red arrows point to *M. tuberculosis* acid-fast bacilli stained in purple. Scale bar corresponds to 250 µm (middle column), 50 µm (right column H&E) and 25

µm (ZN staining). In **B-C** each dot represents an individual mouse and Mean ± SEM are represented for each group. Statistical analysis was performed using unpaired t-test **(B-C)**. *p < 0.05; **p < 0.01; ****p < 0.0001.

In all, the data presented so far show a rapid establishment and progression of HN878 infections, followed by those with 6C4 and lastly, those with 4I2. This experience allowed us to establish the peak of disease for each *M. tuberculosis* strain, which was important to proceed the study. 4I2 infections continue to increase severity throughout the time points, with maximum bacterial loads and pathology of the lung at day 90. In contrast, at day 60 post infection, 6C4 infected lungs reach a peak of severity, presenting severe and extensive lesions occupying the majority of the lung. By day 30 post infection, HN878 already causes severe and necrotic lesions in the lung, explaining the respiratory difficulty, and, consequently, one of the reasons why mice started dying around this time point. Unfortunately, until the date of delivery of this thesis, it was not possible to include data from HN878 infection for all time points, but it would be interesting to address the histopathology of the mice that survive. Probably, lung severity of these mice did not continue to progress, since they were able to cope with the infection.

Evaluation of the immune response

The progression of *M. tuberculosis* infection and the disease outcome are strongly linked to the host immune response (10) ,and, at the same time, the immune response might be modulated by the characteristics of the infecting bacteria (8, 40, 44, 98). So, we next investigated the dynamics of the immune response, such as immune cell recruitment and infiltration to the site of infection and lung cytokine gene expression.

The recruitment of immune cell populations of interest was analyzed by multiparametric flow cytometry (**Figure 17A**) at different time points post-infection. In what regards myeloid cells, *M. tuberculosis* 6C4 infection resulted in a high recruitment of monocytes and neutrophils at day 30 post infection, but lower levels of dendritic cells (**Figure 17B-C**). As for lymphoid cells, higher values of percentages and cell count of CD4+ T cells and CD8+ T cells were found in 6C4 infection, at day 30 and 15 post infection (**Figure 17B-D**).

This general enhanced inflammatory cell recruitment to the lungs of mice infected with *M. tuberculosis* 6C4 supports the more severe profile attributed to this isolate, as compared to isolate 4I2. Over time, the immune cell composition of the lung varies similarly for the two clinical isolates, although the 6C4 infection seems to exhibit a peak of accumulation of immune cells earlier than 4I2. For instance, 6C4 infections reach a maximum of neutrophil percentage at day 15 (**Figure 17B**) and neutrophil number at day 30 (**Figure 17C**). Whether due to halted recruitment of this cell type to the lung or by degeneration into necrotic debris, the frequency of neutrophils decreases after that time point. In contrast, 4I2 infection slowly increase their neutrophil numbers until day 90 (**Figure 17C**).

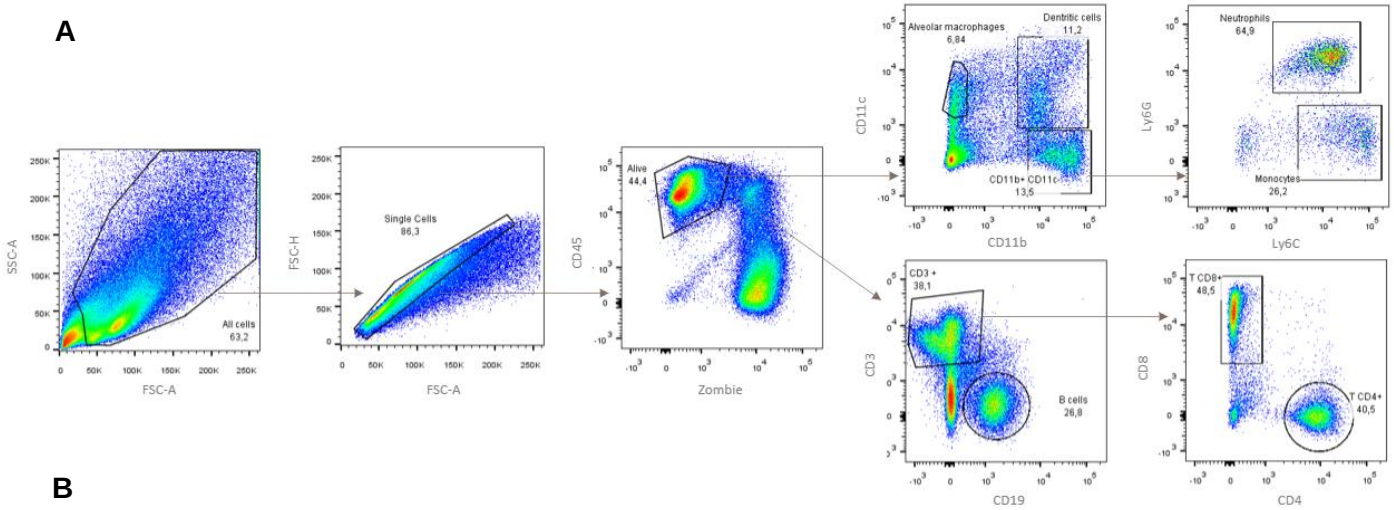
A
SSC-A
FSC-A
All cells
63,2
FSC-H
FSC-A
Single Cells
86,3
CD45
Zombie
Alive
44,4
CD11c
CD11b
Alveolar macrophages
6,84
Dentritic cells
11,2
CD11b+ CD11c+
13,5
Ly6G
Ly6C
Neutrophils
64,9
Monocytes
26,2
CD3
CD19
CD3 +
38,1
B cells
26,8
CD8
CD4
T CD8+
48,5
T CD4+
40,5

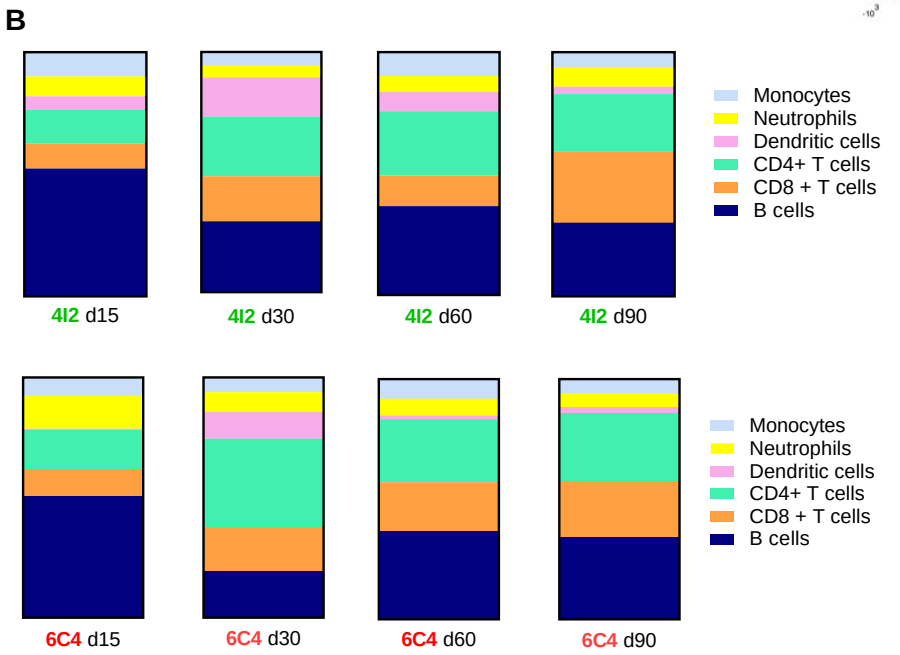
B
Monocytes
Neutrophils
Dendritic cells
CD4+ T cells
CD8 + T cells
B cells
4I2 d15
4I2 d30
4I2 d60
4I2 d90
6C4 d15
6C4 d30
6C4 d60
6C4 d90

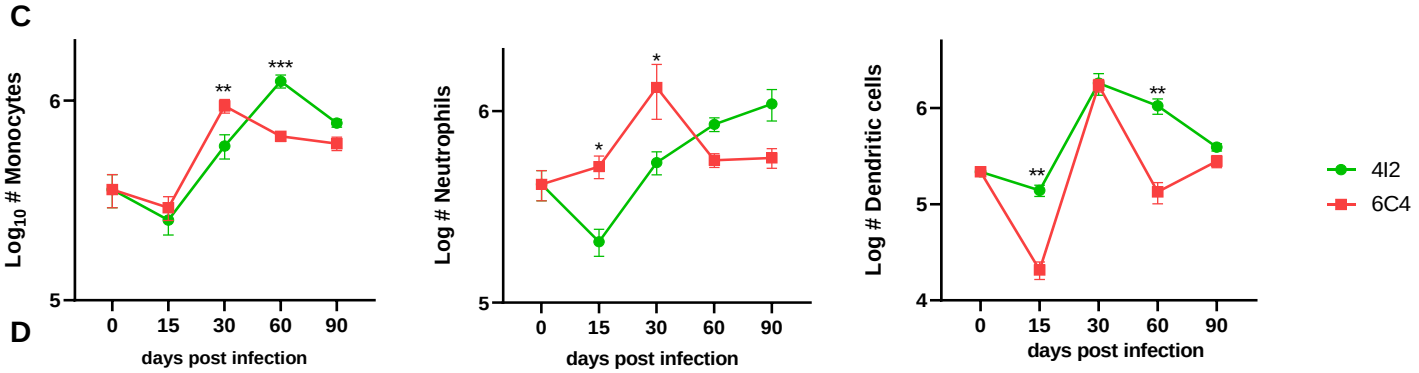
C
Log10 # Monocytes
Log # Neutrophils
Log # Dendritic cells
days post infection
4I2
6C4

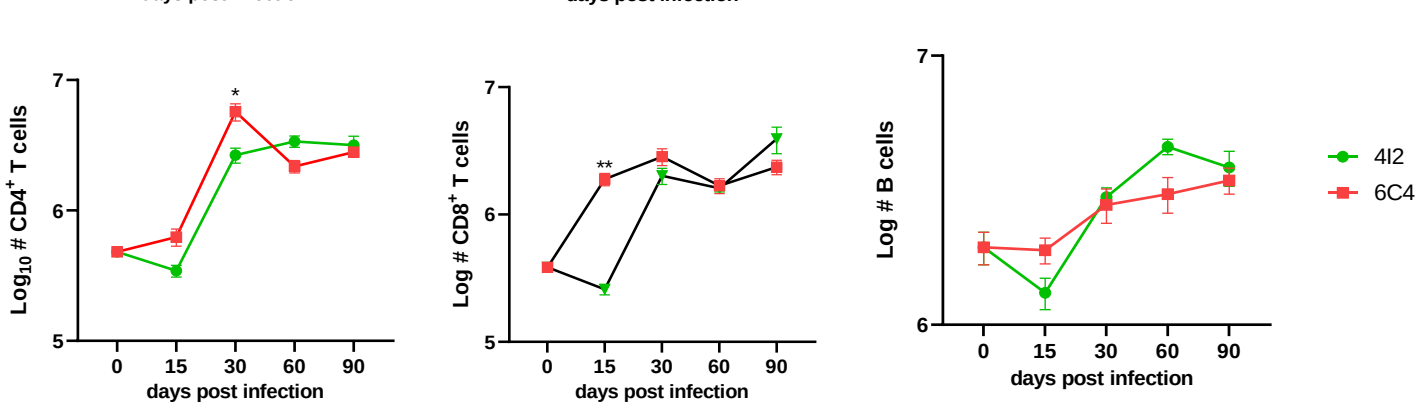
D
Log10 # CD4+ T cells
Log # CD8+ T cells
Log # B cells
days post infection
4I2
6C4

Figure 17. Percentages and cell counts of the indicated immune cell populations in the lung for 4I2, 6C4 and HN878 infections, determined by flow cytometry **(A)** Gating strategy to detect immune cell populations in the lung and BAL of C57BL/6 infected mice. Cell debris and duplets were excluded, and live cells were selected negatively using Zombie Green viability dye. Myeloid cells were gated in the panel above through the expression of specific markers: alveolar macrophages were selected as CD11c+ CD11b-, dendritic cells as CD11b+, CD11c+; within CD11b+ CD11c- population, neutrophils were selected as Ly6G+ Ly6C+ and monocytes were selected as Ly6C+ Ly6G-. Lymphoid cells were gated in the panel below: B cells were selected as CD19+; within the CD3+ population, CD4+ and CD8+ T cells were selected. **(B)** Colour scheme representing the percentage of immune cells in live cells for each infection over time. Number of myeloid **(C)** and lymphoid **(D)** cells in the lungs of mice infected with the clinical isolates 4I2 and 6C4. In **B**, each bar corresponds to the mean of the experimental group; in **C** and D each dot represents the Mean ± SEM. Statistical analysis was performed using multiple t-test (**C-D**). *p < 0.05; **p < 0.01; ****p < 0.0001.

M. tuberculosis initiates the infection in the airways, so, to assess the immune cell populations present in the alveolar space, flow cytometry of BAL was also performed (data available for day 30 only). No significative differences were observed, however it was possible to observe a trend that was in line with what happen in the lung. For instance, infection with isolate 6C4 was associated with a higher recruitment of neutrophils (**Figure 18A-B**) and CD4+ T cells (**Figure 18C**) than infection with isolate 4I2. Furthermore, 4I2 infection led to higher percentages and number of alveolar macrophages (**Figure 18A-B**) and CD8+ T cells (**Figure 18A and C**). More time points and animals will be necessary to confirm these data and substantiate these conclusions.

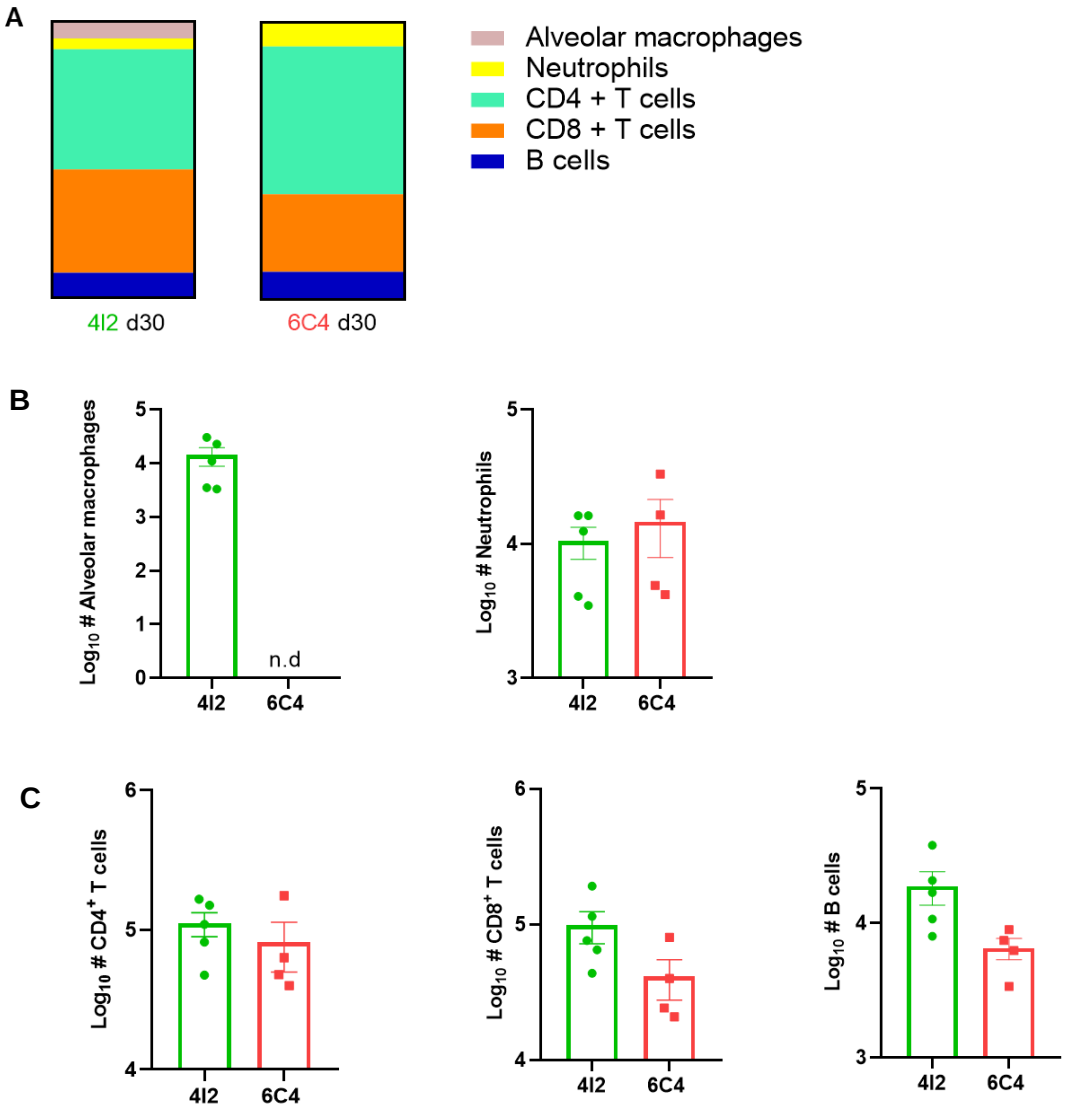

Figure 18. Percentages and cell count of the indicated immune cell populations in the BAL for 4I2, and 6C4 infections, determined by flow cytometry. Gating strategy is as presented in Figure 15. **(A)** Colour scheme representing the percentage of immune cells in live cells for each infection on day 30. Number of myeloid **(B)** and lymphoid **(C)** immune cells in the BAL of mice infected with the clinical isolates 4I2 or 6C4 at day 30 post infection. Alveolar macrophages were not detected (n.d) in the BAL of mice infected with Mtb 6C4. In **A**, each bar corresponds to the mean of the experimental group; in **B** and **C** each dot represents an individual mouse and Mean ± SEM are represented for each group. Statistical analysis was performed using unpaired *t*-test (**B-C**).

Finally, we investigated possible differences in cytokine gene expression as a result of the *in vivo* infection by the *M. tuberculosis* clinical isolates 4I2 and 6C4. For that, RNA was purified from the lung suspension and the expression of *Tnfa*, *Il1b, Il6, Il10, Ifng* and *Il17* analysed by qPCR. These cytokines were selected based on the expected proinflammatory profile that *M. tuberculosis* causes. As a control, expression of anti-inflammatory gene *Il10* was analyzed.

The expression of *Tnfa*, *Il1b*, *Il10* and *Il17* was enhanced in *M. tuberculosis* 6C4 infected lungs as compared to *M. tuberculosis* 4I2 infected ones, whereas that of *Il6* and *Ifng* did not vary between the two infections (**Figure 19**). Throughout time, the expression of most genes reached a peak on day 30 post infection, and then dropped. The expression of *Il6* did not follow this tendency, as higher levels were observed in early time points and after that, reduced almost totally (**Figure 19**).

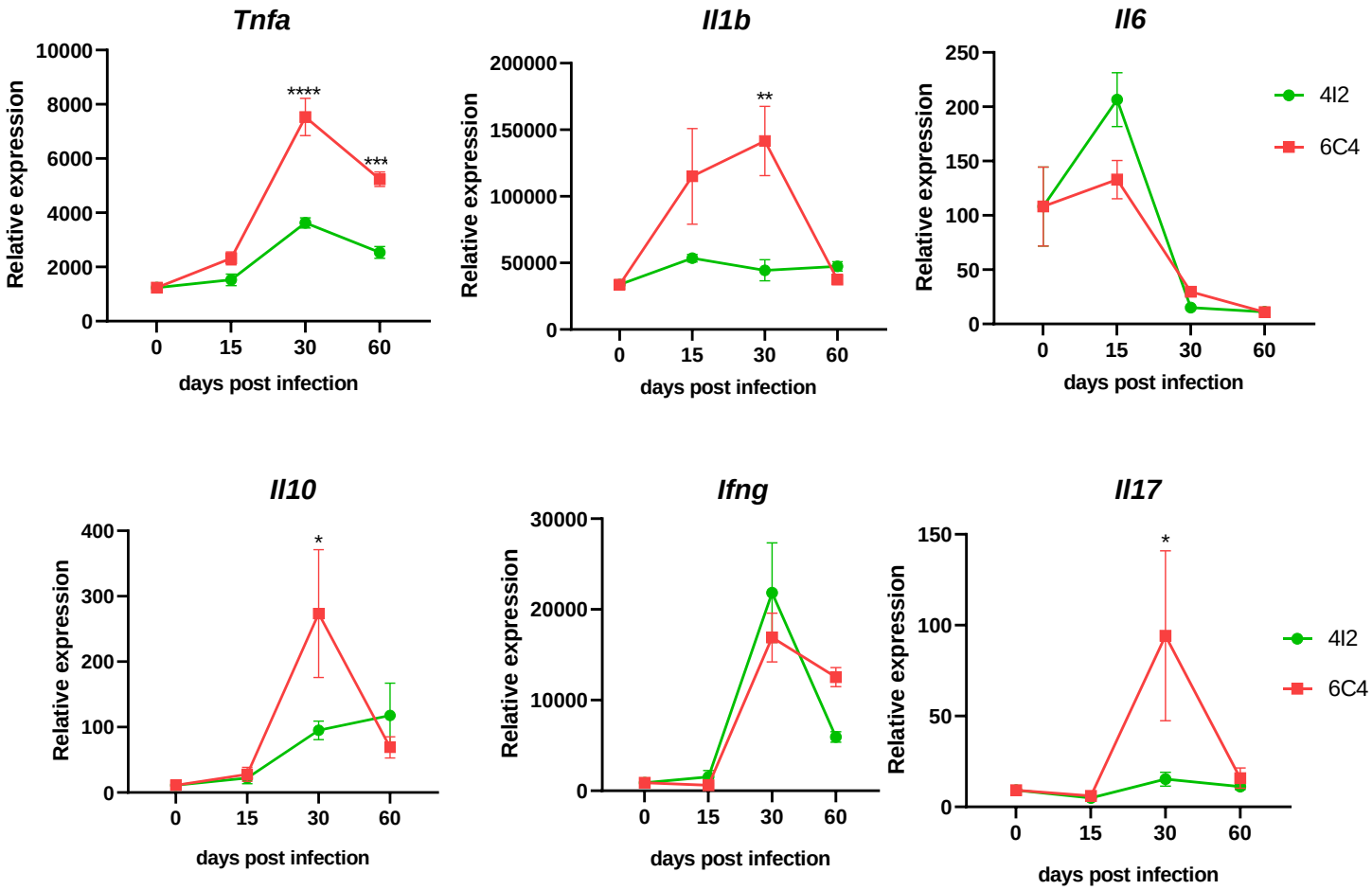

Figure 19. Relative expression of various genes encoding cytokines associated with immune responses in TB, in the lungs of mice infected with 4I2 or 6C4 in different time points. The relative expression of the indicated genes was determined against ubiquitin by real-time PCR. Each dot represents the Mean ± SEM. Statistical analysis was performed using multiple *t*-test. *$p < 0.05$; **$p < 0.01$; ****$p < 0.0001$.

In vitro, *M. tuberculosis* 4I2 is a higher inducer of IL-1β, but the increased production of this cytokine was found to be regulated post-transcriptionally (44). Therefore, the increased expression of *Il1b* observed *in vivo* during *M. tuberculosis* 6C4 infections does not necessarily imply higher levels of this cytokine. To clarify this issue, in the future, we will perform protein quantification using immunoassays, as ELISA (Enzyme-Linked Immunosorbent Assay) or bead assays. This will be done in the BAL and the blood. Still, the higher upregulation of proinflammatory genes such as *Tnfa*, *Il17* and *Il1b* and anti-inflammatory genes, as *Il10*, is compatible with a stronger immune response occurring in the case of the 6C4 isolate. This may in turn associate with the increased severity observed upon infection with 6C4 as compared to 4I2. It is important to refer that for this set of experiments, considerable variability was observed and can reflect the heterogeneous contributions of different lung cells. Also of note, is the observation of an increased *Il17* expression in the case of infection with *M. tuberculosis* 6C4, which may link this isolate with a favoured differentiation of Th17 cells and thus increased neutrophil mobilization, as seen by flow cytometry. To test this hypothesis, we could perform T cell analysis through intracellular staining, immunofluorescence for detection of neutrophils in the lung or even, a neutrophil depletion to verify if 6C4 infection become less virulent as described in these studies (46, 55).

In conclusion, by combining several parameters allowing the evaluation of disease severity and immunology studies, the results evidence that a certain spectrum of disease severity is observable in the mouse model upon infection with different *M. tuberculosis* clinical isolates. Bacterial burdens, histopathology, characterization of immune cell populations and gene expression results guided the stratification of *M. tuberculosis* 6C4 as a more severe isolate, with faster establishment and progression of infection, as compared to *M. tuberculosis* isolate 4I2. Furthermore, our findings position HN878 as the isolate leading to worst outcomes, reinforcing its classification as an hypervirulent isolate. In a simple way, **Figure 20** represent this spectrum of severities revealed by infecting C57BL/6 mice with distinct *M. tuberculosis* isolates.

Despite the promising results obtained thus far, showing a stratification of disease severity due to distinct clinical isolates, compatible with TB in humans, the mouse model used has some limitations. Granuloma is a hallmark of human TB pathology, however, lesions in C57BL/6 mice do not exhibit the same level of organization and composition of human granuloma (99). For instance, the necrotic centre involved by epithelioid cells, multinucleated giant cells and the fibrotic capsule are not present in infected C57BL/6 mice (99). Importantly, recent evidence show that another strain of mice, the C3HeB/FeJ, do form necrotizing lesions upon *M. tuberculosis* infection, resembling the active human TB, so being a better mouse model to gain insights on disease pathogenesis (97). For this reason, in the future, we will complement these results using the C3HeB/FeJ mouse model of infection.

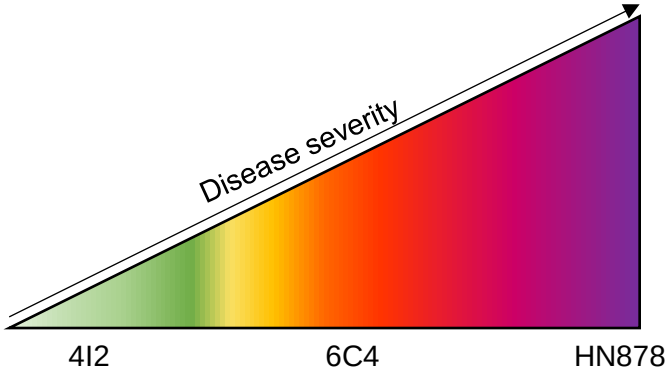

Figure 20. Representation of a possible spectrum of disease severity among *in vivo* infection with different clinical isolates: 4I2, 6C4 and HN878. Severity increased from the left to the right, as the colour intensifies.

The impact of myeloid specific IL-1 receptor signalling on the pathogenesis of TB

According to the results described in the previous section, *M. tuberculosis* strains that manipulate IL-1 responses, drive different courses of infection in mice, in what regards lung invasion and pathology. Given the indisputable role of IL-1 signalling in protection against TB, the modulation of this pathway by the pathogen could be, directly or indirectly, impacting the evolution and outcome of infection. IL-1β protection is classically associated to the potentiation of antimicrobial mechanisms in infected macrophages (76). So, our hypothesis is that differential induction of IL-1β driven by each *M. tuberculosis* isolate may affect microbicidal responses *in vivo*. Therefore, ultimately, the lower *in vivo* severity of *M. tuberculosis* isolate 4I2 may be linked to the higher induction of IL-1β. To unveil the impact of IL-1 receptor signalling on the pathogenesis of TB, mice lacking IL-1R in the myeloid compartment (IL-1R^{flox} LyzM.Cre^{+} mice) were infected with the clinical isolates in study. Similar to the previous section, the dynamic of infection was evaluated through bacterial burden enumeration in lung and BAL, analysis of lung pathology, and characterization of the immune response.

Evaluation of disease severity

IL-1R^{flox} LyzM.Cre mice were infected with high doses of *M. tuberculosis* 4I2, 6C4 or HN878 to define the dynamics of disease at day 30 post infection and possible differences in TB severity (**Figure 21**). Infections with isolates 4I2 and 6C4 were monitored over 60 days, whereas those with HN878 were monitored for 30 days. Once again, we monitored the survival and general welfare of infected mice as compared to control non-infected mice. At day 30 post infection, the lungs were harvested, and the bacterial burden and histopathology examined.

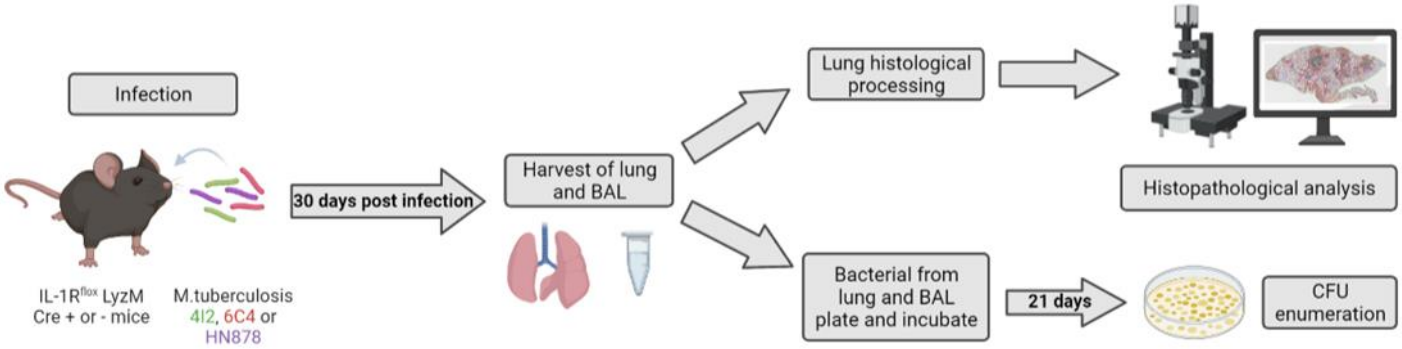

Figure 21. Experimental setup for the evaluation of disease in IL-1R^{flox} LyzM.Cre^{-} or $^{+}$ aerosol infected with Mtb clinical isolates 4I2, 6C4 and HN878. After 30 days of infection, lung and BAL of each animal were harvested. Histological images of the lung were obtained, and histopathology was evaluated through relative disease score and morphometric analysis. Bacteria from lung and BAL were cultured and incubated and after 21 days, CFU ere enumerated. Weights and animal welfare were also monitored.

Upon infection with *M. tuberculosis* 4I2 isolate, IL-1R^{flox} LyzM.Cre^{+} mice did not gain weight at the same rate as LyzM.Cre- mice, showing a significative lower weights throughout the 60 days of experiment (**Figure 22A**). Of note, one mouse of the Cre^{+} genotype had to be humanely euthanized on day 32 due to a 24 % weight loss and signs of distress and stillness. In contrast, during the experimental period, both Cre^{+} and Cre^{-} mice infected with *M. tuberculosis* 6C4 survived and showed similar weight variations (**Figure 22A**). Similar patterns of weight loss were also observed in Cre^{+} and Cre^{-} mice infected with *M. tuberculosis* HN878, with two IL-1R^{flox} LyzM.Cre^{+} and two IL-1R^{flox} LyzM.Cre^{-} reaching 20% of weight loss 30 days post infection (**Figure 22A**). These first results suggest that IL-1R signaling in myeloid cells may be needed for host protection in the case of infection with *M. tuberculosis* 4I2. Contrary, lack of IL-1 signaling in myeloid cells did not seem to impact infections with *M. tuberculosis* 6C4 and HN878 isolates.

Next, to further investigate if these evidences were also present at the lung level, lung and BAL bacterial burden and lung pathology were evaluated on day 30 post infection. In **Figure 22B,** it is possible to observe a significative increase in bacterial loads in the lungs of IL-1R^{flox} LyzM.Cre^{+} infected with *M. tuberculosis* 4I2, but not with 6C4 or HN878. Nonetheless, the bacterial burden in the BAL did not show significative differences across the three infections, although in the case of 4I2 infections a tendency to higher bacteria loads is observed for IL-1R^{flox} LyzM.Cre^{+} mice (**Figure 22C)**. Importantly, analysis of the lung histopathology revealed a superior lesion score for IL-1R^{flox}

LyzM.Cre^{+} infected with *M. tuberculosis* 4I2 as compared to Cre^{-} mice (**Figure 22D**). Once again, this difference between Cre^{+} and Cre^{-} mice was not observed in infections with the other isolates (**Figure 22D**).

Collectively, our findings suggest that in the case of *M. tuberculosis* 4I2, the host benefits from the induction of IL-1β and lack of IL-1R signalling in myeloid cells associates with increased susceptibility to infection. Additionally, the manipulation of the host response towards lower induction of IL-1β by *M. tuberculosis* 6C4 may indeed be a mechanism associated with increased disease severity, where presence or absence of IL-1R in myeloid cells is no longer important. Interestingly, we report that IL-1R signalling in myeloid cells is not a key part of the *in vivo* disease mechanism in *M. tuberculosis* HN878 infections. In this case, the mechanism of severity, as described in literature (81,82), is likely to be mainly dependent on the induction of high levels of type I IFN. For that reason, hereinafter, we focused on the two *M. tuberculosis* clinical isolates 4I2 and 6C4.

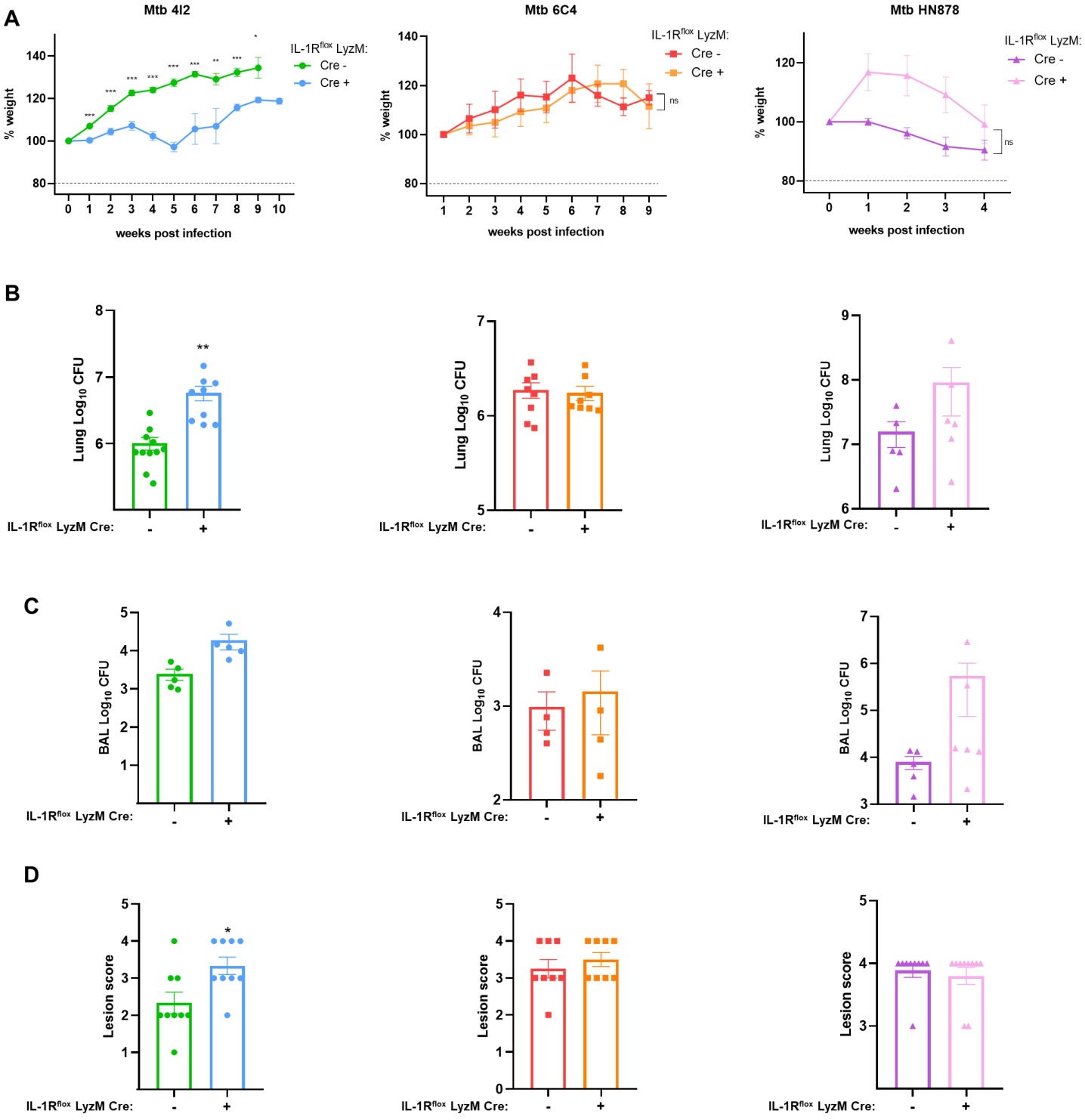

Figure 22. Disease severity of IL-1R^{flox} LyzM.Cre $^{-}$ or $^{+}$ mice infected with high doses of Mtb isolates 4I2, 6C4 or HN878, evaluated through weight loss, bacterial loads in the lung and BAL and lung pathology. **(A)** The weight of the animals was monitored and mice with percentage of weight above 80 % (dotted line) were humanely euthanized. At day 30 post-infection, the lungs **(B)** and BAL **(C)** of infected mice were collected and the bacteria burden determined by CFU

enumeration. **(D)** The histopathology of the infected lungs was assessed, and a relative disease score attributed at day 30 post infection. In **A** each dot represents Mean ± SEM and in **B**, **C** and **D** each dot represents an individual mouse, and Mean ± SEM are represented for each group. Statistical analysis was performed using multiple *t*-test (**A**) or unpaired *t*-test (**B-D**). *$p < 0.05$; **$p < 0.01$; ***$p < 0.01$.

For a more detailed analyses of lung pathology, the area of lesion/cell infiltrates was quantified for the two selected infections on day 30 post infection (**Figure 23**). The quantitative analysis of lung lesions was compatible with the aforementioned qualitative disease score, in which IL-1R^{flox} LyzM.Cre^{+} infected with *M. tuberculosis* 4I2 presented larger areas of lung lesion than IL-1R^{flox} LyzM.Cre^{-}, whereas infection with *M. tuberculosis* 6C4 yielded similar % of lung lesions independent of the presence or absence of the IL-1R in myeloid cells (**Figure 23A**). In the case of *M. tuberculosis* 4I2 infection, the presence of foamy macrophages, mainly mixed with lymphocyte infiltrates, is seen infected lungs of both mouse strains **(Figure 23B)**. Interestingly, in *M. tuberculosis* 4I2 infected IL-1R^{flox} LyzM.Cre^{+} mice, extensive areas of cell infiltrates enriched in neutrophils and small foci of cell debris were observed, overall, indicative of a severe lesion.

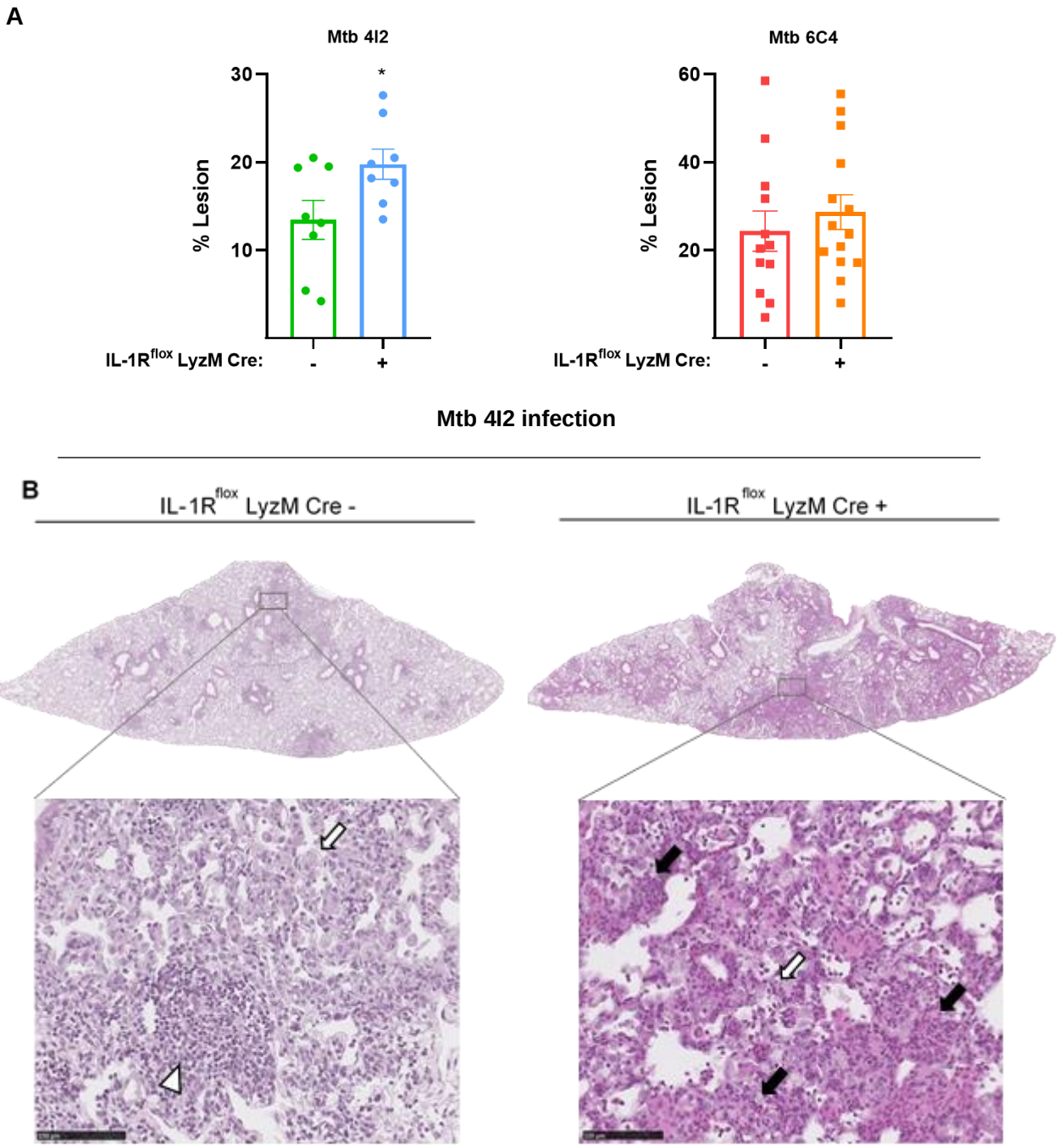

Figure 23. Histopathology analysis of IL-1R^{flox} LyzM.Cre $^{-}$ or $^{+}$ mice infected with high doses of Mtb 4I2 or 6C4. **(A)** At 30 days post infection, lung pathology was defined as the percentage of cell infiltrates per lobe, determined upon H&E staining and morphometric analysis of infected lungs. **(B)** Representative H&E staining images of lungs from mice infected with Mtb 4I2 are shown. Black arrows point to neutrophil infiltrates, white arrows point to foamy macrophages, white arrowhead points to perivascular lymphocytes. Scale bar corresponds to 100 µm. In **A** each dot represents an individual mouse, and Mean ± SEM are represented for each group. Statistical analysis was performed using unpaired *t*-test (**A**). *$p < 0.05$.

Therefore, our results show that abrogation of the IL-1R signalling in the myeloid compartment affected the disease severity of animals infected with *M. tuberculosis* 4I2, leading to a substantial increase in weight loss, bacterial burden and histopathology of the lung. Although preliminary, these results support that the low severity of the *M. tuberculosis* 4I2 isolate may be linked to the bacteria inability to modulate IL-1β induction (7), and that this could help in the control of infection in early stages. Thus, when the IL-1R signaling cascade is blocked, the protection afforded by IL-1 is lost and the severity of the disease worsens. In contrast, in *M. tuberculosis* isolates that modulate IL-1, such as *M. tuberculosis* 6C4, the outcome of infection is not affected when IL-1R is compromised.

Evaluation of immune response

To investigate how differential induction of IL-1β by *M. tuberculosis* isolates may lead to distinct disease outcomes, we explored the dynamics of the immune response in the local of infection on day 30 post infection (**Figure 24**). For that, immune cell populations in the lung and BAL of IL-1R^{flox} LyzM.Cre $^{-}$ or $^{+}$ mice infected with *M. tuberculosis* 4I2 or 6C4 were analysed by flow cytometry. Furthermore, lung suspensions were also used to quantify the relative expression of genes associated with inflammatory responses, by real time PCR. This allowed us to infer how the absence of IL-1R signaling in the myeloid compartment may affect the immune cells recruited to the lung and the expression of genes encoding cytokines of relevance to the immune response in TB.

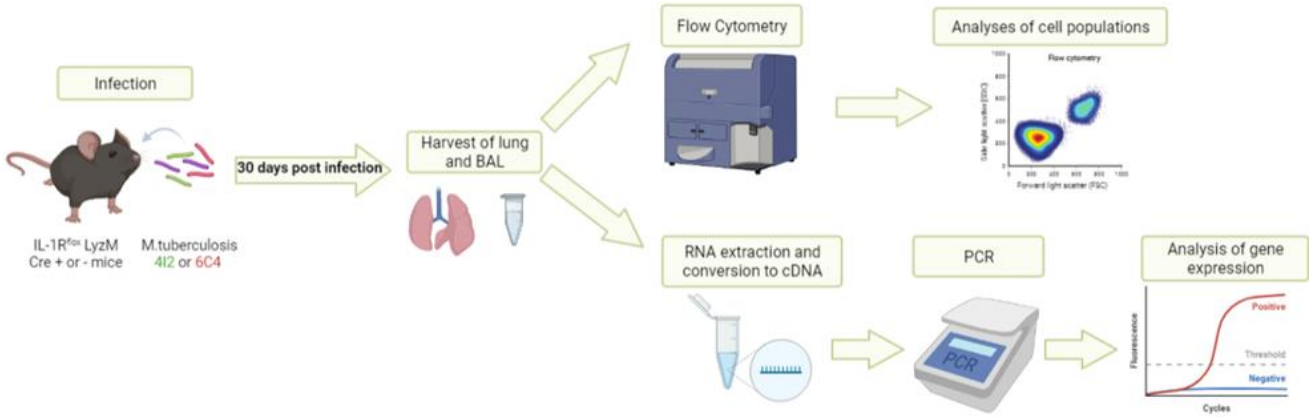

Figure 24. Experimental setup for the evaluation of the immune response in IL-1R^{flox} LyzM.Cre $^{-}$ or $^{+}$ aerosol infected with Mtb clinical isolates 4I2 or 6C4. After 30 days of infection, lung and BAL of each animal were harvested. Cell populations in the lung and BAL were analysed through flow cytometry. Relative gene expression in the lung and BAL were evaluated by real time qPCR, after RNA extraction and conversion to cDNA.

Cell populations in the lung were analysed in terms of percentage in live cells (**Figure 25A**) and total cell number (**Figure 25B-C**). It is possible to observe an increase of percentage of neutrophils, dendritic cells, CD4+ T cells and a decrease in percentage of B cells in IL-1R^{flox} LyzM.Cre^{+} mice infected with *M. tuberculosis* 4I2, as compared to IL-1R^{flox} LyzM.Cre^{-} mice (**Figure 25A**). This increase of neutrophils is in line with what we observed in our histology analysis (**Figure 25B**). The differences in cell frequencies were paralleled in terms of cell counts, with significative higher values observed in numbers of myeloid cells, such as monocytes, neutrophils and dendritic cells (**Figure 25B)**, higher

numbers of lymphoid CD4+ T cells and lower B cell counts (**Figure 25C)** in IL-1R^{flox} LyzM.Cre^{+} mice infected with *M. tuberculosis* 4I2. In contrast, infections of both mouse genotypes with *M. tuberculosis* 6C4 resulted in similar patterns of immune cell populations in the infected lungs, with exception of a rise in B cell percentages and numbers in the case of IL-1R^{flox} LyzM.Cre^{+} mice.

It is important to note that increased immune cell recruitment in *M. tuberculosis* 4I2 IL-1R^{flox} LyzM.Cre^{+} infected mice may be a consequence of the increased bacterial loads observed in these mice. However, if that was the case, similar increases were expected across the different populations. Yet, the increase in neutrophils and CD4 T cells is particularly visible, suggesting a subtler alteration. Interestingly, the accumulation of neutrophils in the lung has been widely associated with lung pathology, which we also report here. Another interesting finding related to this set of experiments is that the overall immune cell profile and disease features observed in IL-1R^{flox} LyzM.Cre^{+} mice are similar to those observed in mice infected with 6C4. This suggests that *M. tuberculosis* 6C4 is likely manipulating the host response and creating a low IL-1b environment suring the early stages of *in vivo* infection.

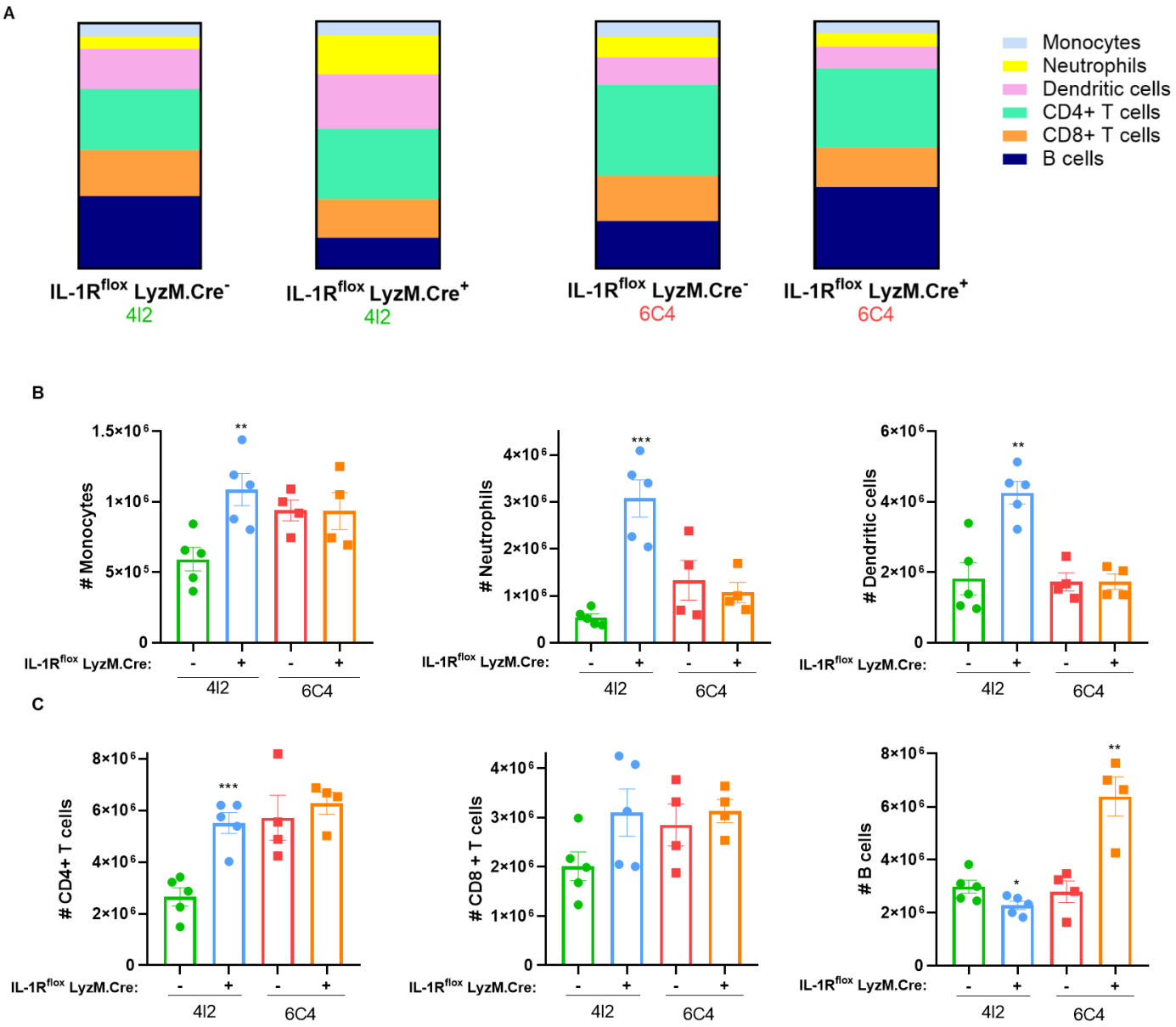

Figure 25. Percentages and cell counts of the indicated immune cell populations in the lung of mice infected with Mtb 4I2 or 6C4 at day 30 post infection, determined by flow cytometry. The gating strategy was identical to the one shown in **Figure 15A**. **(A)** Colour scheme representing the percentage of immune cells in live cells for each experimental group. Percentage of myeloid **(B)** and lymphoid **(C)** immune cells in the lung of IL-1R^{flox} LyzM.Cre $^{-}$ or $^{+}$ infected with the clinical isolates 4I2 or 6C4. In **A**, each bar corresponds to the mean of the experimental group; in **B** and **C** each dot represents an individual mouse, and Mean ± SEM are represented for each group. Statistical analysis was performed using unpaired *t*-test (**B-C**). *$p < 0.05$; **$p < 0.01$; ***$p < 0.01$.

In parallel, we assessed the immune cell composition of the alveolar space, by flow cytometry analysis of BAL samples obtained from the same experimental groups (**Figure 26**). It is interesting to observe in BAL an increase of frequencies and numbers of neutrophils and CD4+ T cell in IL-1R^{flox} LyzM.Cre^{+} mice infected with *M. tuberculosis* 4I2 (**Figure 26A-C**), which parallels the lung interstitium data. The other detected cell populations did not change significantly in the two mouse genotypes upon *M. tuberculosis* 4I2 infection (**Figure 26A-C**). Also, similarly to the lung data, the BAL immune cell composition in mice infected with *M. tuberculosis* 6C4 was not affected by the lack of IL-1R in myeloid cells (**Figure 26A-C**).

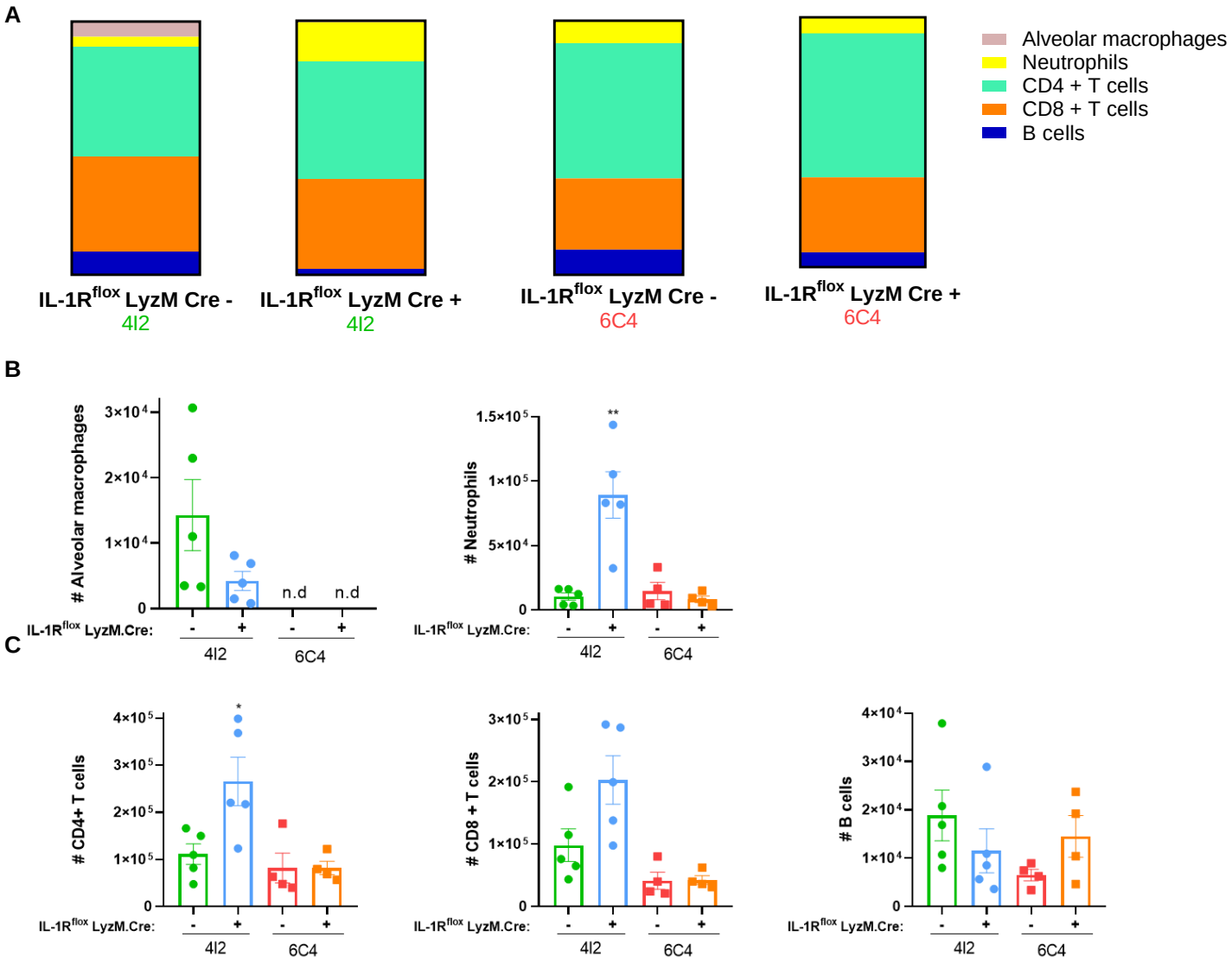

Figure 26. Percentages and cell counts of the indicated immune cell populations in the BAL of mice infected with Mtb 4I2 or 6C4 at day 30 post infection, determined by flow cytometry. The gating strategy was identical to the one shown in **Figure 15A**. **(A)** Colour scheme representing

the percentage of immune cells in live cells for each experimental group. Percentage of myeloid **(B)** and lymphoid **(C)** immune cells in the BAL of IL-1R^{flox} LyzM.Cre $^{-}$ or $^{+}$ infected with Mtb clinical isolates 4I2 or 6C4. Alveolar macrophages in the lungs of mice infected with Mtb 6C4 were not detected (n.d). In **A**, each bar corresponds to the mean of the experimental group; in **B** and **C** each dot represents an individual mouse and Mean ± SEM are represented for each group. Statistical analysis was performed using unpaired *t*-test (**B-C**). **p* < 0.05; ***p* < 0.01.

Together, the results from lung and BAL were compatible, showing differences in *M. tuberculosis* 4I2 infection in mice lacking IL-1R signalling in myeloid cells. Most notably, higher percentages and numbers of neutrophils and CD4+ T cells were observed in IL-1R^{flox} LyzM.Cre^{+} mice infected with Mtb 4I2 as compared to IL-1R^{flox} LyzM.Cre^{-}. These findings complement the results from disease severity presented in the previous section and suggest a possible deregulation of neutrophil responses leading to damage in mice infected with Mtb 4I2 and lacking the IL-1R in myeloid cells.

Finally, we investigated the expression of some immune mediators in response to each infection in each mouse genotype. We focused in the expression of genes encoding *Tnfa*, *Il1b, IL6, Il10, Ifng* and *Il17*, in lung at day 30 post infection (**Figure 27**). Through analysis of **Figure 27** it is possible to observe an increase of *Tnfa* and *Il1b* expression in *M. tuberculosis* 4I2-infected IL-1R^{flox} LyzM.Cre^{+} mice, which is compatible with a higher inflammatory response taking place, perhaps due to increased bacterial burdens. It is important to refer that despite the higher expression of *Il1b* and eventually higher production of IL-1β, this cytokine will not exert their action in myeloid cells, since this pathway is abrogated in IL-1R^{flox} LyzM.Cre^{+} mice. Surprisingly, *Il6* expression was significatively downregulated in IL-1R^{flox} LyzM.Cre^{+} mice, although the values obtained were very low and should thus be interpreted with caution. Interestingly, the biggest difference observed between Cre^{+} and Cre^{-} mice infected with *M. tuberculosis* isolate 4I2 was on the expression of *Il17*, which was significatively higher in IL-1R^{flox} LyzM.Cre^{+} mice. In contrast, and in line with our previously presented data, infection of in either strain of mice with *M. tuberculosis* 6C4 was not reflected in significative differences in gene expression (**Figure 27**). In the future, it would be helpful to confirm these data and perform ELISA assays for cytokine quantification.

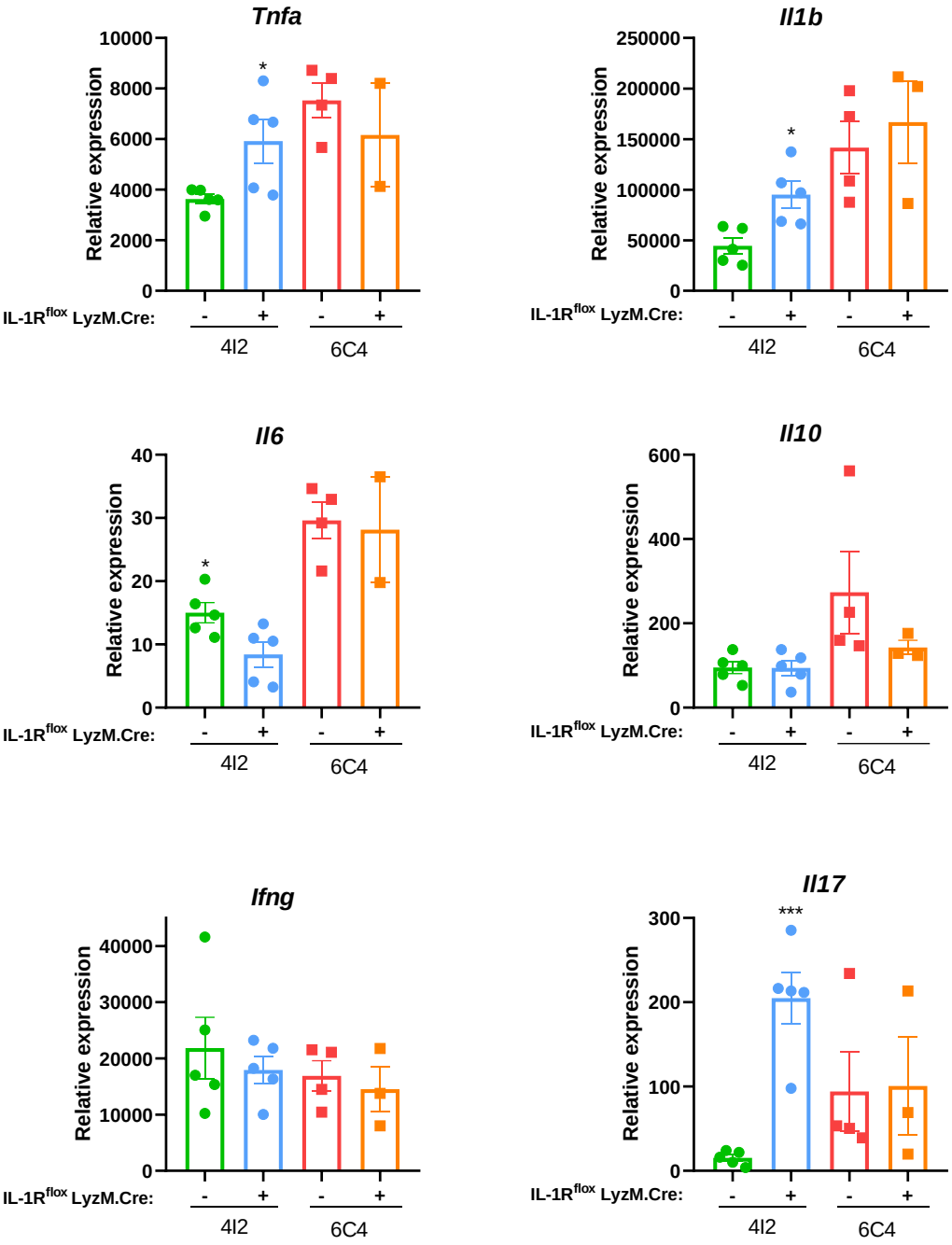

Figure 27. Relative expression of cytokine genes associated with immune response, in the lungs of IL-1R^{flox} LyzM.Cre $^{-}$ or $^{+}$ mice infected with 4I2 or 6C4. The relative expression of the indicated genes was determined against ubiquitin by real-time PCR. Each dot represents an individual mouse and Mean ± SEM are represented for each group. Statistical analysis was performed using unpaired *t*-test. *$p < 0.05$; ***$p < 0.01$.

Collectively, our results offer interesting insights on the relation between IL-1R signaling in the myeloid compartment and the dynamics of the immune response occurring *in vivo*. Overall, IL-1R^{flox} LyzM.Cre^{+} mice infected with a higher IL-1β inducer strain (*M. tuberculosis* 4I2) resulted in higher recruitment of neutrophils, CD4+ T cells and other myeloid cells to the lung and BAL, and higher expression of pro inflammatory associated genes, such as *Tnfa*, *Il1b* and *Il17* than IL-1R^{flox} LyzM.Cre^{-} mice. This increase in *Il17* may underlie the mechanism associated with the increased recruitment of neutrophils reported above. Although associated with protective immunity through pro inflammatory mechanisms, a pathological role for IL-17 in TB has been highlighted (100). During chronic phases of infection, immune responses developed towards excessive IL-17 production may lead to extensive neutrophil recruitment and tissue damage (60, 100). Indeed, some studies show a link between Th17 cells and autoimmune and inflammatory diseases such as collagen-induced arthritis (59). Also, neutrophil damage is common in genetically susceptible mice, such as IFN-γ -/- mice (100). In humans, a blood transcriptional signature marked by neutrophils accumulation is associated with active TB, rather than a latent TB profile (57). Moreover, the increased expression of *Il17*, and potentially the stronger Th17 response, observed in *M. tuberculosis* 4I2 infections in the absence of IL-1R pathway in myeloid cells may underlie a role for this pathway in regulating protective vs pathological responses in TB (**Figure 28**). Due to these findings, we have an on-going work with the aim of analysing the phenotype of T cells upon infection with *M. tuberculosis* 4I2, through intracellular staining. Also, it would be interesting to perform immunofluorescence analysis of the infected lungs to address the localization and distribution of the various cell populations, particularly of neutrophils. Furthermore, to complement this work, we could analyse the expression of genes encoding chemokines involved in the recruitment of neutrophils, such as *Cxcl1, Cxcl2* and *Cxcl5* (55). As discussed in the previous section, we also could perform a depletion of neutrophils to investigate their specific contribution to the increased susceptibility seen in IL-1R^{flox} LyzM.Cre^{+} mice. In contrast, infection with the lower IL-1β inducer strain (*M. tuberculosis* 6C4) did not show indicative differences between strains of mice, suggesting that the threshold of IL-1 induced by this isolate is such that the IL-1R pathway does not play an important role in the protection against infection.

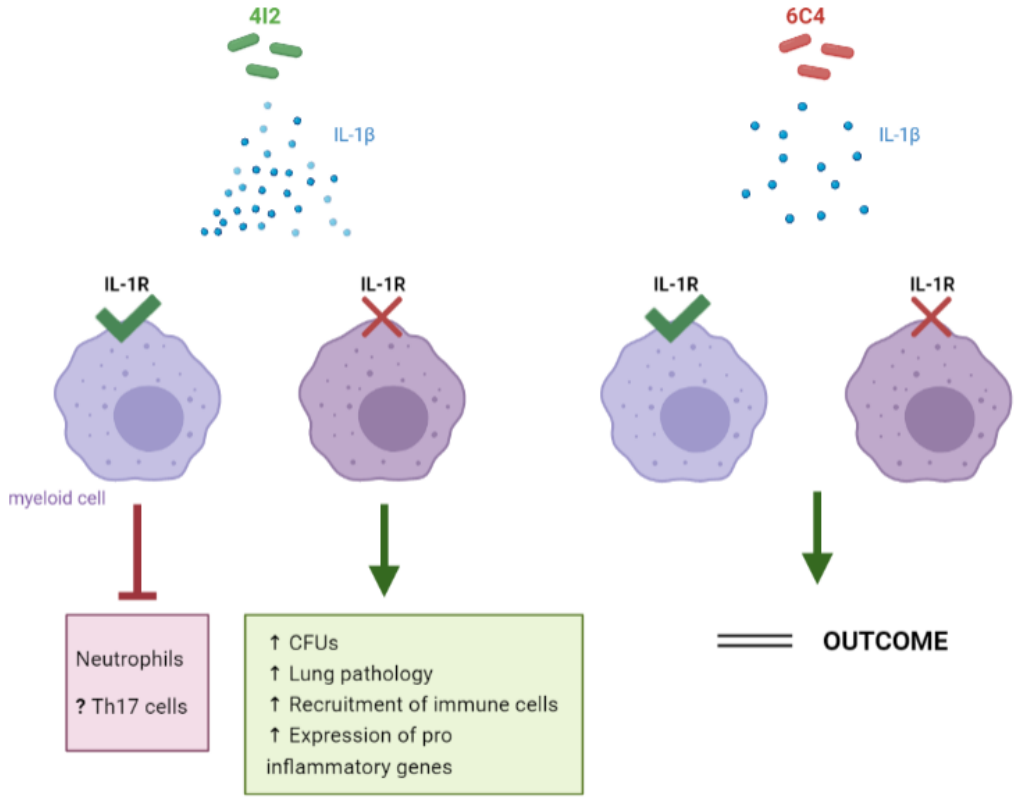

Figure 28. Working model for the impact of IL-1 modulation by distinct Mtb isolates in the regulation of the immune response triggered. Figure created in Biorender.

Chapter IV. Conclusion and future perspectives

TB remains a major health problem, causing an enormous death toll every year (4). To tackle this disease a better understanding of the complex immune response and the host-pathogen interactions is needed. Indeed, a wide range of disease severity and clinical presentations are characteristic of the dynamic spectrum of TB (11). Although classically associated with host factors, rising evidence validates that genetic diversity of the bacteria is linked to TB heterogeneity (8). In fact, *M. tuberculosis* diversity has been associated with different virulence, transmission potential and more recently, by our group, with different disease outcomes and modulation of immune responses (44).

In this thesis, we investigated if TB severity could be modelled *in vivo* using *M. tuberculosis* clinical isolates associating with distinct disease presentation in human TB patients. According to the results it was possible to recapitulate, in the mouse model, different severities of disease provoked by diverse *M. tuberculosis* strains. Briefly, *M. tuberculosis* 6C4 that caused severe TB in a human patient, presented higher bacterial loads in the lung, larger and more severe lesions, higher recruitment of immune cells to the site of infection and increased expression of genes encoding proinflammatory cytokines, as compared to infection with *M. tuberculosis* 4I2, a mild TB associated isolate. Furthermore, different evolution and peaks of infection were observed. Whereas *M. tuberculosis* 4I2 infection appeared to have a slower progression of disease, *M. tuberculosis* 6C4 infection reached maximum of response already at day 30 post infection. Importantly, these findings suggest that early events upon infection may guide the severity of disease. *M. tuberculosis* HN878 used as a hypervirulent strain control, displayed the expected results, in which some mice succumbed to disease. Taken together, these results allow us to position the three *M. tuberculosis* isolates in order of disease severity *in vivo*, from mild infection with 4I2, severe with 6C4 and acutely severe with HN878.

The second part of this work was the study of the contribution of the myeloid IL-1R signaling to the pathogenesis of TB. To decipher if the severity of the *M. tuberculosis* isolates under study was associated with induction of IL-1β, knock out mice lacking IL-1R in myeloid cells were used. IL-1R-myeloid deficient mice when infected with the higher IL-1 inducer strain, were less able to control the infection in comparison with WT mice. Specifically, higher bacterial loads, severe pathology, more infiltrations and increased inflammatory responses were observed, which was very similar to the response to 6C4 infection in WT mice. The same was not observed for the other *M.*

tuberculosis strains (6C4 and HN878). Therefore, these findings highlight that the low severity of 4I2 is linked to the high induction of IL-1β.

In the future, it will be interestingly to address the contribution of the IL-1R signaling on other cell compartments for TB protection. Indeed, several studies highlight the role of epithelial and endothelial cells as *in vivo* targets of IL-1 (50, 68, 101). In fact, IL-1 induces the expression of several adhesion molecules that can promote tissue permeability and consequently allow the infiltration of other immune cells in response to infection (80). More recently, the migration of *M. tuberculosis* infected alveolar macrophages into the lung interstitium was shown to be dependent on IL-1R signaling triggering in lung epithelial cells (50). Therefore, IL-1R signaling not only in the hematopoietic, but also in stromal compartments could reveal important features of protection/disease during the establishment of TB.

References

1. Morse D, Brothwell DR, Ucko PJ. Tuberculosis in Ancient Egypt. American Review of Respiratory Disease. 1964;90(4):524-41.
2. Pezzella AT. History of Pulmonary Tuberculosis. Thoracic Surgery Clinics. 2019;29(1):1-17.
3. Kim PS, Swaminathan S. Ending TB: the world's oldest pandemic. J Int AIDS Soc. 2021;24(3):e25698.
4. WHO. Global tuberculosis Report. World Health Organization. 2020.
5. Grundner C. To fight tuberculosis, fund basic research. PLoS Biol. 2018;16(9):e3000037.
6. WHO. Global strategy and targets for tuberculosis prevention, care and control after 2015. 2013.
7. Pai M, Behr MA, Dowdy D, Dheda K, Divangahi M, Boehme CC, et al. Tuberculosis. Nat Rev Dis Primers. 2016;2:16076.
8. Bastos HN, Osorio NS, Gagneux S, Comas I, Saraiva M. The Troika Host-Pathogen-Extrinsic Factors in Tuberculosis: Modulating Inflammation and Clinical Outcomes. Front Immunol. 2017;8:1948.
9. Sousa J, Saraiva M. Paradigm changing evidence that alter tuberculosis perception and detection: Focus on latency. Infect Genet Evol. 2019;72:78-85.
10. O'Garra A, Redford PS, McNab FW, Bloom CI, Wilkinson RJ, Berry MP. The immune response in tuberculosis. Annu Rev Immunol. 2013;31:475-527.
11. Cadena AM, Fortune SM, Flynn JL. Heterogeneity in tuberculosis. Nat Rev Immunol. 2017;17(11):691-702.
12. Lin PL, Flynn JL. The End of the Binary Era: Revisiting the Spectrum of Tuberculosis. J Immunol. 2018;201(9):2541-8.
13. Houben RMGJ, Dodd PJ. The Global Burden of Latent Tuberculosis Infection: A Re-estimation Using Mathematical Modelling. PLOS Medicine. 2016;13(10):e1002152.
14. Lönnroth K, Castro KG, Chakaya JM, Chauhan LS, Floyd K, Glaziou P, et al. Tuberculosis control and elimination 2010-50: cure, care, and social development. Lancet. 2010;375(9728):1814-29.
15. Chai Q, Zhang Y, Liu CH. Mycobacterium tuberculosis: An Adaptable Pathogen Associated With Multiple Human Diseases. Frontiers in Cellular and Infection Microbiology. 2018;8(158).

16. van Crevel R, Critchley JA. The Interaction of Diabetes and Tuberculosis: Translating Research to Policy and Practice. Tropical Medicine and Infectious Disease. 2021;6(1):8.

17. Tiemersma EW, van der Werf MJ, Borgdorff MW, Williams BG, Nagelkerke NJ. Natural history of tuberculosis: duration and fatality of untreated pulmonary tuberculosis in HIV negative patients: a systematic review. PLoS One. 2011;6(4):e17601.

18. Pai M, Sotgiu G. Diagnostics for latent TB infection: incremental, not transformative progress. European Respiratory Journal. 2016;47(3):704-6.

19. Pai M, Denkinger CM, Kik SV, Rangaka MX, Zwerling A, Oxlade O, et al. Gamma interferon release assays for detection of Mycobacterium tuberculosis infection. Clin Microbiol Rev. 2014;27(1):3-20.

20. Rangaka MX, Wilkinson KA, Glynn JR, Ling D, Menzies D, Mwansa-Kambafwile J, et al. Predictive value of interferon-γ release assays for incident active tuberculosis: a systematic review and meta-analysis. The Lancet Infectious Diseases. 2012;12(1):45-55.

21. Detjen AK, DiNardo AR, Leyden J, Steingart KR, Menzies D, Schiller I, et al. Xpert MTB/RIF assay for the diagnosis of pulmonary tuberculosis in children: a systematic review and meta-analysis. Lancet Respir Med. 2015;3(6):451-61.

22. Fu H, Lewnard JA, Frost I, Laxminarayan R, Arinaminpathy N. Modelling the global burden of drug-resistant tuberculosis avertable by a post-exposure vaccine. Nature Communications. 2021;12(1):424.

23. Lange C, Chesov D, Heyckendorf J, Leung CC, Udwadia Z, Dheda K. Drug-resistant tuberculosis: An update on disease burden, diagnosis and treatment. Respirology. 2018;23(7):656-73.

24. Law S, Piatek AS, Vincent C, Oxlade O, Menzies D. Emergence of drug resistance in patients with tuberculosis cared for by the Indian health-care system: a dynamic modelling study. Lancet Public Health. 2017;2(1):e47-e55.

25. Seung KJ, Keshavjee S, Rich ML. Multidrug-Resistant Tuberculosis and Extensively Drug-Resistant Tuberculosis. Cold Spring Harb Perspect Med. 2015;5(9):a017863.

26. Düzgüneş N, Sessevmez M, Yildirim M. Bacteriophage Therapy of Bacterial Infections: The Rediscovered Frontier. Pharmaceuticals. 2021;14(1):34.

27. Scriba TJ, Netea MG, Ginsberg AM. Key recent advances in TB vaccine development and understanding of protective immune responses against Mycobacterium tuberculosis. Seminars in Immunology. 2020;50:101431.

28. Delogu G, Provvedi R, Sali M, Manganelli R. Mycobacterium tuberculosis virulence: insights and impact on vaccine development. Future Microbiol. 2015;10(7):1177-94.

29. Ernst JD. Mechanisms of M. tuberculosis Immune Evasion as Challenges to TB Vaccine Design. Cell Host Microbe. 2018;24(1):34-42.

30. Franco AR, Peri F. Developing New Anti-Tuberculosis Vaccines: Focus on Adjuvants. Cells. 2021;10(1):78.

31. Wirth T, Hildebrand F, Allix-Béguec C, Wölbeling F, Kubica T, Kremer K, et al. Origin, Spread and Demography of the Mycobacterium tuberculosis Complex. PLOS Pathogens. 2008;4(9):e1000160.

32. Coscolla M, Gagneux S. Consequences of genomic diversity in Mycobacterium tuberculosis. Seminars in Immunology. 2014;26(6):431-44.

33. An Wang R. Why is Mycobacterium Tuberculosis Hard to Grow? The Principle of Biorelativity Explains. Journal of Clinical & Experimental Pathology. 2014;04(03).

34. Coscolla M, Brites D, Menardo F, Loiseau C, Borrell S, Otchere ID, et al. Phylogenomics of Mycobacterium africanum reveals a new lineage and a complex evolutionary history. bioRxiv. 2020:2020.06.10.141788.

35. Ngabonziza JCS, Loiseau C, Marceau M, Jouet A, Menardo F, Tzfadia O, et al. A sister lineage of the Mycobacterium tuberculosis complex discovered in the African Great Lakes region. Nature Communications. 2020;11(1):2917.

36. Napier G, Campino S, Merid Y, Abebe M, Woldeamanuel Y, Aseffa A, et al. Robust barcoding and identification of Mycobacterium tuberculosis lineages for epidemiological and clinical studies. Genome Medicine. 2020;12(1):114.

37. Ejo M, Torrea G, Uwizeye C, Kassa M, Girma Y, Bekele T, et al. Genetic diversity of the Mycobacterium tuberculosis complex strains from newly diagnosed tuberculosis patients in Northwest Ethiopia reveals a predominance of East-African-Indian and Euro-American lineages. International Journal of Infectious Diseases. 2021;103:72-80.

38. Comas I, Coscolla M, Luo T, Borrell S, Holt KE, Kato-Maeda M, et al. Out-of-Africa migration and Neolithic coexpansion of Mycobacterium tuberculosis with modern humans. Nature Genetics. 2013;45(10):1176-82.

39. Brites D, Gagneux S. Co-evolution of Mycobacterium tuberculosis and Homo sapiens. Immunol Rev. 2015;264(1):6-24.

40. Gagneux S. Ecology and evolution of Mycobacterium tuberculosis. Nat Rev Microbiol. 2018;16(4):202-13.

41. Uren C, Hoal EG, Möller M. Mycobacterium tuberculosis complex and human coadaptation: a two-way street complicating host susceptibility to TB. Human Molecular Genetics. 2020;30(R1):R146-R53.

42. Cá B, Fonseca KL, Sousa J, Maceiras AR, Machado D, Sanca L, et al. Experimental Evidence for Limited in vivo Virulence of Mycobacterium africanum. Frontiers in Microbiology. 2019;10(2102).

43. Gehre F, Otu J, DeRiemer K, de Sessions PF, Hibberd ML, Mulders W, et al. Deciphering the Growth Behaviour of Mycobacterium africanum. PLOS Neglected Tropical Diseases. 2013;7(5):e2220.

44. Sousa J, Cá B, Maceiras AR, Simões-Costa L, Fonseca KL, Fernandes AI, et al. Mycobacterium tuberculosis associated with severe tuberculosis evades cytosolic surveillance systems and modulates IL-1β production. Nature Communications. 2020;11(1):1949.

45. Liu CH, Liu H, Ge B. Innate immunity in tuberculosis: host defense vs pathogen evasion. Cell Mol Immunol. 2017;14(12):963-75.

46. Moreira-Teixeira L, Stimpson PJ, Stavropoulos E, Hadebe S, Chakravarty P, Ioannou M, et al. Type I IFN exacerbates disease in tuberculosis-susceptible mice by inducing neutrophil-mediated lung inflammation and NETosis. Nat Commun. 2020;11(1):5566.

47. Stanley SA, Johndrow JE, Manzanillo P, Cox JS. The Type I IFN Response to Infection with Mycobacterium tuberculosis Requires ESX-1-Mediated Secretion and Contributes to Pathogenesis. The Journal of Immunology. 2007;178(5):3143-52.

48. Donovan ML, Schultz TE, Duke TJ, Blumenthal A. Type I Interferons in the Pathogenesis of Tuberculosis: Molecular Drivers and Immunological Consequences. Frontiers in immunology. 2017;8:1633-.

49. Moreira-Teixeira L, Mayer-Barber K, Sher A, O'Garra A. Type I interferons in tuberculosis: Foe and occasionally friend. The Journal of experimental medicine. 2018;215(5):1273-85.

50. Cohen SB, Gern BH, Delahaye JL, Adams KN, Plumlee CR, Winkler JK, et al. Alveolar Macrophages Provide an Early Mycobacterium tuberculosis Niche and Initiate Dissemination. Cell Host Microbe. 2018;24(3):439-46 e4.

51. Nair VR, Franco LH, Zacharia VM, Khan HS, Stamm CE, You W, et al. Microfold Cells Actively Translocate Mycobacterium tuberculosis to Initiate Infection. Cell Rep. 2016;16(5):1253-8.

52. Maertzdorf J, Tonnies M, Lozza L, Schommer-Leitner S, Mollenkopf H, Bauer TT, et al. Mycobacterium tuberculosis Invasion of the Human Lung: First Contact. Front Immunol. 2018;9:1346.

53. Huang L, Nazarova EV, Tan S, Liu Y, Russell DG. Growth of Mycobacterium tuberculosis in vivo segregates with host macrophage metabolism and ontogeny. J Exp Med. 2018;215(4):1135-52.

54. Eruslanov EB, Lyadova IV, Kondratieva TK, Majorov KB, Scheglov IV, Orlova MO, et al. Neutrophil responses to Mycobacterium tuberculosis infection in genetically susceptible and resistant mice. Infect Immun. 2005;73(3):1744-53.

55. Fonseca KL, Maceiras AR, Matos R, Simoes-Costa L, Sousa J, Ca B, et al. Deficiency in the glycosyltransferase Gcnt1 increases susceptibility to tuberculosis through a mechanism involving neutrophils. Mucosal Immunol. 2020;13(5):836-48.

56. Muefong CN, Sutherland JS. Neutrophils in Tuberculosis-Associated Inflammation and Lung Pathology. Frontiers in Immunology. 2020;11(962).

57. Berry MPR, Graham CM, McNab FW, Xu Z, Bloch SAA, Oni T, et al. An interferon-inducible neutrophil-driven blood transcriptional signature in human tuberculosis. Nature. 2010;466(7309):973-7.

58. Dorhoi A, Kaufmann SH. Pathology and immune reactivity: understanding multidimensionality in pulmonary tuberculosis. Semin Immunopathol. 2016;38(2):153-66.

59. Hu S, He W, Du X, Yang J, Wen Q, Zhong XP, et al. IL-17 Production of Neutrophils Enhances Antibacteria Ability but Promotes Arthritis Development During Mycobacterium tuberculosis Infection. EBioMedicine. 2017;23:88-99.

60. Teixeira-Coelho M, Cruz A, Carmona J, Sousa C, Ramos-Pereira D, Saraiva AL, et al. TLR2 deficiency by compromising p19 (IL-23) expression limits Th 17 cell responses to Mycobacterium tuberculosis. Int Immunol. 2011;23(2):89-96.

61. Bruchfeld J, Correia-Neves M, Källenius G. Tuberculosis and HIV Coinfection. Cold Spring Harb Perspect Med. 2015;5(7):a017871.

62. Lin PL, Flynn JL. CD8 T cells and Mycobacterium tuberculosis infection. Semin Immunopathol. 2015;37(3):239-49.

63. Hunter RL. Tuberculosis as a three-act play: A new paradigm for the pathogenesis of pulmonary tuberculosis. Tuberculosis. 2016;97:8-17.

64. Coscolla M, Copin R, Sutherland J, Gehre F, de Jong B, Owolabi O, et al. M. tuberculosis T Cell Epitope Analysis Reveals Paucity of Antigenic Variation and Identifies Rare Variable TB Antigens. Cell Host Microbe. 2015;18(5):538-48.

65. Dinarello CA. Overview of the IL-1 family in innate inflammation and acquired immunity. Immunol Rev. 2018;281(1):8-27.

66. Van Den Eeckhout B, Tavernier J, Gerlo S. Interleukin-1 as Innate Mediator of T Cell Immunity. Frontiers in Immunology. 2021;11(3605).

67. Kaneko N, Kurata M, Yamamoto T, Morikawa S, Masumoto J. The role of interleukin-1 in general pathology. Inflammation and Regeneration. 2019;39(1):12.

68. Bohrer AC, Tocheny C, Assmann M, Ganusov VV, Mayer-Barber KD. Cutting Edge: IL-1R1 Mediates Host Resistance to Mycobacterium tuberculosis by Trans-Protection of Infected Cells. J Immunol. 2018;201(6):1645-50.

69. Mayer-Barber KD, Barber DL, Shenderov K, White SD, Wilson MS, Cheever A, et al. Caspase-1 independent IL-1beta production is critical for host resistance to mycobacterium tuberculosis and does not require TLR signaling in vivo. J Immunol. 2010;184(7):3326-30.

70. Yamada H MS, Horai R, Iwakura Y, Sugawara I. Protective role of interleukin-1 in mycobacerial infection in IL-1 α/β double-knockout mice Lab Investig. 2000;80:759-67.

71. Di Paolo NC, Shafiani S, Day T, Papayannopoulou T, Russell DW, Iwakura Y, et al. Interdependence between Interleukin-1 and Tumor Necrosis Factor Regulates TNF-Dependent Control of Mycobacterium tuberculosis Infection. Immunity. 2015;43(6):1125-36.

72. Mayer-Barber KD, Andrade BB, Oland SD, Amaral EP, Barber DL, Gonzales J, et al. Host-directed therapy of tuberculosis based on interleukin-1 and type I interferon crosstalk. Nature. 2014;511(7507):99-103.

73. Juffermans NP FS, Camoglio L, Verbon A, Kolk AH, Speelman P, et al. Interleukin-1 Signaling Is Essential for Host Defense during Murine Pulmonary Tuberculosis. The Journal of Infectious Diseases. 2000;182:902-8.

74. Sugawara I, Yamada H, Hua S, Mizuno S. Role of interleukin (IL)-1 type 1 receptor in mycobacterial infection. Microbiol Immunol. 2001;45(11):743-50.

75. Liu X, Boyer MA, Holmgren AM, Shin S. Legionella-Infected Macrophages Engage the Alveolar Epithelium to Metabolically Reprogram Myeloid Cells and Promote Antibacterial Inflammation. Cell Host Microbe. 2020;28(5):683-98 e6.

76. Jayaraman P, Sada-Ovalle I, Nishimura T, Anderson AC, Kuchroo VK, Remold HG, et al. IL-1beta promotes antimicrobial immunity in macrophages by regulating TNFR signaling and caspase-3 activation. J Immunol. 2013;190(8):4196-204.

77. Winchell CG, Mishra BB, Phuah JY, Saqib M, Nelson SJ, Maiello P, et al. Evaluation of IL-1 Blockade as an Adjunct to Linezolid Therapy for Tuberculosis in Mice and Macaques. Front Immunol. 2020;11:891.

78. Hitzler I, Sayi A, Kohler E, Engler DB, Koch KN, Hardt WD, et al. Caspase-1 has both proinflammatory and regulatory properties in Helicobacter infections, which are differentially mediated by its substrates IL-1beta and IL-18. J Immunol. 2012;188(8):3594-602.

79. Kim B, Jin Y-H, Meng L, Hou W, Kang H, Park H, et al. IL-1 signal affects both protection and pathogenesis of virus-indduced chronic CNS demyelinating disease. J Neuroinflammation. 2012;9(217).

80. Mantovani A, Dinarello CA, Molgora M, Garlanda C. Interleukin-1 and Related Cytokines in the Regulation of Inflammation and Immunity. Immunity. 2019;50(4):778-95.

81. Kleinnijenhuis J, Joosten LA, van de Veerdonk FL, Savage N, van Crevel R, Kullberg BJ, et al. Transcriptional and inflammasome-mediated pathways for the induction of IL-1beta production by Mycobacterium tuberculosis. Eur J Immunol. 2009;39(7):1914-22.

82. Gringhuis SI, Kaptein TM, Wevers BA, Theelen B, van der Vlist M, Boekhout T, et al. Dectin-1 is an extracellular pathogen sensor for the induction and processing of IL-1β via a noncanonical caspase-8 inflammasome. Nature Immunology. 2012;13(3):246-54.

83. Wassermann R, Gulen MF, Sala C, Perin SG, Lou Y, Rybniker J, et al. Mycobacterium tuberculosis Differentially Activates cGAS- and Inflammasome-Dependent Intracellular Immune Responses through ESX-1. Cell Host Microbe. 2015;17(6):799-810.

84. Cheng Y, Schorey JS. Mycobacterium tuberculosis-induced IFN-beta production requires cytosolic DNA and RNA sensing pathways. J Exp Med. 2018;215(11):2919-35.

85. Novikov A, Cardone M, Thompson R, Shenderov K, Kirschman KD, Mayer-Barber KD, et al. Mycobacterium tuberculosis triggers host type I IFN signaling to regulate IL-1beta production in human macrophages. J Immunol. 2011;187(5):2540-7.

86. Shah S, Bohsali A, Ahlbrand SE, Srinivasan L, Rathinam VA, Vogel SN, et al. Cutting edge: Mycobacterium tuberculosis but not nonvirulent mycobacteria inhibits IFN-beta and AIM2 inflammasome-dependent IL-1beta production via its ESX-1 secretion system. J Immunol. 2013;191(7):3514-8.

87. Master SS, Rampini SK, Davis AS, Keller C, Ehlers S, Springer B, et al. Mycobacterium tuberculosis prevents inflammasome activation. Cell Host Microbe. 2008;3(4):224-32.

88. Sousa J, Cá B, Maceiras AR, Simões-Costa L, Fonseca KL, Fernandes AI, et al. Mycobacterium tuberculosis associated with severe tuberculosis evades cytosolic surveillance systems and modulates IL-1β production. Nature Communications. 2020;11(1).

89. Gleeson LE, Sheedy FJ, Palsson-McDermott EM, Triglia D, O'Leary SM, O'Sullivan MP, et al. Cutting Edge: Mycobacterium tuberculosis Induces Aerobic Glycolysis in Human Alveolar Macrophages That Is Required for Control of Intracellular Bacillary Replication. J Immunol. 2016;196(6):2444-9.

90. Hackett EE, Charles-Messance H, O'Leary SM, Gleeson LE, Munoz-Wolf N, Case S, et al. Mycobacterium tuberculosis Limits Host Glycolysis and IL-1beta by Restriction of PFK-M via MicroRNA-21. Cell Rep. 2020;30(1):124-36 e4.

91. Howard NC, Marin ND, Ahmed M, Rosa BA, Martin J, Bambouskova M, et al. Mycobacterium tuberculosis carrying a rifampicin drug resistance mutation reprograms macrophage metabolism through cell wall lipid changes. Nat Microbiol. 2018;3(10):1099-108.

92. Robson MJ, Zhu CB, Quinlan MA, Botschner DA, Baganz NL, Lindler KM, et al. Generation and Characterization of Mice Expressing a Conditional Allele of the Interleukin-1 Receptor Type 1. PLoS One. 2016;11(3):e0150068.

93. Pinteaux E, Abdulaal WH, Mufazalov IA, Humphreys NE, Simonsen-Jackson M, Francis S, et al. Cell-specific conditional deletion of interleukin-1 (IL-1) ligands and its receptors: a new toolbox to study the role of IL-1 in health and disease. Journal of Molecular Medicine. 2020;98(7):923-30.

94. Shi J, Hua L, Harmer D, Li P, Ren G. Cre Driver Mice Targeting Macrophages. Methods Mol Biol. 2018;1784:263-75.

95. Ordway D, Henao-Tamayo M, Harton M, Palanisamy G, Troudt J, Shanley C, et al. The HypervirulentMycobacterium tuberculosisStrain HN878 Induces a Potent TH1 Response followed by Rapid Down-Regulation. The Journal of Immunology. 2007;179(1):522-31.

96. Choreño-Parra JA, Bobba S, Rangel-Moreno J, Ahmed M, Mehra S, Rosa B, et al. Mycobacterium tuberculosis HN878 Infection Induces Human-Like B-Cell Follicles in Mice. J Infect Dis. 2020;221(10):1636-46.

97. Moreira-Teixeira L, Tabone O, Graham CM, Singhania A, Stavropoulos E, Redford PS, et al. Mouse transcriptome reveals potential signatures of protection and pathogenesis in human tuberculosis. Nat Immunol. 2020;21(4):464-76.

98. Kramnik I, Beamer G. Mouse models of human TB pathology: roles in the analysis of necrosis and the development of host-directed therapies. Semin Immunopathol. 2016;38(2):221-37.

99. Driver ER, Ryan GJ, Hoff DR, Irwin SM, Basaraba RJ, Kramnik I, et al. Evaluation of a mouse model of necrotic granuloma formation using C3HeB/FeJ mice for testing of drugs against Mycobacterium tuberculosis. Antimicrob Agents Chemother. 2012;56(6):3181-95.

100. Torrado E, Cooper AM. IL-17 and Th17 cells in tuberculosis. Cytokine Growth Factor Rev. 2010;21(6):455-62.

101. Dudek M, Puttur F, Arnold-Schrauf C, Kuhl AA, Holzmann B, Henriques-Normark B, et al. Lung epithelium and myeloid cells cooperate to clear acute pneumococcal infection. Mucosal Immunol. 2016;9(5):1288-302.

Attachments

Interleukin-1 manipulation by *Mycobacterium tuberculosis*: impact to the infection establishment and progression

Gonçalves, Rute (rute.goncalves@i3s.up.pt), i3s, FCUP, Portugal
Silvério, Diogo (diogo.f.silverio@gmail.com), i3s, ICBAS, Portugal
Maceiras, Ana R. (raquel.maceiras@gmail.com), i3s, Portugal
Cá, Baltazar (baltazar.ca@ibmc.up.pt), i3s, Portugal
Rocha, Deisy (deisy.rocha@i3s.up.pt), i3s, Portugal
Saraiva, Margarida (margarida.saraiva@ibmc.up.pt), i3s, Portugal

Introduction

Interleukin-1 (IL-1) is a pro-inflammatory cytokine of great importance to the early protection against tuberculosis (TB), since experimental studies in mice show that deficiency in the IL-1 signaling results in rapid establishment of infection and death[1,2]. Our group has recently described that different *Mycobacterium tuberculosis* clinical isolates associated with mild (4I2) or severe (6C4) TB in humans induce high or low levels of IL-1β, respectively, in human macrophages[3,4]. To further investigate how these differences impact the establishment and course of infection, we infected wild type mice and mice lacking IL-1R in the myeloid compartment[4](IL-1R$^{\Delta LyzM}$).

Aim

- **Investigate if different modulation of IL-1β and TB severity could be modelled *in vivo* by *M.tuberculosis* strains.**
- **Decipher if the lower severity of 4I2 strain is linked to the induction of IL-1β, studying the impact of cell specific IL-1 receptor signalling on the pathogenesis of TB.**

Methodology

***M.tuberculosis* strains recovered from patients with different severities of TB.**

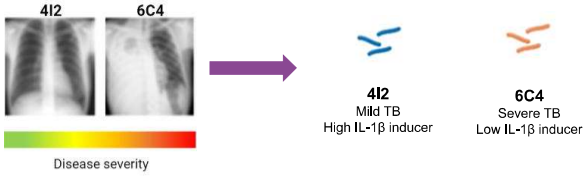

***In vivo* experiment: Wild Type (WT) and IL-1R$^{\Delta LyzM}$ mice were aerosol infected with *M.tuberculosis* 4I2 or 6C4 and the organs were harvested, processed and analyzed at 15 and 30 post infection (p.i) .**

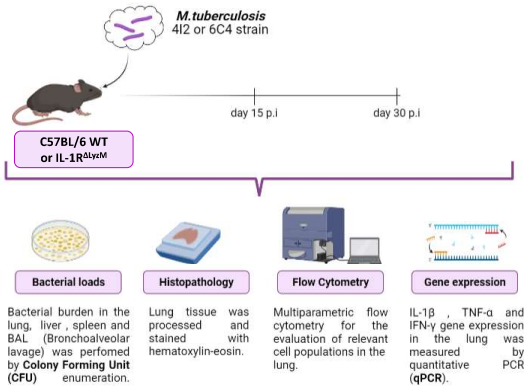

Bacterial burden in the lung, liver , spleen and BAL (Bronchoalveolar lavage) was perfomed by **Colony Forming Unit (CFU)** enumeration.

Lung tissue was processed and stained with hematoxylin-eosin.

Multiparametric flow cytometry for the evaluation of relevant cell populations in the lung.

IL-1β , TNF-α and IFN-γ gene expression in the lung was measured by quantitative PCR (**qPCR**).

Results

C57BL/6 mice infected with *M.tuberculosis* 6C4 present higher bacterial loads in the lung and liver and more severe pathology than mice infected with 4I2.

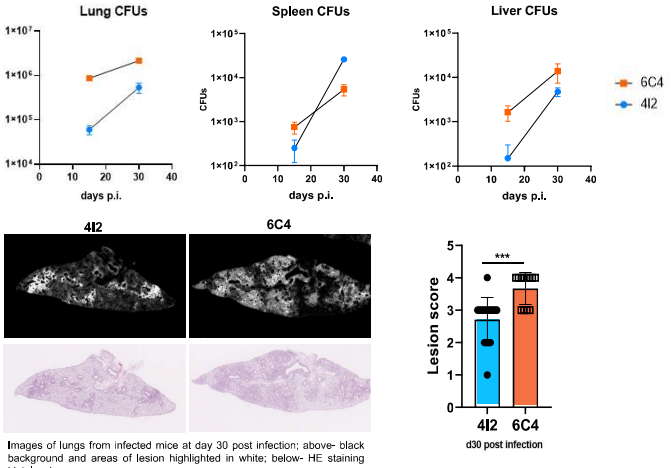

Images of lungs from infected mice at day 30 post infection; above- black background and areas of lesion highlighted in white; below- HE staining histology's.

Lack of IL-1R in the myeloid compartment (LyzM mice) leads to increased bacterial burden in lung and BAL, severe pathology, increased expression of pro inflammatory genes and higher cell recruitment to the local of infection, when mice are infected with the higher IL-1β inducer strain (4I2).

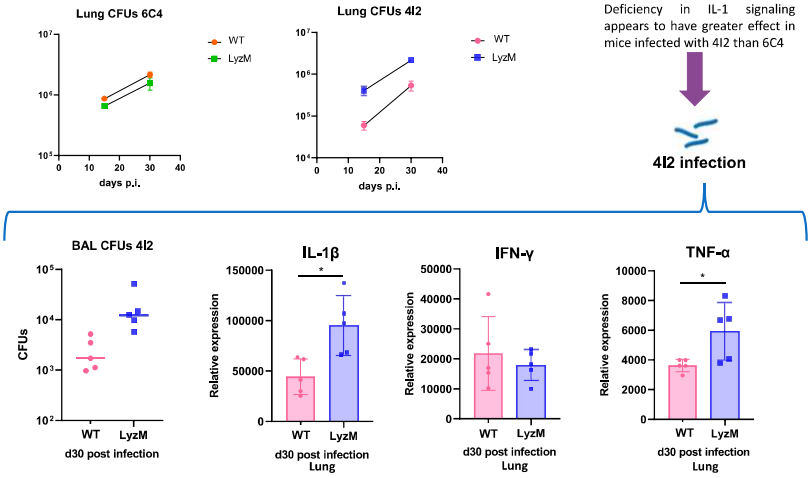

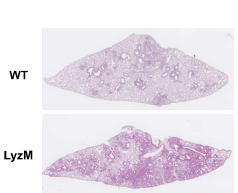

Images of lungs from infected mice at day 30 post infection; HE staining histology's.

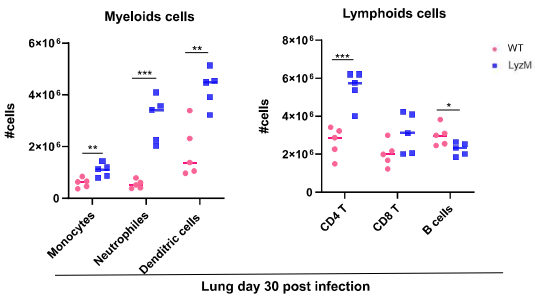

Conclusion

According to the results, it was possible to recapitulate, in the mouse model, distinct severities of disease provoked by different *M.tuberculosis* strains. *M.tuberculosis* 6C4 showed a higher bacterial load at the local of infection, more dissemination to the liver and a larger area of lung lesion than 4I2, compatible with the severe form of TB described in humans. IL-1R-deficient mice in myeloid cells when infected with the higher IL-1β inducer strain (4I2) were less able to control the infection in comparison to WT, showing higher bacterial burden, severe pathology, more cell infiltration and increased inflammatory responses. Therefore, the low severity of 4I2 infection compared to other strains, seems to be linked to the high induction of IL-1β.

Future perspectives include performing a similar experience to compare LyzM and WT mice when infected with 6C4 and study the contribution of other cellular compartments, such as epithelial and endothelial cells in the IL-1 signaling.

With this study and future ones, we expect to better understand the complex immune response of TB.

References

1. Mayer-Barber KD, Barber DL, Shenderov K, White SD, Wilson MS, Cheever A, et al. Caspase-1 independent IL-1beta production is critical for host resistance to mycobacterium tuberculosis and does not require TLR signaling in vivo. J Immunol. 2010;184(7):3326-30
2. Bohrer AC, Tocheny C, Assmann M, Ganusov VV, Mayer-Barber KD. Cutting Edge: IL-1R1 Mediates Host Resistance to Mycobacterium tuberculosis by Trans-Protection of Infected Cells. J Immunol. 2018;201(6):1645-50
3. Sousa J, Cá B, Maceiras AR, Simões-Costa L, Fonseca KL, Fernandes AI, et al. Mycobacterium tuberculosis associated with severe tuberculosis evades cytosolic surveillance systems and modulates IL-1β production. Nature Communications. 2020;11(1):1949.
4. Moreira-Teixeira L, Tabone O, Graham CM, Singhania A, Stavropoulos E, Redford PS, et al. Mouse transcriptome reveals potential signatures of protection and pathogenesis in human tuberculosis. Nat Immunol. 2020;21(4):464-76.

This poster is a result of the project HEALTH-UNORTE: Setting-up biobanks and regenerative medicine strategies to boost research in cardiovascular, musculoskeletal, neurological, oncological, immunological and infectious diseases (NORTE-01-0145-FEDER-000039), supported by Norte Portugal Regional Operational Programme (NORTE 2020), under the PORTUGAL 2020 Partnership Agreement, through the European Regional Development Fund (ERDF).

D. Silvério (SFRH/BD/143536/2019) is supported by the Portuguese Foundation for Science and Technology (FCT) through PhD grants.

M. Saraiva, is funded by FCT through *Estímulo Individual ao Emprego Científico*.

Interleukin-1 manipulation by *Mycobacterium tuberculosis*: impact to the infection establishment and progression

Rute Gonçalves[1,2], Diogo Silvério[1,3] , Ana Raquel Maceiras[1,2], Baltazar Cá[1], Deisy Rocha[1], Margarida Saraiva[1]

[1]Instituto de Investigação e Inovação em Saúde (i3s), Universidade do Porto, Portugal
[2]Faculdade de Ciências, Universidade do Porto, Portugal
[3]Instituto de Ciências Biomédicas Abel Salazar, Universidade do Porto, Portugal

Introduction

Interleukin-1 (IL-1) is a pro-inflammatory cytokine of great importance to the early protection against tuberculosis (TB), since experimental studies in mice show that deficiency in the IL-1 signaling results in rapid establishment of infection and death (1,2). Our group has recently described that different *Mycobacterium tuberculosis* clinical isolates associated with mild (4I2) or severe (6C4) TB in humans induce high or low levels of IL-1β, respectively, in human macrophages (3,4). To further investigate how these differences impact the establishment and course of infection, we infected wild type mice and mice lacking IL-1R in the myeloid compartment (IL-1R$^{\Delta LyzM}$).

Aim

- **Investigate if different modulation of IL-1β and TB severity could be modelled *in vivo* by *M.tuberculosis* strains.**
- **Decipher if the lower severity of 4I2 strain is linked to the induction of IL-1β, studying the impact of cell specific IL-1 receptor signalling on the pathogenesis of TB.**

Methodology

***M.tuberculosis* strains recovered from patients with different severities of TB.**

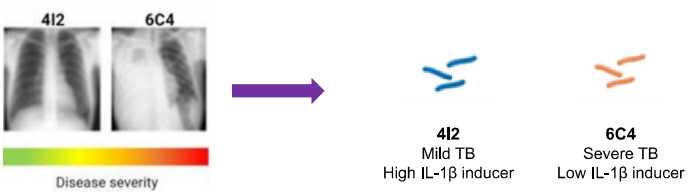

***In vivo* experiment: Wild Type (WT) and IL-1R$^{\Delta LyzM}$ mice were aerosol infected with *M.tuberculosis* 4I2 or 6C4 and the organs were harvested, processed and analyzed at 15 and 30 post infection (p.i) .**

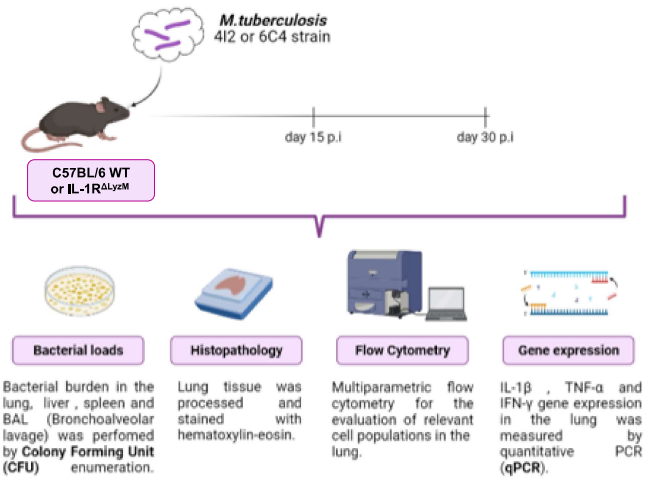

Bacterial burden in the lung, liver , spleen and BAL (Bronchoalveolar lavage) was perfomed by **Colony Forming Unit (CFU)** enumeration.

Lung tissue was processed and stained with hematoxylin-eosin.

Multiparametric flow cytometry for the evaluation of relevant cell populations in the lung.

IL-1β , TNF-α and IFN-γ gene expression in the lung was measured by quantitative PCR (**qPCR**).

Results

I. C57BL/6 mice infected with *M.tuberculosis* 6C4 present higher bacterial loads in the lung and liver and more severe pathology than mice infected with 4I2.

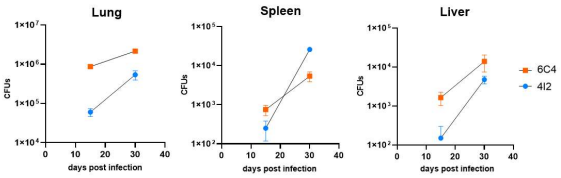

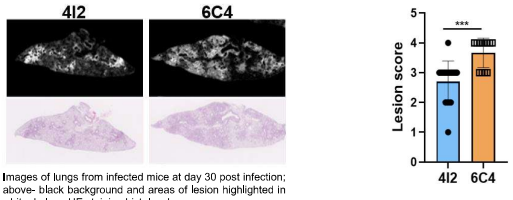

Images of lungs from infected mice at day 30 post infection; above- black background and areas of lesion highlighted in white; below- HE staining histology's

II. Lack of IL-1R in the myeloid compartment (LyzM mice) leads to increased bacterial burden in lung and BAL, severe pathology, increased expression of pro inflammatory genes and higher cell recruitment to the local of infection, when mice are infected with the higher IL-1β inducer strain (4I2).

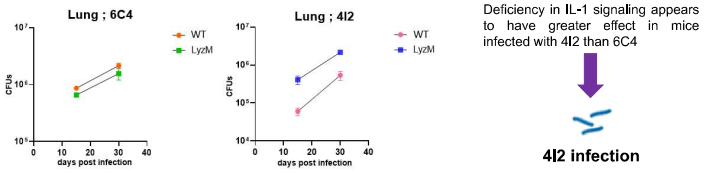

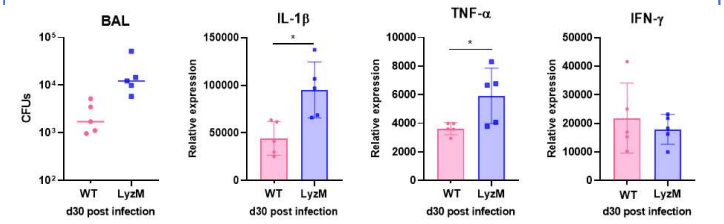

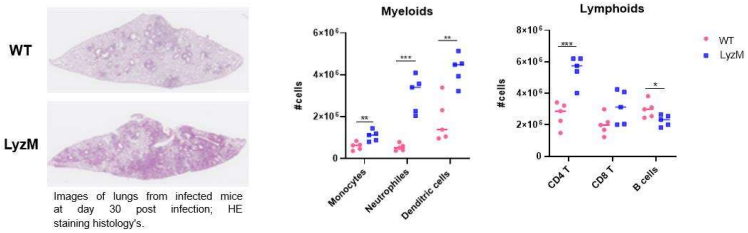

Images of lungs from infected mice at day 30 post infection; HE staining histology's.

Conclusion

According to the results, it was possible to recapitulate, in the mouse model, distinct severities of disease provoked by different *M.tuberculosis* strains. *M.tuberculosis* 6C4 showed a higher bacterial load at the local of infection, more dissemination to the liver and a larger area of lung lesion than 4I2, compatible with the severe form of TB described in humans. IL-1R-deficient mice in myeloid cells when infected with the higher IL-1β inducer strain (4I2) were less able to control the infection in comparison to WT, showing higher bacterial burden, severe pathology, more cell infiltration and increased inflammatory responses. Therefore, the low severity of 4I2 infection compared to other strains, seems to be linked to the high induction of IL-1β.

Future perspectives include performing a similar experience to compare LyzM and WT mice when infected with 6C4 and study the contribution of other cellular compartments, such as epithelial and endothelial cells in the IL-1 signaling. With this study and future ones, we expect to better understand the complex immune response of TB.

References

1. Mayer-Barber KD, Barber DL, Shenderov K, White SD, Wilson MS, Cheever A, et al. Caspase-1 independent IL-1beta production is critical for host resistance to mycobacterium tuberculosis and does not require TLR signaling in vivo. J Immunol. 2010;184(7):3326-30
2. Bohrer AC, Tocheny C, Assmann M, Ganusov VV, Mayer-Barber KD. Cutting Edge: IL-1R1 Mediates Host Resistance to Mycobacterium tuberculosis by Trans-Protection of Infected Cells. J Immunol. 2018;201(6):1645-50
3. Sousa J, Cá B, Maceiras AR, Simões-Costa L, Fonseca KL, Fernandes AI, et al. Mycobacterium tuberculosis associated with severe tuberculosis evades cytosolic surveillance systems and modulates IL-1β production. Nature Communications. 2020;11(1):1949.
4. Moreira-Teixeira L, Tabone O, Graham CM, Singhania A, Stavropoulos E, Redford PS, et al. Mouse transcriptome reveals potential signatures of protection and pathogenesis in human tuberculosis. Nat Immunol. 2020;21(4):464-76.